

TRANSCRIPTIONAL REGULATION OF NEURAL CREST-DERIVED
PHARYNGEAL ARCH ARTERY DEVELOPMENT

APPROVED BY SUPERVISORY COMMITTEE

Carole R. Mendelson, Ph.D.

Jane E. Johnson, Ph.D.

Tom Sato, Ph.D.

Deepak Srivastava, M.D.

To my Mom and Dad
for their love and encouragement.

And to my husband, Chris
for sharing his life with me.

TRANSCRIPTIONAL REGULATION OF NEURAL CREST-DERIVED
PHARYNGEAL ARCH ARTERY DEVELOPMENT

by

KATHRYN NICOLE IVEY

DISSERTATION

Presented to the Faculty of the Graduate School of Biomedical Sciences

The University of Texas Southwestern Medical Center at Dallas

In Partial Fulfillment of the Requirements

For the Degree of

DOCTOR OF PHILOSOPHY

The University of Texas Southwestern Medical Center at Dallas

Dallas, Texas

December, 2004

ACKNOWLEDGEMENTS

This body of work, and my success as a graduate student, would not have been realized without the support of my mentor, Deepak Srivastava. Deepak was able to recognize my strengths and make use of them while gently helping me to improve on my weaknesses. As he taught me to be a good scientist, he also helped me to gain the confidence that is required to be a success in any field. While I am proud of the thesis that I have completed under his tutelage, I am more proud and surprised by the person that I have become through his patient guidance.

I would also like to thank current and past members of the Srivastava Lab who have been my good friends and teachers. I think that my graduate school experience was more enjoyable than most because of the kind-hearted and fun people that shared the lab with me. I also thank my friend Jennifer for providing a reprieve from the lab in spite of our busy schedules and my friend and yoga instructor Liz, who taught me new ways to strengthen my body, clear my mind, and be at peace.

Finally, my deepest thanks go to my family—my Mom and Dad and my husband, Chris. They have been my biggest supporters before and during graduate school and I couldn't have done it without them. Thank you for all of the guidance, encouragement, and for being there through all of my frustrations. So much of my success is owed to you and I hope that this accomplishment will bring many opportunities that we can share together.

Copyright

by

Kathryn Nicole Ivey, Ph.D.

All Rights Reserved

TRANSCRIPTIONAL REGULATION OF NEURAL CREST-DERIVED
PHARYNGEAL ARCH ARTERY DEVELOPMENT

Publication No. _____

Kathryn Nicole Ivey, Ph.D.

The University of Texas Southwestern Medical Center at Dallas, 2004

Supervising Professor: Deepak Srivastava, M.D.

The heart is the first organ to form and is required for growth and development of mammalian embryos. As the heart matures, formation of the outflow tract is vital to establish appropriate connections with the vasculature. This process requires contribution from specialized neural crest cells, which originate in the neural folds and migrate to give rise to specific segments of the great vessels as well as particular facial structures. Many syndromic birth defects in humans affecting the heart and face arise as a result of inappropriate development of neural crest cells and can be modeled in animals through

ablation of premigratory neural crest cells or targeted deletion of genes required for their proliferation, migration or survival. However, the transcription factors and signaling molecules that specify unique subsets of neural crest cells are still being detailed. This thesis represents efforts to understand those particulars.

Endothelin-1 (Et-1), a small signaling peptide, is important for development of neural crest-derived structures and targeted deletion of the gene encoding Et-1 or its receptor, Endothelin-A (Et_A), results in craniofacial and outflow tract anomalies along with downregulation of particular neural crest-derived pharyngeal arch mesenchyme markers. Mice deficient for both $G\alpha_q$ and $G\alpha_{11}$ are phenotypically similar to Et_A or $Et-1$ -null mice. My analysis of expression patterns of Et-1 dependent and independent transcription factors in $G\alpha_q/G\alpha_{11}$ -deficient embryos revealed that expression of genes encoding Et-1 dependent transcription factors was specifically downregulated in the pharyngeal arches of $G\alpha_q/G\alpha_{11}$ -deficient mice indicating that $G\alpha_q$ and $G\alpha_{11}$ proteins serve as intracellular mediators of Et-1 signaling in the pharyngeal arch mesenchyme.

Et-1 is also important for development of the neural crest-derived fetal vessel, the ductus arteriosus, which bridges the pulmonary and systemic circulations during gestation and must close at birth for extrauterine survival. The ductus arteriosus is composed of highly differentiated, contractile smooth muscle. I found that Et-1 is expressed specifically in the smooth muscle of the ductus arteriosus during development along with Hif2 α and Ap2 β and that, through epistatic relationships and negative feedback regulation, these three factors cooperatively regulate development of the specialized, neural crest-derived smooth muscle of this vessel.

TABLE OF CONTENTS

TABLE OF CONTENTS.....	viii
PUBLICATIONS.....	xi
LIST OF FIGURES.....	xii
CHAPTER ONE: INTRODUCTION.....	1
The Heart.....	1
The Outflow Tract.....	2
Neural Crest Cells and the Great Vessels.....	4
Transcriptional Regulation of Neural Crest Development.....	5
References.....	8
 CHAPTER TWO: A COMMON CIS-ACTING SEQUENCE IN THE DIGEORGE CRITICAL REGION REGULATES BI-DIRECTIONAL TRANSCRIPTION OF UFD1L AND CDC45L.....	 11
Background.....	11
Results.....	14
<i>Coexpression of UFD1L and CDC45L.....</i>	<i>14</i>
<i>The UFD1L-CDC45L intergenic region is a conserved CpG island.....</i>	<i>15</i>
<i>The UFD1L-CDC45L intergenic region contains regulatory elements sufficient for bi-directional transcription.....</i>	<i>18</i>
<i>A 404bp regulatory region is necessary and sufficient to direct bi-directional transcriptional activation of UFD1L and CDC45L.....</i>	<i>22</i>
Discussion.....	25
<i>Bidirectional transcriptional activity of the UFD1L-CDC45L intervening region...25</i>	
<i>The UFD1L-CDC45L intergenic region is a CpG island.....</i>	<i>26</i>
<i>Relation with the 22q11 deletion phenotype.....</i>	<i>27</i>
Materials and Methods.....	29
<i>Radioactive section in situ hybridization.....</i>	<i>29</i>
<i>Cloning of the intergenic human genomic DNA between UFD1L and CDC45L.....</i>	<i>29</i>
<i>Generation of transgenic mice.....</i>	<i>30</i>
<i>β-galactosidase staining.....</i>	<i>30</i>
<i>Neural crest cell culture and transfection.....</i>	<i>31</i>
<i>RNA isolation and Northern blot analysis.....</i>	<i>31</i>
<i>Construction of UFD1L/CDC45L fragment.....</i>	<i>32</i>
<i>Cell culture and transfections.....</i>	<i>33</i>
<i>Luciferase assays.....</i>	<i>34</i>
<i>References.....</i>	<i>35</i>

CHAPTER THREE: $G\alpha_q$ AND $G\alpha_{11}$ PROTEINS MEDIATE ENDOTHELIN-1 SIGNALING IN THE NEURAL CREST-DERIVED PHARYNGEAL ARCH

MESENCHYME.....	39
Background.....	39
Results.....	41
<i>Hand gene expression is downregulated in pharyngeal arches of $G\alpha_q/G\alpha_{11}$-deficient embryos.....</i>	<i>41</i>
<i>$Msx1$ and $Msx2$ expression is maintained in the pharyngeal arches of $G\alpha_q/G\alpha_{11}$-deficient embryos.....</i>	<i>43</i>
<i>$Dlx3$ and $Dlx6$ expression is downregulated in $G\alpha_q/G\alpha_{11}$-deficient embryos and maintained in dHAND-null embryos.....</i>	<i>43</i>
Discussion.....	46
Materials and Methods.....	51
<i>Harvesting and genotyping of embryos.....</i>	<i>51</i>
<i>Whole mount in-situ hybridization.....</i>	<i>52</i>
<i>Radioactive section in situ hybridization.....</i>	<i>52</i>
References.....	53

CHAPTER FOUR: $HIF2\alpha$, $AP2\beta$ AND ET-1 COOPERATIVELY REGULATE DEVELOPMENT OF DUCTUS ARTERIOSUS SMOOTH MUSCLE.....

.....56	56
Background.....	56
Results.....	59
<i>Et-1 is specifically expressed in the smooth muscle of the ductus arteriosus during development.....</i>	<i>59</i>
<i>$Hif2\alpha$, a potential transcriptional regulator of Et-1 is specifically expressed in the smooth muscle of the ductus arteriosus during development.....</i>	<i>62</i>
<i>$Hif2\alpha$ and Et-1 are not required for one another's expression in the smooth muscle of the ductus arteriosus.....</i>	<i>63</i>
<i>$Tfap2\beta$ is expressed in the smooth muscle of the ductus arteriosus and $Tfap2\beta^{-/-}$ mice have delayed ductal closure.....</i>	<i>65</i>
<i>$Tfap2\beta$ is required for ductal smooth muscle expression of $Hif2\alpha$ and Et-1.....</i>	<i>67</i>
<i>Smooth muscle cells are appropriately specified in the ductus arteriosus of $Tfap2\beta^{-/-}$ mice, but fail to maintain their highly differentiated state.....</i>	<i>68</i>
<i>$Hif2\alpha$ blocks transcriptional activation by $Ap2\beta$ by preventing DNA binding by $Ap2\beta$.....</i>	<i>70</i>
<i>The N-terminus of $Hif2\alpha$ containing the PAS domains is required to block DNA binding and transcriptional activation by $Ap2\beta$.....</i>	<i>73</i>
Discussion.....	75
<i>$Hif2\alpha$ protein vs. mRNA expression.....</i>	<i>75</i>
<i>Et-1 expression in the smooth muscle of the ductus arteriosus declines prenatally..</i>	<i>76</i>
<i>Human vs. mouse phenotypes with respect to $Tfap2\beta$.....</i>	<i>78</i>
<i>Clinical implications.....</i>	<i>79</i>
Materials and Methods.....	80

<i>Luciferase reporter assays</i>	80
<i>LacZ staining</i>	80
<i>Embryo harvesting and histology</i>	80
<i>Radioactive section in situ hybridization</i>	81
<i>Transfections, CAT assays, and western analysis</i>	81
<i>Electrophoretic mobility shift assays</i>	82
<i>Hif2α truncations</i>	82
References	84
CHAPTER FIVE: CONSIDERATIONS AND FUTURE DIRECTIONS	87
Dissecting Independent Roles of Endothelin-1	87
Retinoic Acid and the Neural Crest	88
Implications for the Ductus Venosus	90
Technological Advances in Gene Regulation Discovery	92
References	98
VITAE	101

PUBLICATIONS

- Ivey, K.**, Zhao, F., Garg, V., Sutcliffe, D., Richardson, J., Garcia, J., Gelb, B., Srivastava, D. Hif2 α , Ap2 β and Et-1 cooperatively regulate development of the ductus arteriosus. *In preparation*.
- Ivey, K.**, Tyson, B., Ukidwe, P., McFadden, D.G., Levi, G., Olson, E.N., Srivastava, D., Wilkie, T.M. G α_q and G α_{11} proteins mediate endothelin-1 signaling in neural crest-derived pharyngeal arch mesenchyme. *Developmental Biology*. 255: 230-237 (2003).
- *Kunte, A., ***Ivey, K.**, Yamagishi, C., Garg, V., Yamagishi, H., Srivastava, D. A common cis-acting sequence in the DiGeorge critical region regulates bi-directional transcription of UFD1L and CDC45L. *Mechanisms of Development*. 108: 81-92 (2001).
*Authors contributed equally
- Pepper, A.E., Seong-Kim, M., Hebst, S.M., **Ivey, K.N.**, Kwak, S.J., Broyles, D.E. shl, a new set of Arabidopsis mutants with exaggerated developmental responses to available red, far-red, and blue light. *Plant Physiology*. 127: 295-304 (2001).
- Cha, J.H., Brooke, J.S., **Ivey, K.N.**, Eidels, L. Cell surface monkey CD9 antigen is a coreceptor that increases diphtheria toxin sensitivity and diphtheria toxin receptor affinity. *Journal of Biological Chemistry*. 275: 6901-6907 (2000).

LIST OF FIGURES

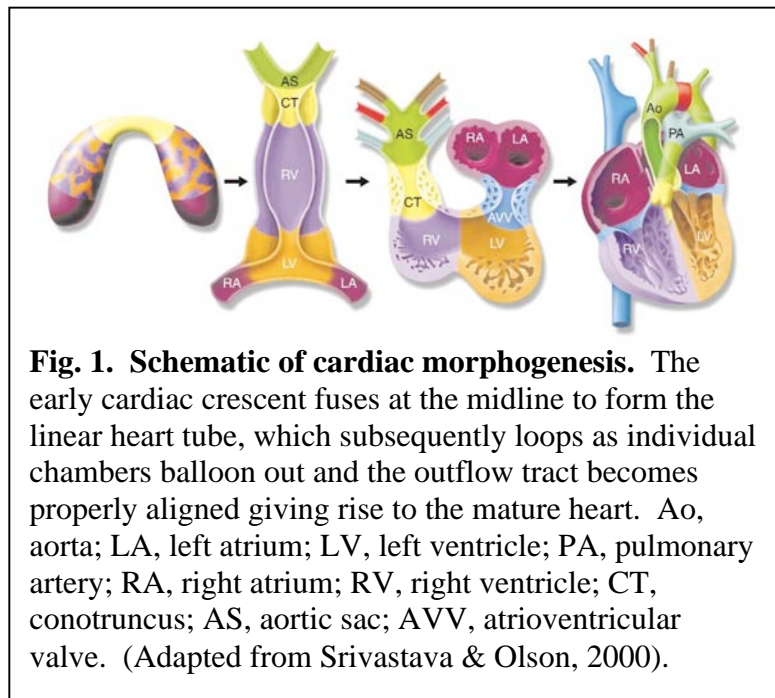
CHAPTER ONE.....	1
Figure 1. Schematic of cardiac morphogenesis.....	1
Figure 2. Transition from fetal to neonatal circulation.....	2
Figure 3. Aorticopulmonary septation defects.....	3
Figure 4. Progression of mammalian pharyngeal arch artery development.....	4
CHAPTER TWO.....	10
Figure 1. Gene expression of <i>UFD1L</i> and <i>CDC45L</i>	15
Figure 2. Analysis of the <i>UFD1L-CDC45L</i> intergenic sequence.....	17
Figure 3. Bidirectional transcriptional activity of the <i>UFD1L-CDC45L</i> intervening sequence in neural crest cells.....	18
Figure 4. Bi-directional transcriptional activity of the <i>UFD1L-CDC45L</i> intervening sequence in cell lines.....	20
Figure 5. Deletion analysis of the <i>UFD1L – CDC45L</i> intervening region.....	23
CHAPTER THREE.....	38
Figure 1. <i>Hand</i> genes are downregulated in $G\alpha_q/G\alpha_{11}$ -deficient pharyngeal arches.....	41
Figure 2. Pharyngeal arch expression of <i>Msx1</i> in wild-type and $G\alpha_q/G\alpha_{11}$ -deficient mice.....	42
Figure 3. <i>Dlx3</i> and <i>Dlx6</i> pharyngeal arch expression is regulated by $G\alpha_q/G\alpha_{11}$ in a dose-dependent manner.....	43
Figure 4. <i>Dlx3</i> and <i>dHAND</i> function in independent pathways in developing pharyngeal arches.....	45
Figure 5. Model of $G\alpha_q/G\alpha_{11}$ –coupled Et_A activation of <i>Dlx</i> and <i>Hand</i> expression in pharyngeal arch mesenchyme.....	48
CHAPTER FOUR.....	55
Figure 1. Endothelin and <i>Hif2α</i> in the smooth muscle of the ductus arteriosus.....	60
Figure 2. <i>Hif2α</i> activates an <i>Et-1</i> enhancer in cultured vascular smooth muscle cells but is not necessary in vivo at E13.5.....	63
Figure 3. <i>Tfap2β</i> is expressed in the smooth muscle of the ductus arteriosus.....	65
Figure 4. <i>Tfap2β</i> is required for ductal smooth muscle expression of <i>Hif2α</i> and <i>Et-1</i>	66
Figure 5. Smooth muscle cells are appropriately specified in the ductus arteriosus of <i>Tfap2β^{-/-}</i> mice, but fail to maintain their highly differentiated state.....	68
Figure 6. <i>Hif2α</i> negatively regulates <i>Ap2β</i> activity through inhibition of DNA binding.....	71

CHAPTER ONE

INTRODUCTION

The Heart

The heart is the first organ to form and its function during embryogenesis is required for complete development of all mammalian species. This is evidenced by the large number of targeted gene deletions in mice that result in embryonic lethality due to inappropriate organogenesis of the heart in the absence of those gene products (reviewed in Conway et al., 2003). Heart precursor cells form very early in the embryo, arising as a crescent-shaped mass of cells that fuse at the midline to form the linear heart tube. Up to this point in development, the embryo is small and only a few cell layers thick, so diffusion is sufficient to provide nutrients, exchange gases and remove cellular waste. During the eighth day of gestation (E8.0) in the mouse, when the embryo begins to grow exponentially, the linear heart tube starts to contract, pumping blood through the developing vasculature to provide the



necessary exchange of nutrients and gases for all of the cells of the growing body. Around E8.5, the heart starts to loop to the right and each of the four chambers begin to develop, expressing their own unique markers and undergoing various processes of invasion, differentiation, proliferation and apoptosis (Fig. 1).

The Outflow Tract

Alignment of the heart with the great vessels is essential to provide adequate blood flow to all of the organs. By E11.5, the outflow tract of the heart has come to sit above the developing left and right ventricular chambers, allowing blood exiting both of the ventricles to mix and enter the circulation. Shortly afterwards, the outflow tract begins to septate and rotate so that each half ultimately becomes contiguous with a single ventricle and one of the great vessels. Through this process of septation and rotation, the aorta and pulmonary artery become aligned with their appropriate ventricular chamber, the left and right ventricle, respectively. Were

it not for the fetal shunts, the ductus arteriosus and the foramen ovale, this would effectively separate the pulmonary and systemic

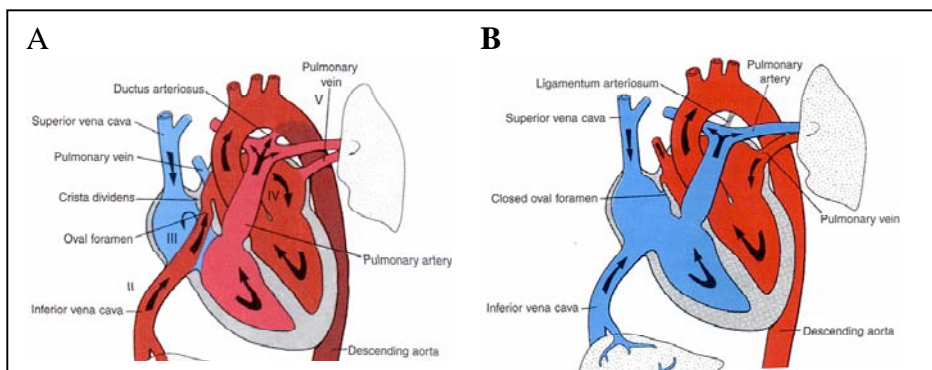
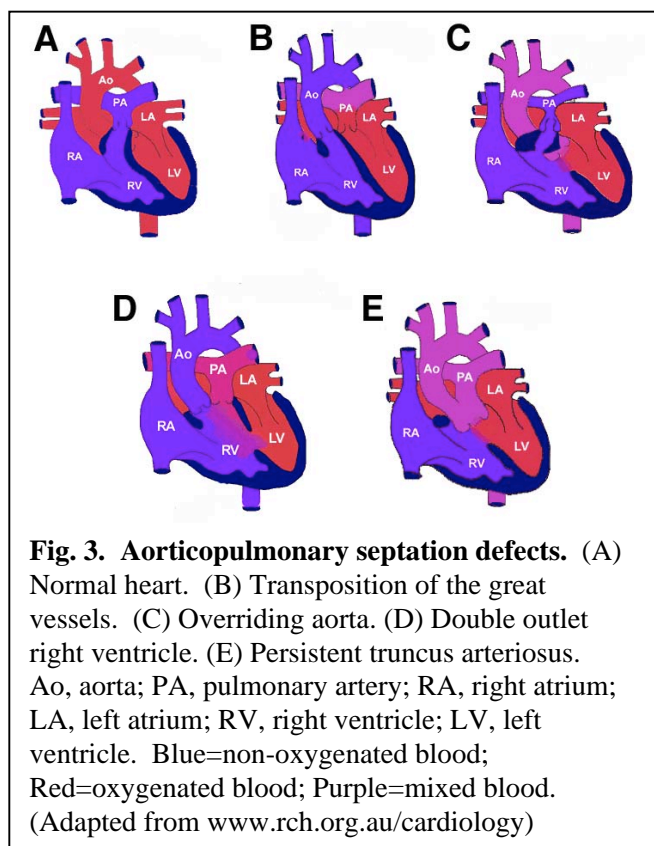


Fig. 2. Transition from fetal to neonatal circulation in mammals. Shunting through the ductus arteriosus and foramen ovale allows blood to bypass the lungs and maintains communication between the pulmonary and systemic circulations during gestation (A). At birth, both structures close, separating the two circulations and allowing blood to travel to the lungs for oxygenation (B). (Adapted from Langman & Sadler, 2000)

circulations (Fig. 2.). However, shunting of blood through these structures allows for communication between the two circulatory pathways until the time of parturition when the foramen ovale and ductus arteriosus begin to close.

In some cases, the aorta and pulmonary artery do not become aligned with the correct ventricular chamber and this results in aorticopulmonary septation defects, namely, transposition of the great vessels, overriding aorta, or double-outlet right ventricle (Warkany,



1971; Moss et al., 1977; Kieth et al., 1977). In other cases, septation of the outflow tract does not occur at all giving rise to what is called persistent truncus arteriosus (Fig. 3). While none of these conditions affect fetal survival, they are detrimental to the neonate who relies on separated pulmonary and systemic circulations for extrauterine life. Perturbations of hemodynamic flow arising from aorticopulmonary septation defects can also adversely

affect growth and expansion of the ventricular chambers. This often results in insufficient chamber volume and decreased contractile force of one or both of the ventricles which is inadequate to supply blood to the entire body and, therefore, is incompatible with separate pulmonary and systemic circulations. In the case of particular outflow tract defects or

ventricular malformations, maintenance of fetal circulation is required postnatally to provide blood to all of the body. This can be achieved temporarily through pharmacological means, but treatment is often accompanied by undesirable side effects.

Neural Crest Cells and the Great Vessels

Septation of the outflow tract relies on the contribution of specialized cells known as the neural crest. In addition, specific segments of the great vessels arise directly from the neural crest-derived pharyngeal

arch arteries. During early development, as the linear heart tube first forms at the midline, neural crest cells, which develop along the dorsal aspect of the neural folds, begin to migrate ventrally to populate the pharyngeal arch. These neural crest cells make up much of the pharyngeal arch mesenchyme, giving rise to smooth muscle cells of the pharyngeal arch arteries. After the heart has looped and as the individual

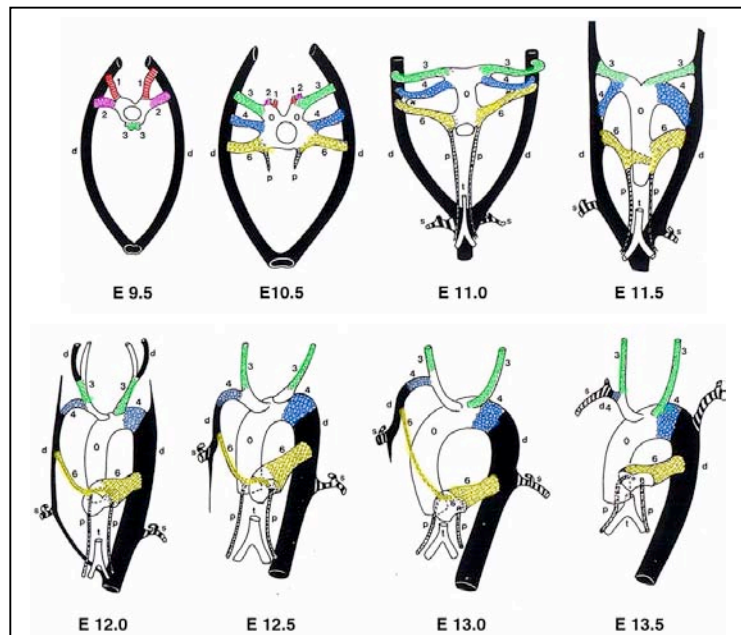


Fig. 4. Progression of mammalian pharyngeal arch artery development. The pharyngeal arch arteries (1-6) arise as bilaterally paired vessels extending from the aortic sac to the dorsal aorta. By E11.5, they begin an asymmetric remodeling program to give rise to specific segments of the great vessels. d, dorsal aorta; o, aorta; p, pulmonary artery; s, subclavian artery; t, trachea (Adapted from Kaufman, 1992).

chambers of the heart further differentiate and grow, the pharyngeal arch arteries remodel into the left-sided aortic arch present in all mammals.

The pharyngeal arch arteries remodel in an asymmetric fashion, differentially regressing or expanding depending on which side of the midline they arise from, with the left-sided arch arteries predominantly persisting (Fig. 4). The first and second arch arteries disappear entirely before asymmetry is observed, while the fifth never fully form. The remaining left third, fourth, and sixth arch arteries remodel to become the proximal carotid, the arch of the aorta, and the ductus arteriosus, respectively. Ablation of premigratory neural crest cells in avian embryos results in abnormal development of each of these structures (Bockman et al., 1987) as well as the outflow tract itself, which receives neural crest cells from the mesenchyme of the third, fourth, and sixth pharyngeal arches (Kirby et al., 1985; Nishibatake et al., 1987).

Another lineage contributed from the pharyngeal region is the anterior or secondary heart field (Mjaatvedt et al., 2001; Waldo et al., 2001; Kelly et al., 2001). Cells of the anterior heart field arise dorsal and anterior to the heart tube and later migrate through the pharyngeal mesoderm into the outflow tract and part of the right ventricles where they differentiate into mesocardium and endocardium (Liu et al., 2002). Signals from the anterior heart field are required for neural crest cell development and loss or inappropriate development of the anterior heart field adversely affects development of neural crest-derived structures in a non cell-autonomous fashion (Liu et al., 2002; Hu et al., 2004; Xu et al., 2004).

Transcriptional Regulation of Neural Crest Development

Inappropriate development of the neural crest in humans results in several different types of birth defects affecting the heart, outflow tract, and face. While cardiac defects occur in about 1% of all live births (Hoffman, 1995), for parents of a child born with a congenital heart defect, the chance of a cardiac defect in their subsequent children increases to 2-6% (Hoffman, 1990) suggesting that congenital heart defects can be attributed, in part, to heritable genetic polymorphisms that present as disease under particular genetic backgrounds or environmental conditions.

Many transcription factors and signaling molecules are known to be important for development of the neural crest-derived outflow tract and great vessels. Among these are endothelin-1, a small signaling peptide, and its G protein-coupled receptor, endothelin-A. Disruption of the endothelin signaling cascade during development of the rat or mouse has been demonstrated to adversely affect formation of neural crest cell-derived structures throughout the body (Kurihara et al., 1994; Clouthier et al., 1998; Yanagisawa et al., 1998; Taniguchi et al., 2003). Similarly, interfering with retinoic acid signaling pathways through ablation of combinations of retinoic acid receptors (Mendelsohn et al., 1994) or metabolizing enzymes (Niederreither et al., 2000), as well as vitamin A over-availability or deficiency (Warkany et al., 1948; Wilson et al., 1953), disrupts development of the neural crest-derived outflow tract, aortic arch, and head structures in addition to other organs and tissues.

One well-studied syndrome affecting development of the neural crest arises as a result of heterozygous chromosomal deletions of the 22q11 region. This condition, known as DiGeorge syndrome, velocardiofacial syndrome, or conotruncal anomaly face syndrome, has

been largely attributed to decreased dosage of a transcription factor, *Tbx1*, whose coding region is commonly deleted in affected individuals. (reviewed in Yamagishi and Srivastava, 2003; Baldini, 2004). *Tbx1* is expressed in the secondary heart field where it regulates Fgf signals controlling neural crest development (Hu et al., 2004; Xu et al., 2004). However, rare patients with DiGeorge syndrome have presented with deletions not encompassing the *Tbx1* coding region suggesting that other genes or regulatory elements may contribute to the etiology of this disease.

Although many genes are known to be important for global neural crest development (reviewed in Meulemans and Bronner-Fraser, 2004), transcriptional control of particular segments of the cardiac neural crest and regulation of distinct neural crest-derived structures such as the arch of the aorta or the ductus arteriosus are less understood. In humans, isolated cases of patent ductus arteriosus or interrupted aortic arch are observed clinically suggesting that development of these neural crest-derived structures is independently controlled, leading to the hypothesis that uniquely expressed transcription factors specify these individual vessels. While mouse knockouts have identified *Mfh1* as a likely determinant of the aortic arch (Winnier et al., 1999), more recently, human genetics studies have identified *TFAP2 β* as a gene that controls development of the ductus arteriosus (Satoda et al., 2000; Zhao et al., 2001). However, the mechanisms for developmental control by these transcription factors, including interacting protein partners and direct transcriptional targets within the tissue of interest, remain uncharacterized.

References

- Baldini A. 2004. DiGeorge syndrome: an update. *Curr Opin Cardiol.* **19**:201-4.
- Bockman, D.E., M.E. Redmond, K. Waldo, H. Davis, and M.L. Kirby. 1987. Effect of neural crest ablation on development of the heart and arch arteries in the chick. *Am J Anat* **180**: 332-41.
- Clouthier, D.E., K. Hosoda, J.A. Richardson, S.C. Williams, H. Yanagisawa, T. Kuwaki, M. Kumada, R.E. Hammer, and M. Yanagisawa. 1998. Cranial and cardiac neural crest defects in endothelin-A receptor-deficient mice. *Development* **125**: 813-24.
- Conway, S.J., A. Kruzynska-Frejtag, P.L. Kneer, M. Machnicki, and S.V. Koushik. 2003. What cardiovascular defect does my prenatal mouse mutant have, and why? *Genesis* **35**: 1-21.
- Hoffman, J.I. 1990. Congenital heart disease: incidence and inheritance. *Pediatr Clin North Am* **37**: 25-43.
- Hoffman, J.I. 1995. Incidence of congenital heart disease: I. Postnatal incidence. *Pediatric Cardiology* **16**: 103-13.
- Hu, T., H. Yamagishi, J. Maeda, J. McAnally, C. Yamagishi, and D. Srivastava. 2004. Tbx1 regulates fibroblast growth factors in the anterior heart field through a reinforcing autoregulatory loop involving forkhead transcription factors. *Development* **131**: 5491-502.
- Kaufman, M.H. 1992. The Atlas of Mouse Development. Academic Press, San Diego, California: 131-133.
- Kelly, R.G., N.A. Brown, and M.E. Buckingham. 2001. The arterial pole of the mouse heart forms from Fgf10-expressing cells in pharyngeal mesoderm. *Dev Cell* **1**: 435-40.
- Kieth, J.D., Rowe, R.D. and Vlad, P. 1977. *Heart Disease in Infancy and Childhood*. Macmillan, New York, Ed. 3: 452-517 and 590-637.
- Kirby, M.L., K.L. Turnage, 3rd, and B.M. Hays. 1985. Characterization of conotruncal malformations following ablation of "cardiac" neural crest. *Anat Rec* **213**: 87-93.
- Kurihara, Y., H. Kurihara, H. Suzuki, T. Kodama, K. Maemura, R. Nagai, H. Oda, T. Kuwaki, W.H. Cao, and N. Kamada. 1994. Elevated blood pressure and craniofacial abnormalities in mice deficient in endothelin-1. *Nature* **368**: 703-10.
- Liu, C., W. Liu, J. Palie, M.F. Lu, N.A. Brown, and J.F. Martin. 2002. Pitx2c patterns

- anterior myocardium and aortic arch vessels and is required for local cell movement into atrioventricular cushions. *Development* **129**: 5081-91.
- Mjaatvedt, C.H., T. Nakaoka, R. Moreno-Rodriguez, R.A. Norris, M.J. Kern, C.A. Eisenberg, D. Turner, and R.R. Markwald. 2001. The outflow tract of the heart is recruited from a novel heart-forming field. *Dev Biol* **238**: 97-109.
- Mendelsohn, C., D. Lohnes, D. Decimo, T. Lufkin, M. LeMeur, P. Chambon, and M. Mark. 1994. Function of the retinoic acid receptors (RARs) during development (II). Multiple abnormalities at various stages of organogenesis in RAR double mutants. *Development* **120**: 2749-71.
- Mendelsohn, C., M. Mark, P. Dolle, A. Dierich, M.P. Gaub, A. Krust, C. Lampron, and P. Chambon. 1994. Retinoic acid receptor beta 2 (RAR beta 2) null mutant mice appear normal. *Dev Biol* **166**: 246-58.
- Meulemans, D. and M. Bronner-Fraser. 2004. Gene-regulatory interactions in neural crest evolution and development. *Dev Cell* **7**: 291-9.
- Moss, A.J., Adams, F.H., and Emmanouilides, G.C. 1977. *Heart Disease in Infants, Children, and Adolescents*. Williams and Wilkins, Baltimore, Ed. 2: 301-380.
- Niederreither, K., J. Vermot, B. Schuhbaur, P. Chambon, and P. Dolle. 2000. Retinoic acid synthesis and hindbrain patterning in the mouse embryo. *Development* **127**: 75-85.
- Nishibatake, M., M.L. Kirby, and L.H. Van Mierop. 1987. Pathogenesis of persistent truncus arteriosus and dextroposed aorta in the chick embryo after neural crest ablation. *Circulation* **75**: 255-64.
- Sadler, T.W. and Langman, Jan. 2000. *Langman's Medical Embryology*. Lippincott Williams & Wilkins, Ed. 8: 225-7.
- Satoda, M., F. Zhao, G.A. Diaz, J. Burn, J. Goodship, H.R. Davidson, M.E. Pierpont, and B.D. Gelb. 2000. Mutations in TFAP2B cause Char syndrome, a familial form of patent ductus arteriosus. *Nat Genet* **25**: 42-6.
- Srivastava, D. and E.N. Olson. 2000. A genetic blueprint for cardiac development. *Nature* **407**: 221-6.
- Taniguchi, T. and I. Muramatsu. 2003. Pharmacological knockout of endothelin ET(A) receptors. *Life Sci* **74**: 405-9.
- Waldo, K.L., D.H. Kumiski, K.T. Wallis, H.A. Stadt, M.R. Hutson, D.H. Platt, and M.L. Kirby. 2001. Conotruncal myocardium arises from a secondary heart field.

- Development* **128**: 3179-88.
- Warkany, J. 1971. *Congenital Malformations*. Year Book Medical Publishers, Chicago: 515-525.
- Warkany, J., Roth, C.B., and Wilson, J.G. 1948. Multiple congenital malformations : a consideration of etiologic factors. *Pediatrics* **1**: 462-471
- Wilson, J.G., C.B. Roth, and J. Warkany. 1953. An analysis of the syndrome of malformations induced by maternal vitamin A deficiency. Effects of restoration of vitamin A at various times during gestation. *Am J Anat* **92**: 189-217.
- Winnier, G.E., T. Kume, K. Deng, R. Rogers, J. Bundy, C. Raines, M.A. Walter, B.L. Hogan, and S.J. Conway. 1999. Roles for the winged helix transcription factors MF1 and MFH1 in cardiovascular development revealed by nonallelic noncomplementation of null alleles. *Dev Biol* **213**: 418-31.
- Xu, H., M. Morishima, J.N. Wylie, R.J. Schwartz, B.G. Bruneau, E.A. Lindsay, and A. Baldini. 2004. Tbx1 has a dual role in the morphogenesis of the cardiac outflow tract. *Development* **131**: 3217-27.
- Yamagishi H, and Srivastava D. 2003. Unraveling the genetic and developmental mysteries of 22q11 deletion syndrome. *Trends Mol Med*. **9**:383-9.
- Yanagisawa, H., M. Yanagisawa, R.P. Kapur, J.A. Richardson, S.C. Williams, D.E. Clouthier, D. de Wit, N. Emoto, and R.E. Hammer. 1998. Dual genetic pathways of endothelin-mediated intercellular signaling revealed by targeted disruption of endothelin converting enzyme-1 gene. *Development* **125**: 825-36.
- Zhao, F., C.G. Weismann, M. Satoda, M.E. Pierpont, E. Sweeney, E.M. Thompson, and B.D. Gelb. 2001. Novel TFAP2B mutations that cause Char syndrome provide a genotype-phenotype correlation. *Am J Hum Genet* **69**: 695-703.

CHAPTER TWO

A COMMON CIS-ACTING SEQUENCE IN THE DIGEORGE CRITICAL REGION REGULATES BI-DIRECTIONAL TRANSCRIPTION OF *UFD1L* AND *CDC45L*

Background

Deletions within the q11.2 region of chromosome 22 are associated with a variety of cardiac and craniofacial abnormalities that are characteristic of three clinical syndromes - DiGeorge syndrome (DGS), velocardiofacial syndrome (VCFS) and conotruncal anomaly face syndrome (CTAFS) (Emanuel et al., 1998). Based on their common phenotypic features and genetic etiology, these three clinical entities are referred to as the 22q11 deletion syndrome. Nearly 40 developmental defects are associated with this syndrome, the most common including malformations of the cardiac outflow tract and aortic arch, hypoplasia of the thymus and parathyroid glands, and the presence of a cleft palate. A common feature in the normal development of all these structures is a contribution by cranial neural crest cells that migrate through the pharyngeal arches. Neural crest ablation in chick embryos causes cardiac defects similar to those seen in the 22q11 deletion syndrome (Kirby and Waldo, 1990). These observations suggest that development of neural crest-derived tissues is affected by deletion of segments of 22q11.2, and that one or more factors responsible for normal neural crest development are encoded in this region.

A variety of overlapping deletions within the commonly deleted DiGeorge critical region (DGCR), typically measuring 2-3 Mb, have been reported in patients with the 22q11 deletion syndrome. Interestingly, the phenotype does not correlate with the size or region of the deletion. In addition, a number of non-overlapping deletions have been reported in patients clinically diagnosed with the syndrome (Carlson et al., 1997; Novelli et al., 2000) some of which are outside the DGCR. Furthermore, no single point mutation has been reported in patients who have the disease phenotype but do not have a 22q11 deletion.

Recent evidence in mice indicates that haploinsufficiency of *Tbx1*, a T-box family member that is expressed in the developing pharyngeal arches (Chapman et al., 1996) may be a major contributor to aortic arch defects in the 22q11 deletion phenotype. A subset of mice heterozygous for *Tbx1* display defects in aortic arch patterning that are reminiscent of defects seen in the 22q11 deletion syndrome (Jerome and Papaioannou, 2001; Merscher et al., 2001) although no other features of the syndrome are present. Furthermore, aortic arch defects seen in mouse chromosomal deletions syntenic to 22q11 can be rescued by a transgene carrying *Tbx1* (Merscher et al., 2001; Lindsay et al., 2001). The 22q11 deletion phenotype has, however, also been detected in patients with deletions that do not include *TBX1*. Additionally, no patients have been identified with point mutations of *TBX1*.

These observations suggest a complex molecular mechanism underlying the pathogenesis of the 22q11 deletion syndrome. There are two popular explanations that may account for the observed discrepancies. The DGCR may contain common regulatory regions, such as locus control regions, that affect gene expression over a long range (Novelli

et al., 2000; Dallapiccola et al., 1996). Such a region may affect expression of important distant genes even though they are not included in the deletion. Alternatively, the DGCR may contain multiple genes that function, either individually or in a combinatorial fashion, to regulate neural crest development (Lindsay et al., 2001; Lindsay and Baldini, 1998).

We had earlier described a patient, JF, who demonstrated many of the clinical features commonly associated with the 22q11 deletion syndrome (Yamagishi et al., 1999). JF did not have the typical 22q11 deletion, but rather had only a 20kb microdeletion that encompassed the first three exons of the gene encoding the ubiquitin fusion degradation protein, *UFDIL*, the first five exons of *CDC45L* and an 884 base pair intergenic region. During embryogenesis, *Ufdil* gene expression is enhanced in regions of the mouse embryo derived from the cranial neural crest. Furthermore, expression of *Ufdil* is downregulated in mice lacking dHAND, a basic helix-loop-helix transcription factor necessary for cranial neural crest development. Mice heterozygous for *Ufdil* do not, however, have any detectable anomalies (Lindsay et al., 1999). This fact, in conjunction with the observation that both genes were disrupted in the patient JF led us and others to speculate that deletion of *UFDIL* alone is not likely to be responsible for the phenotype of JF, and that combinatorial deletion of *UFDIL* and *CDC45L*, and/or the 884bp intergenic region may contribute to the phenotype (Yamagishi et al., 1999; Baldini, 1999; Srivastava and Yamagishi, 1999).

UFDIL and *CDC45L* are organized with their coding regions oriented in a head to head fashion and thus with their promoters presumably located in the 884bp intergenic sequence. This unusual genomic organization has been described previously for genes that are functionally related and co-regulated (Gaston and Fried, 1995; Guarguaglini et al., 1997;

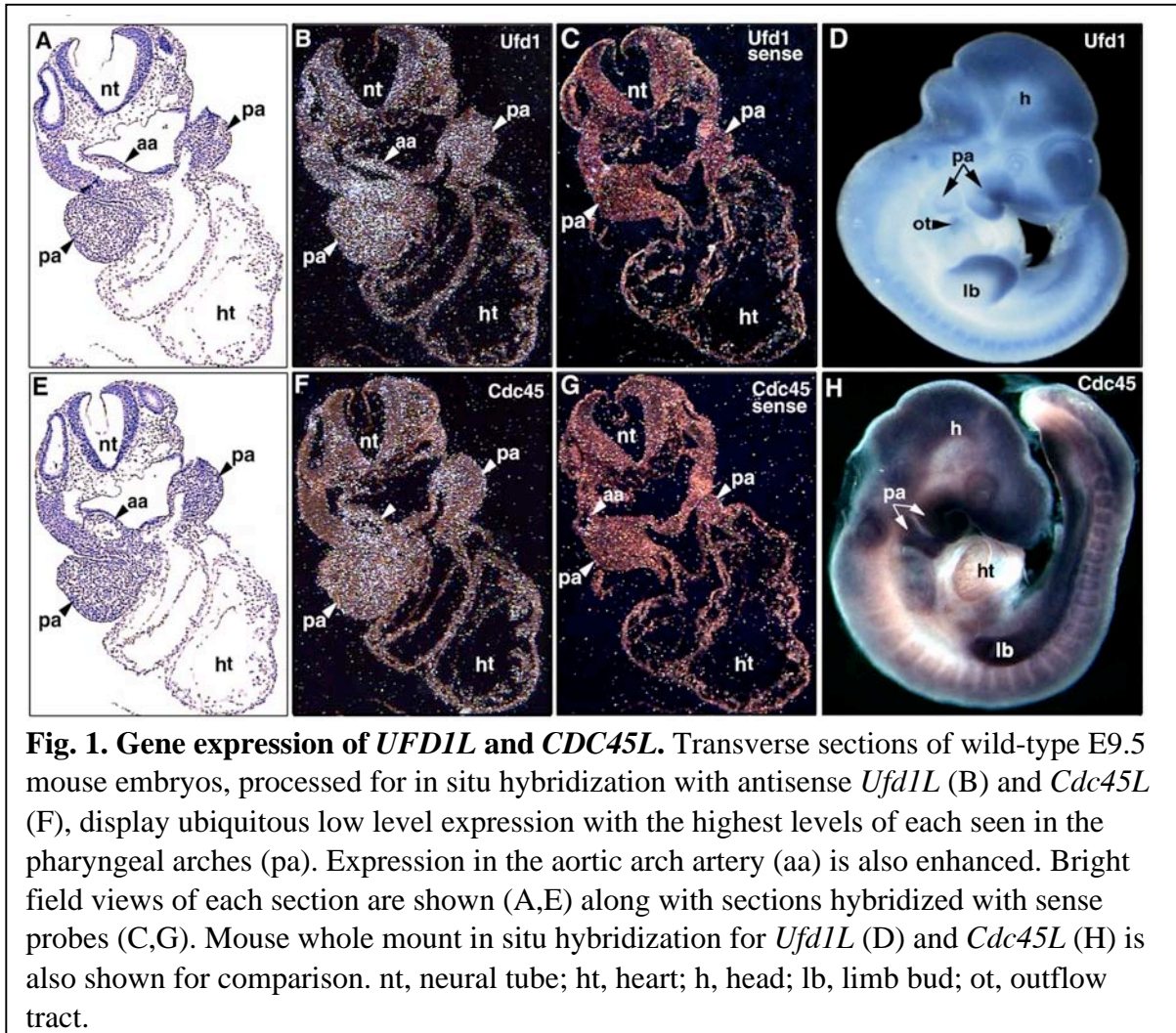
Schilling and Farnham, 1995). Here, we show that expression of *UFDIL* and *CDC45L* is enhanced in similar regions of the developing embryo. Furthermore, we demonstrate that the 884bp intergenic region contains the regulatory sequences necessary to recapitulate the pattern of endogenous *UFDIL* expression *in vivo*, and that it directs bi-directional transcriptional activity in a variety of cell lines, including neural crest cells. The critical sequences necessary for transcription in both the *UFDIL* as well as the *CDC45L* directions localize to a 404bp region upstream of the *UFDIL* gene, suggesting that the two genes may be partly co-regulated in some cell types. We speculate that the two genes may be related functionally, either directly or indirectly by responding to the same metabolic need and therefore may play a combinatorial role in neural crest development.

Results

Coexpression of UFDIL and CDC45L

Both *UFDIL* and *CDC45L* are expressed widely at low levels in the developing embryo, but there are specific regions where enhanced expression of the genes can be detected. In order to compare the expression patterns of these genes in the precursors of tissues affected in the 22q11 deletion syndrome, we performed section in situ hybridization experiments for the *Ufd1L* and *Cdc45L* mRNA on E9.5 mouse embryos. Hybridizations were performed on serial transverse sections at the level of the second pharyngeal arch and demonstrated a remarkably similar pattern of expression for the two genes (Fig.1). Both genes were expressed maximally in the neural crest-derived pharyngeal arch and aortic arch artery. Lower levels of expression were detected in other areas of the section, such as the

heart mesenchyme and in the cleft between the second and third pharyngeal arches. Similar results were observed at E10.5 (data not shown).



The UFD1L-CDC45L intergenic region is a conserved CpG island

Because *UFD1L* and *CDC45L* expression was enhanced in similar tissues during development, we analyzed the 884bp intergenic region separating the two genes for potential regulatory sequences. The sequence of the entire human *UFD1L-CDC45L* intergenic region

(accession no. AC 000087; human cosmid 83c5) and the corresponding mouse sequence (accession no. NT 002584) were obtained from Genbank. Alignment of the human and mouse sequences revealed a number of stretches of conserved residues throughout the region (Fig. 2A). The human sequence appeared to contain a region that fits the consensus for a TATA box in the direction of *UFDIL*. This sequence is not, however, conserved in the mouse intergenic region. TATA-less promoters have been frequently reported (Gaston and Fried, 1995; Burbelo et al., 1988; Gavalas et al., 1993; Ikeda et al., 2000; Zhang et al., 1998) and are usually driven by initiator elements (Smale, 1997). Transcription from such genes has also been found to initiate from multiple sites in either direction (Lavia et al., 1987). A number of conserved initiator consensus sites (26) were found in either orientation in the *UFDIL-CDC45L* intergenic region (Fig. 2A). Conserved potential binding sites for a number of transcription factors such as Sp1, Ets family proteins, CCAAT binding factors, p53 and Interferon Response Factor-1 were also observed at various places in the intergenic region (Fig. 2A), as determined by the TESS algorithm (Schug and Overton, 1997).

Analysis of the human sequence revealed a high G+C content. The G+C content of the entire 884 intergenic sequence was 55.2%, while the first and last 200bp within the region had a G+C content of 69.5% and 60.2% respectively (Fig. 2A). The average G+C content of bulk genomic DNA is 40% (Bird, 1986). This suggested to us the possibility that this region might be a CpG island. We therefore calculated both the observed frequency of CpG dinucleotides as well as the expected frequency assuming random base composition, and used the ratio of the two values as an indicator of the relative CpG content of a given DNA segment (Fig. 2B). This was performed for the entire 884bp intergenic region and a

number of contiguous 884bp segments of genomic DNA on either side of the region. The intergenic region had an observed/expected ratio of 0.82 while the ratio for bulk genomic DNA is 0.2–0.25 (Lavia et al., 1987). The ratio dropped steeply to one resembling bulk genomic DNA on either side of the intergenic region, indicating that the region is indeed a

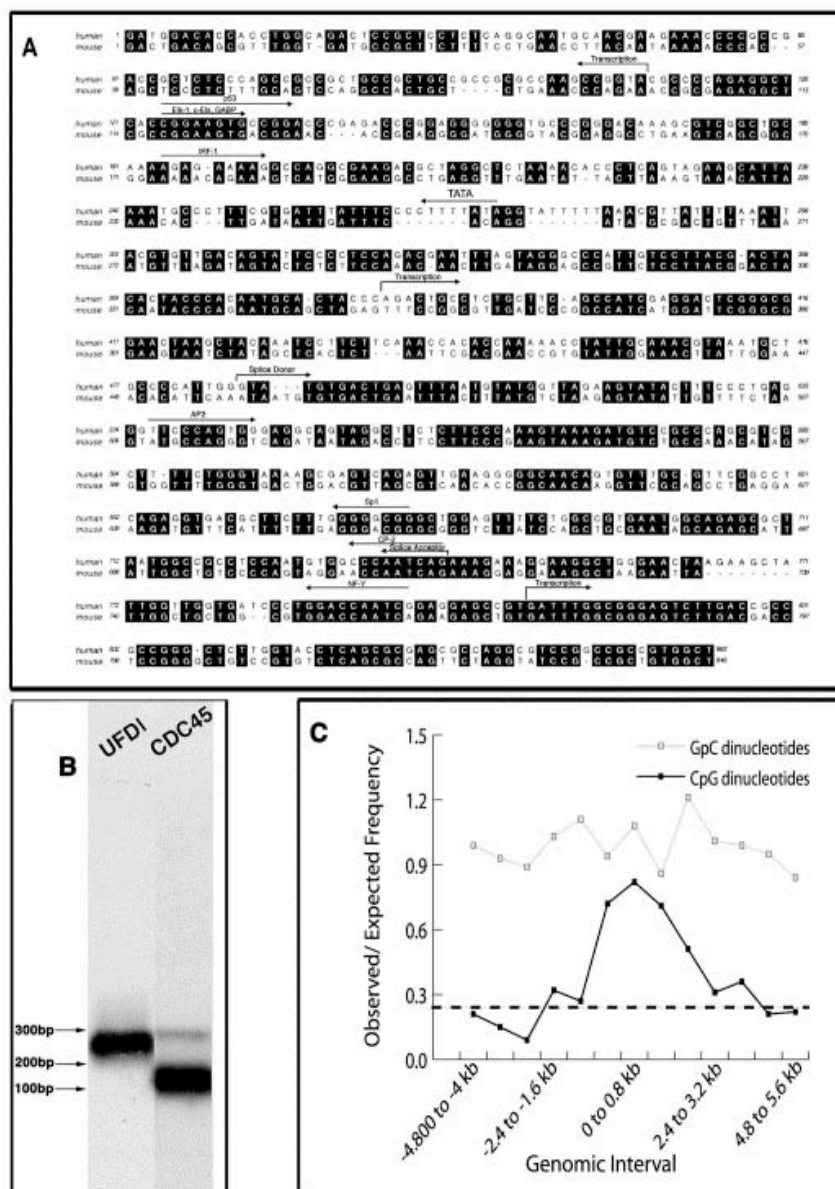


Fig. 2. Analysis of the *UFD1L*–*CDC45L* intergenic sequence.

(A) Alignment of the human and mouse intergenic sequences demonstrates stretches of conserved residues, shaded in black. Position 1 denotes the *UFD1L* end.

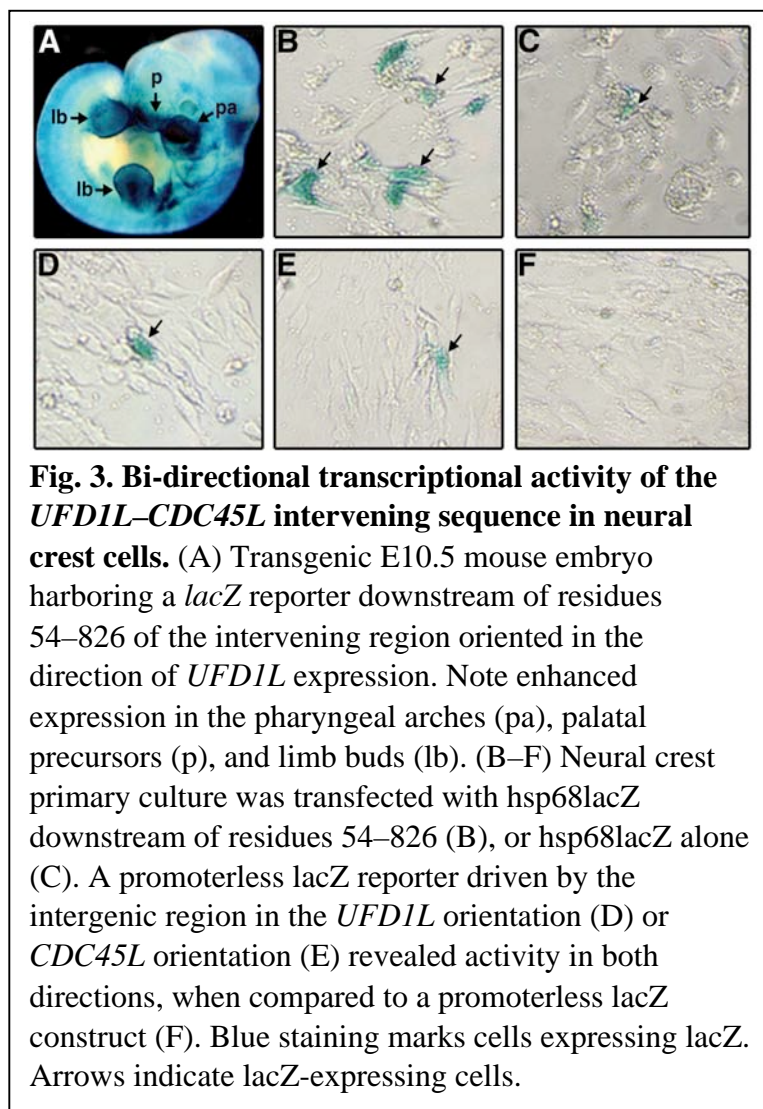
Transcription start sites, splice sites, and conserved transcription factor binding sites are indicated. (B) Southern analysis of the *UFD1L* and *CDC45L* 5'-RACE products was performed using sequences from the entire intervening region as probe. A broad band was detected for *UFD1L* corresponding multiple start sites with the longest at position 108, as revealed by sequencing of the product shown. A major broad band was also detected for *CDC45L* with the longest genomic DNA. This ratio was plotted as a function of

genomic intervals including the intervening region and 884 bp intervals on either side of it. The 0–0.8 kb segment represents the intergenic region. Points on the x-axis indicate consecutive 884 bp segments on either side of the intergenic region. Negative numbers indicate distances from the *UFD1L* end and positive numbers indicate distances from the *CDC45L* end of the intergenic region. A similar analysis for the frequency of GpC dinucleotides serves as a negative control. The dotted line represents the frequency of CpG dinucleotides in bulk genomic DNA.

CpG island. The frequency of GpC dinucleotides serves as a control and remained near an observed/expected ratio of 1 throughout the sequence analyzed.

The UFD1L-CDC45L intergenic region contains regulatory elements sufficient for bi-directional transcription

Based on the above-mentioned observations and previously available information



about *UFD1L* and *CDC45L* mRNA sequence, we amplified the region from nucleotides 54–826 of the 884 bp intervening region between the coding sequences of the two genes and tested this sequence in a number of reporter gene assays. In order to test whether the *UFD1L-CDC45L* intervening region contained regulatory elements in addition to a core promoter, we generated transgenic mice

carrying the *UFD1L-CDC45L* intergenic region upstream of a -galactosidase reporter with a

minimal promoter (*hsp68-lacZ*), the reporter being in the direction of *UFDIL* transcription.

Whole mount X-gal staining of E10.5 F0 transgenic embryos revealed a pattern of expression similar to the expression of the *Ufd1L* and *Cdc45L* genes in 80% of embryos (Fig. 3A).

Expression was detected maximally in the pharyngeal arches and palatal precursors, which are both structures containing neural crest-derived cells. Expression was also detected in the limb bud, the otocyst, and throughout the embryo at lower levels. In this assay, the presence of a heterologous promoter would result in a summation of enhancer activity in both directions.

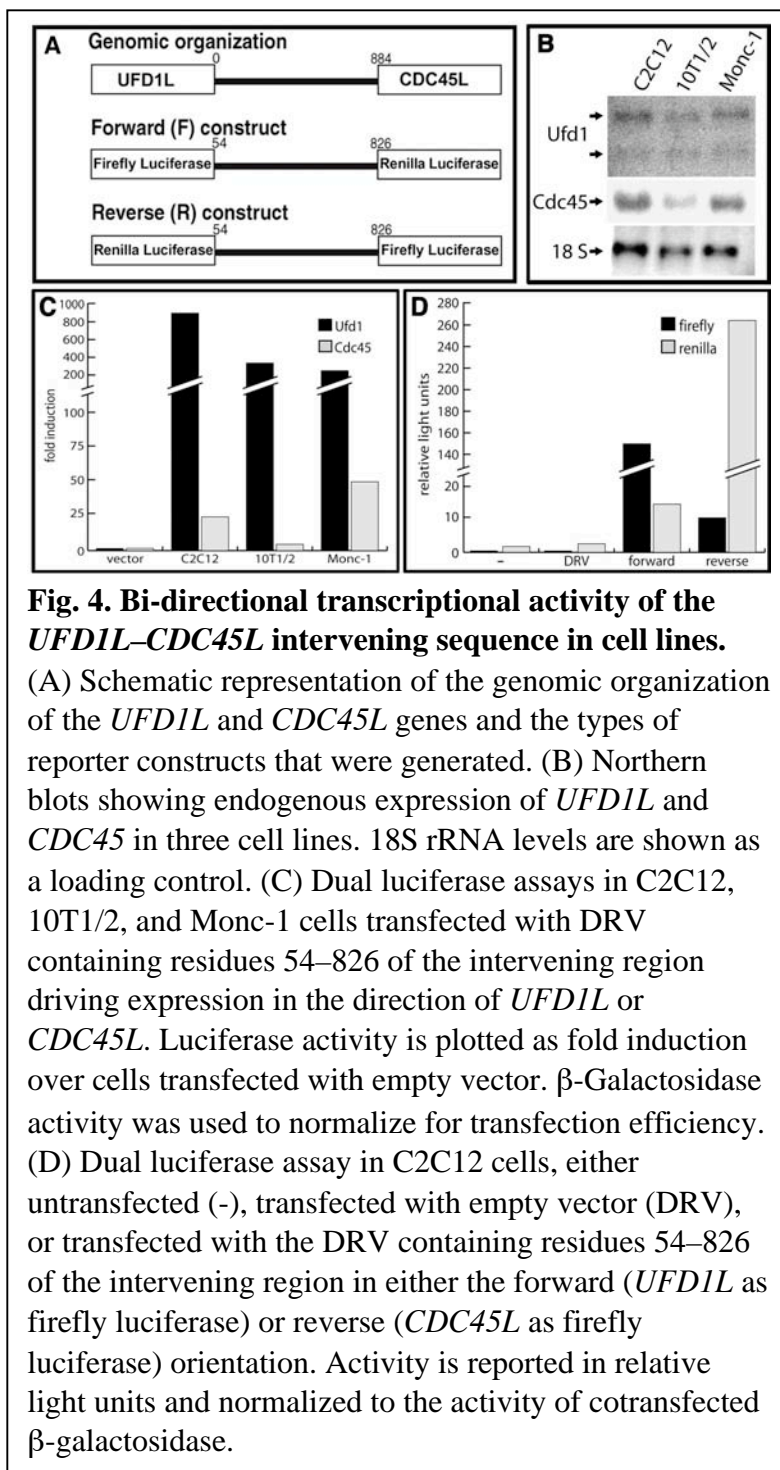
As the *UFDIL–CDC45L* intervening region contained enhancer activity in mouse embryos but was less than 1 kb, further dissection and analysis of this region was performed in primary or immortalized cell cultures. Examination of the activity of this region in neural crest cell lineages was performed by transfecting chick primary neural crest cells with the same reporter construct. The total number of lacZ positive cells that migrated off the neural folds was counted in wells transfected with the above-mentioned construct and wells transfected with the empty *hsp68-lacZ* construct. An average of three independent experiments demonstrated a consistently higher proportion of positive cells in wells transfected with the construct carrying the intergenic region, the ratio being approximately 2.5:1 (Fig. 3B,C). Transfection of a promoterless *lacZ* gene did not produce any lacZ positive cells (Fig. 3F). In contrast, transfection of constructs carrying the intergenic region cloned in the ‘forward’ and ‘reverse’ orientations into a promoterless vector produced 15 and 12

positive cells per well, respectively (Fig. 3D,E). Finally, one well transfected with the

intergenic region upstream of *hsp68-lacZ* was double stained for HNK, which is a marker of migrating neural crest cells.

Out of 144 lacZ positive cells, 93 (64.5%) were also positive for HNK, indicating that the reporter is indeed active in migrating neural crest cells.

We next sought to determine whether the entire intergenic region was sufficient to direct bi-directional transcriptional activation in a variety of cell lines. This was done by subcloning a fragment including residues 54-826 of the intergenic region into a dual reporter vector in the 'forward (F)' orientation (Fig.



4A; Materials & Methods). This vector contains a multiple cloning site flanked by a firefly luciferase reporter gene in one orientation and a renilla luciferase reporter gene in the other orientation. To identify cell lines that normally express *UFD1L* and *CDC45L* and would thus express the appropriate trans-acting factors necessary for the expression of these genes, Northern blot analysis was performed on RNA derived from multiple cell lines (Fig. 4B). *UFD1L* and *CDC45L* mRNA transcripts were identified, at varying levels, in a mouse skeletal muscle cell line (C2C12 cells; ATCC no.CRL-1772), a mouse fibroblast cell line (C3H/10T1/2 cells; ATCC no. CCL-226) and a mouse neural crest cell line (Monc-1 cells; (Rao and Anderson, 1997)). The dual reporter constructs were tested in a transient transfection assay in each of the cell lines described above, enabling simultaneous detection of transcriptional activity in the *UFD1L* and/or the *CDC45L* direction. In all three cell lines, transcriptional activity was detected in both directions. Consistently, the fold activation was higher in the *UFD1L* direction (~ 600 fold in C2C12, ~350 fold in 10T1/2 and ~270 fold in Monc-1 cells) compared to the *CDC45L* direction (~ 20 fold in C2C12, 5 fold in 10T1/2 and 45 fold in Monc-1 cells) (Fig.4C).

In order to be certain that the observed difference in transcriptional activity did not reflect a difference in the activity or stability of the two different luciferases, or a difference in transcription due to vector construction, we reversed the orientation of the fragment in the dual reporter vector in order to generate a 'reverse (R)' construct (see Fig. 4A and Materials & Methods). We tested this construct in a similar transient transfection assay in C2C12 cells. The activity of the renilla luciferase (*UFD1L* direction) was now found to be much higher than that of the firefly luciferase (*CDC45L* direction), indicating directional specificity of the

UFD1L-CDC45L regulatory regions (Fig. 4D). In summary, the entire *UFD1L-CDC45L* intergenic region was sufficient to drive transcription of both genes and this activity was an order of magnitude higher in the direction of *UFD1L* transcription.

A 404bp regulatory region is necessary and sufficient to direct bi-directional transcriptional activation of UFD1L and CDC45L

In order to further dissect the *UFD1L-CDC45L* bi-directional transcriptional activity, we generated progressive deletions of approximately 200bp in the 826bp fragment starting from either direction. Each of these shorter fragments was then subcloned into the dual reporter vector, in both orientations, and tested for transcriptional activity by transient transfection into C2C12 cells. The *UFD1L* end of the intergenic region was designated as position 0 and the *CDC45L* end as position 884. The two different orientations were designated as ‘forward (F)’ or ‘reverse(R)’ as depicted in Fig.4A.

The activities of the various fragments were first compared by measuring, as activity of firefly luciferase, the fold induction of transcription over a promoterless fragment (Fig. 5A). In a series of deletions starting from the *CDC45L* end of the fragment, keeping the *UFD1L* end constant, we found that activity in the *UFD1L* direction was not affected more than twofold by deletion of approximately 400bp and was over 800-fold greater than control (Fig. 5A). Further deletion of 200bp decreased the transcriptional activity by an order of magnitude. Some residual transcriptional activity was maintained (30-fold over control). A fragment containing residues between 264-458bp from the *UFD1L* end of the intergenic region similarly activated at only a 20-fold higher level compared to control.

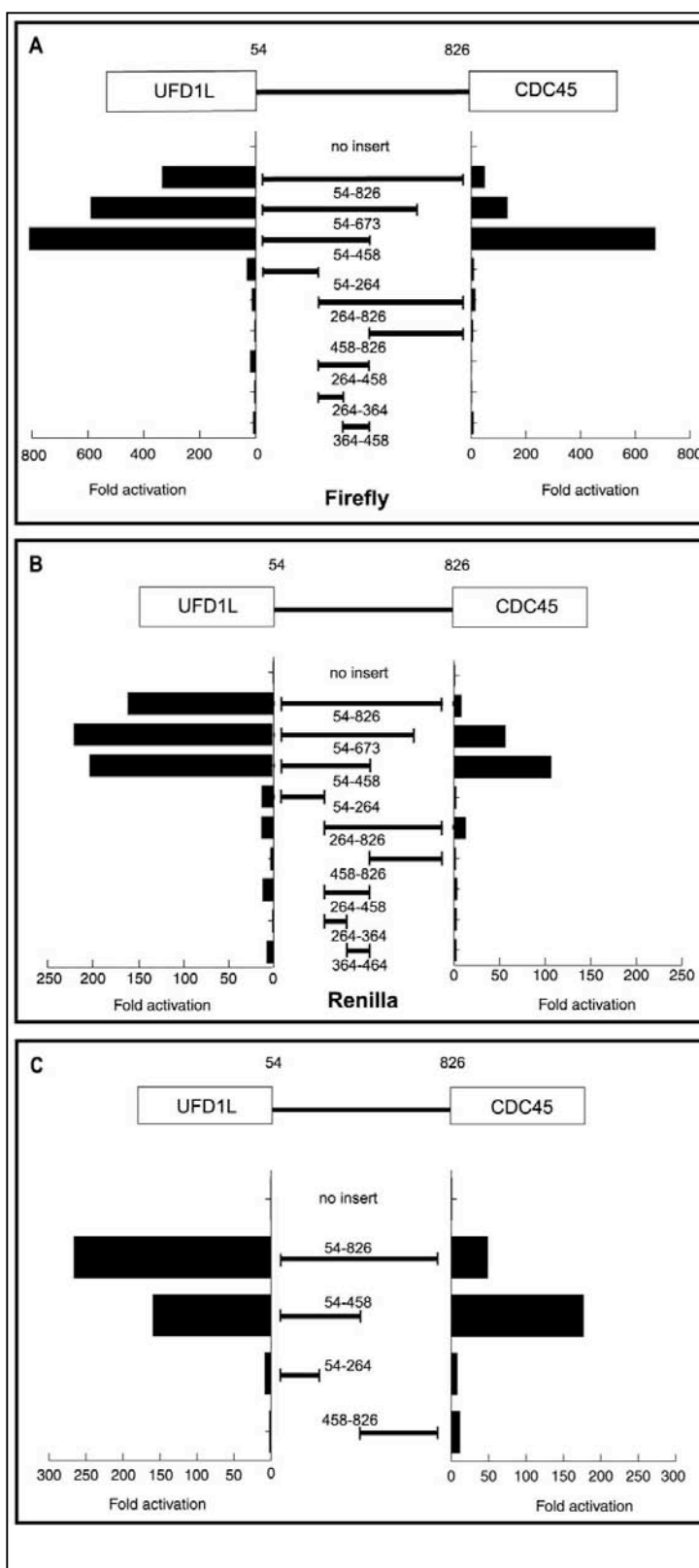


Fig. 5. Deletion analysis of the *UFD1L*–*CDC45L* intervening region.

Fragments of the intervening region were cloned into the DRV in both orientations and tested for bi-directional activity in C2C12 cells.

Transcriptional activity in both the *UFD1L* as well as the *CDC45L* directions is represented either by firefly luciferase activity (A) or renilla luciferase activity (B). Fold induction of

transcription over basal activity of a promoterless construct is plotted on the value axis. β -Galactosidase activity was used to normalize for transfection efficiency. Data is an average of experiments done in duplicate. Black lines between the graphs indicate the particular nucleotides used in the construct.

(C) Selected fragments of the intergenic region were cloned into the DRV in the ‘reverse’ orientation (Materials and methods). Transcriptional activity in the *UFD1L* direction is measured as renilla luciferase activity while activity in the *CDC45L* direction is measured as firefly luciferase activity. Fold induction of transcription over basal activity of a promoterless construct is plotted on the value axis. β -Galactosidase activity was used to normalize for transfection efficiency. Black lines between the graphs indicate the particular nucleotides used in the construct.

Unexpectedly, deletion of 200bp from the *CDC45L* end resulted in an increase in activity in the *CDC45L* direction from 50-fold to 130-fold. Deletion of 200bp more resulted in a further increase in transcriptional activity up to 670-fold. The activity of this 404bp fragment in the *CDC45L* direction was an order of magnitude higher than the activity of the full length intergenic region. Also, the fold increase of luciferase activity for the 54-458bp fragment was approximately equivalent in either direction (~800 and 670 fold over control in the *UFDIL* and *CDC45L* directions, respectively). Deletion of the next 200bp decreased activity to approximately 10-fold, which is below that seen with the full length fragment. The 264-458bp fragment did not, however, reproduce the increase seen with the 54-458bp fragment, nor did fragments containing nucleotides 264-364 or 364-458.

In a complementary series of deletions from the *UFDIL* end of the intergenic region, activity in the *UFDIL* direction was diminished by an order of magnitude after deletion of the first 200bp. Deletion of the next 200bp did not cause a significant change. In the *CDC45L* direction, transcriptional activity after deletion of the first 200bp was lower than that observed with the full length fragment (~ 50 and 15-fold for the 826 and 673bp constructs respectively). The activity was only 6 fold greater than control after deletion of a further 200bp, which is a level of activity significantly below that seen with the full length fragment. All the above findings regarding relative activities of all fragments were reproduced when the activity was measured as renilla luciferase (Fig. 5B). Thus, a 404bp fragment of the intergenic region near the *UFDIL* end is capable of driving maximal transcription in both directions and further deletion of this fragment causes a loss of this ability.

Since a neural crest cell defect is thought to be the major contributor to the pathogenesis of the 22q11 deletion syndrome, we tested the activity of the deletion constructs indicated in Fig. 5C by transient transfection into Monc-1 cells. The results confirmed, in neural crest cells, the major conclusions drawn from the above experiments. Transcription in the *UFDIL* direction was unaffected by deletion of approximately 400bp from the *CDC45L* end and diminished by further deletions. A deletion from the *UFDIL* end abolished transcriptional activity in the *UFDIL* direction. Transcriptional activity in the *CDC45L* direction increased after deletion of 400bp from the *CDC45L* end but was abolished after deletion of a further 200bp. The activity was diminished, compared to the full length fragment, after deletion of 400bp from the *UFDIL* end. Thus, even in neural crest cells, the first 458bp of the intergenic region is capable of driving maximal transcriptional activity in both directions and further deletion of this fragment disrupts the necessary cis elements.

Discussion

Bidirectional transcriptional activity of the UFDIL-CDC45L intervening region

We have described here an analysis of the 884bp intergenic region between the *UFDIL* and *CDC45L* genes that is located on chromosome 22 in the DGCR. The entire 884bp region has the ability to direct transcription simultaneously in both directions. This ability was present in a variety of cell lines, including a neural crest cell line. Deletion analyses helped us narrow the region necessary for maximal transcriptional activity to a 404bp fragment closest to *UFDIL*. Further deletions of this fragment caused a loss of activity. This may be attributable to a synergy between regulatory elements located in the

54-264 and 264-458bp fragments. Alternatively, it may be caused by separation of initiator sequences from their regulatory elements.

In the direction of the *CDC45L* gene, the 54-458bp fragment has an activity which is an order of magnitude higher than the full length fragment, suggesting the presence of a repressive element in the 458-826bp fragment. This conclusion is further supported by the fact that the 264-826bp fragment has an activity similar to the full length fragment and that the 458-826bp fragment has activity lower than that of the full length fragment. An alternative explanation for this finding is that the initiator element is present in the 54-458bp fragment and that the elevated activity is a result of a shortened untranslated region in the luciferase mRNA. Nevertheless, it is possible to conclude that all the elements necessary for bi-directional transcriptional activation reside in this 54-458bp fragment of the intergenic region. It is also worth noting that the fold activation shown by the 54-458bp fragment is similar in both directions. This is evident when activity in either direction is measured using either firefly luciferase (Fig.5A), or renilla luciferase (Fig. 5B). We consider this finding to be indirect evidence that the two genes are co-regulated, possibly by the sharing of bi-directional regulatory elements. Such bi-directional elements responsive to factors such as Ets (Gaston and Fried, 1995; Ikeda et al., 2000), Sp1, and E2F (Guarguaglini et al., 1997) have been previously described in the context of similarly organized promoters.

The UFD1L-CDC45L intergenic region is a CpG island

CpG islands are commonly associated with the 5' end of both housekeeping as well as some tissue specific genes (Bird, 1986). It has been proposed that CpG islands frequently

mark coding sequences that are organized head-to-head and contain bi-directional promoter activity (Lavia et al., 1987). This hypothesis has been borne out by a large number of studies. A number of genes that have been found to be organized in this manner encode proteins that are members of the same structural complex, including a) histone 2A and histone 2B (Osley et al., 1986) b) α_1 and α_2 subunits of collagen 4 (Burbelo et al., 1988) and c) α and β subunits of the human mitochondrial trifunctional protein involved in fatty acid metabolism (Orii et al., 1999). In other cases, genes encoding enzymes that participate in sequential steps of an enzymatic pathway have been found to be organized in this fashion, such as genes in the purine biosynthetic pathway (Gavalas et al., 1993). Yet other genes have been found to respond to a common cellular need, such as growth induction (Guarguaglini et al., 1997; Schilling and Farnham, 1995) and are thus co-expressed. These genes either share a common bi-directional start site and thus have a common promoter in the true sense (Lavia et al., 1987) or have closely spaced transcription initiation sites and share regulatory elements (Gaston and Fried, 1995; Ikeda et al., 2000; Orii et al., 1999). We cannot presently distinguish between these possibilities in the case of *UFDIL* and *CDC45L*.

Relation with the 22q11 deletion phenotype

Our study, together with previous studies (Yamagishi et al., 1999; Novelli et al., 1998; Shaikh et al., 1999) demonstrated that *UFDIL* and *CDC45L* are expressed widely throughout the embryo and are enhanced in specific regions. In particular, we have examined their expression in the pharyngeal arches because of the relevance to the 22q11 deletion phenotype and found that transcripts of both genes were similarly enhanced in this

region. The 884bp region between *UFD1L* and *CDC45L*, which can direct transcription in both directions *in vitro* was capable of directing expression of a reporter gene *in vivo* in a pattern that reproduces expression of endogenous *UFD1L* and *CDC45L*. Furthermore, the intergenic region was sufficient to drive expression of a reporter gene in primary neural crest cells. This finding points to the possibility that the two genes may be coregulated during neural crest development by cis elements within the intergenic region.

Recent evidence indicates that *Tbx1*, a member of the T-box family that is expressed in the developing pharyngeal arches (Chapman et al., 1996), may be a major contributor to some features of the 22q11 deletion phenotype. A subset of mice heterozygous for *Tbx1* display defects in aortic arch patterning that are reminiscent of the defects seen in the 22q11 deletion syndrome (Jerome and Papaioannou, 2001; Merscher et al., 2001). Furthermore, aortic arch defects seen in the *Df1/+* or *Lgdel/+* mice (Merscher et al., 2001; Lindsay et al., 1999), which are heterozygous for large chromosomal deletions encompassing *Tbx1* and surrounding genes, can be rescued by a transgene carrying *Tbx1* (Merscher et al., 2001; Lindsay et al., 2001). These results provide strong support for a role of *TBX1* in the production of aortic arch defects in the 22q11 deletion syndrome. They do not, however, explain the occurrence of the phenotype in patients bearing deletions that exclude *Tbx1*.

In this regard, Guris et al (Guris et al., 2001) have reported the occurrence of a phenotype resembling that of the 22q11 deletion in mice homozygous for a null mutation in *Crkl*, an SH2 and SH3 domain containing adapter protein that is enriched in neural crest derived tissues. This finding supports the hypothesis that other genes within the DGCR, which are involved in neural crest development, may also contribute to the 22q11 deletion

phenotype. Our results regarding the presence of bi-directional transcriptional activity, a characteristic genomic organization and similar embryonic expression patterns suggest that *UFD1L* and *CDC45L* might be, at least in part, co-regulated and therefore might be functionally related, either directly in a molecular pathway or indirectly by responding to the same cellular needs. Clarification of these possibilities awaits elucidation of the precise cellular functions of the UFD1L and CDC45L proteins during development. Current studies implicate *UFD1L* in post-ubiquitination processing of proteins (Hoppe et al., 2000; Johnson et al., 1995; Meyer et al., 2000). *CDC45L* orthologs have been shown to be essential for the initiation of DNA replication in yeast and metazoans (Loebel et al., 2000; Saha et al., 1998; Zou et al., 1998). Although these functions are seemingly unrelated, the fact that a number of cell cycle regulators are regulated by ubiquitin-dependent proteolysis may be a clue to a possible functional relationship between these proteins (Koepp et al., 1999; Tyers and Jorgenson, 2000). Elucidation of the biochemical pathways in which *UFD1L* and *CDC45L* function may thus help determine their contribution to neural crest development and to the 22q11 deletion phenotype.

Materials and Methods

Radioactive section in situ hybridization

A 415bp *Cdc45L* mouse cDNA fragment was amplified by reverse-transcriptase-polymerase chain reaction (RT-PCR) using whole mouse embryo RNA (upper, 5'-ACCACTTCATCCAGGCTCTC-3'; lower, 5'-GGTGCTTTCTGCTGCCTTCT-3') under the following conditions: 94°C for 5 min; 94°C for 30s, 60°C for 30s, 72°C for 30s (35

cycles); 72°C for 7 min. A plasmid containing the 700bp open reading frame of mouse *Ufd1L* cDNA was utilized. ³⁵S-labeled antisense riboprobes for *Cdc45L* and *Ufd1L* were synthesized with T7 or SP6 RNA polymerase, respectively (MAXIScript; Ambion Inc.). Radioactive section in situ hybridization was performed on paraffin-embedded serial sections of E9.5 and E10.5 mouse embryos.

Cloning of the intergenic human genomic DNA between UFD1L and CDC45L

To obtain human genomic DNA containing *UFD1L* and *CDC45L*, a 388bp fragment was amplified from the 3' flanking sequence of *UFD1L* by PCR (primers: 5'-GGTGGGTAGACAGCCTTCAT-3'; 5'-GGAATGACACTGGGACAGAC-3') and used to screen a human PAC genomic library (kindly provided by R. Schultz). A genomic DNA fragment of 884bp containing the intergenic region between *UFD1L* and *CDC45L* was amplified by PCR from the PAC clone (primers: 5'-AAAAAGCTTAAACCCCGCCGACCGCTCTC-3'; 5'-ACTAAGCTTTCAAGACTCCCGCCAAATCA-3').

Generation of transgenic mice

Residues 54-826 of the human *UFD1L-CDC45L* intergenic region were cloned upstream of the *hsp68lacZ* reporter gene (Kothary et al., 1989). DNA for pronuclear injection was linearized, gel-purified and eluted using a QIAEXII kit (Qiagen). Fertilized eggs from B6C3F1 female mice were collected for pronuclear injection. Injected eggs were implanted into ICR female mice and foster mothers were sacrificed to collect F0 embryos at embryonic

day (E) 10.5. DNA from yolk sacs of embryos was used for genotyping by PCR-amplification of the *lacZ* gene. Primer sequences are available upon request.

β -galactosidase staining

Methods for analysis of transgenic mice were described previously (Yamagishi et al., 2000). Briefly, embryos were dissected in 4°C PBS and fixed in 2% paraformaldehyde/PBS with phenol red for 30 min. on ice. After rinsing with PBS, embryos were incubated overnight at room temperature in 0.1% X-gal, 5mM potassium ferricyanide, 5mM potassium ferrocyanide, 1mM magnesium chloride, 0.002% NP-40, 0.1% sodium deoxycholate, PBS, pH 7.0. After staining, the embryos were rinsed in PBS and postfixed at 4°C overnight in 4% paraformaldehyde, 0.1% glutaraldehyde, PBS.

Neural crest cell culture and transfection

The region of the cranial neural folds from the otic vesicle to somite 3 of stage 9-11 chick embryos was dissected and treated with 0.5mg/ml of collagenase type II in PBS at 37°C for 2-3 minutes to remove the mesenchyme surrounding the neural tube. Isolated neural tube was washed in Dulbecco's Modified Eagle Medium (DMEM) (Gibco) supplemented with 10% FBS, then placed on gelatin coated culture plates. The dissected neural tubes were cultured at 37°C for 2h in DMEM with 10% FBS, to allow neural crest cells to begin migrating from the neural tube onto the culture plates. A plasmid containing residues 54-826 of the *UFD1L-CDC45L* intergenic region upstream of the hsp68lacZ reporter was transfected into the migrating neural crest cells using FuGENE6 (Roche) according to the manufacturer's

instructions. After culture at 37°C for 24 hours, the neural crest cells were fixed and stained for β -galactosidase activity as described above.

RNA isolation and Northern blot analysis

Total RNA was extracted with TRIzol reagent (Life Technologies). Two micrograms of total RNA were size-fractionated on a 1% agarose/formaldehyde gel and transferred to a nylon membrane (Amersham Pharmacia Biotech). Ethidium bromide staining of the 18s rRNA band was used to ensure integrity and equal loading of the RNA samples. Blots were hybridized to ³²P-radiolabeled mouse *Cdc45L* (400 bp 3' UTR) and *Ufd1L* (700 bp ORF) DNA probes in Rapid-hyb (Amersham) at 62°C for 16 hours. The blots were washed twice at 62°C with 2X SSC, 0.1% SDS and once at 62°C with 0.1X SSC, 0.1% SDS preheated to 62°C.

Construction of UFD1L/CDC45L fragment

Fragments of the *UFD1L/CDC45L* intergenic region were amplified by PCR using the original 884bp genomic DNA as template with appropriate pairs of the following primers. The 54bp 5' and 826 bp3' primers are located in known 5' untranslated regions of *UFD1L* and *CDC45L* as reported in the Genbank database.

054bp5': 5'-AAAAAGCTTAACCCCGCCGACCGCTCT-3'

264bp5': 5'-ATGCCCTTTCGTGATTTATTTCC-3';

364bp5': 5'-CGACTACACTACCCACAATGCACT-3';

458bp5': 5'-TCAAACCACACCAAAAACCT-3';

264bp3': 5'-GGAAATAAATCACGAAAGGGCAT-3'

364bp3': 5'-AGTGCATTGTGGGTAGTGTAGTCG-3';

458bp3': 5'-AGGTTTTTGGTGTGGTTTGA-3'

673bp3': 5'-CCCCAAAGAAGCGTCACCTC-3'

826bp3': 5'-TCAAGACTCCCGCCAAATCAAAAAGCTT-3'

Individual PCR products were cloned into a dual reporter vector (kindly provided by A. Strauss, Vanderbilt University) by blunt-end ligation into a SmaI site. This vector was constructed by ligating bases 77-1498 of pRL Null Runilla (Promega) into the KpnI site of pGL3 Basic (Promega) such that the two luciferase orthologs (runilla and firefly) were transcribed in opposite directions with a polylinker separating their 5' ends. Clones containing each insert in either direction were then used for transfection into multiple cell lines. Constructs containing firefly luciferase in the direction of *UFDIL* were designated 'forward' while constructs containing renilla luciferase in the *UFDIL* direction were designated 'reverse' (Fig 3A inset).

Cell culture and transfections

The mouse fibroblast cell line, C3H/10T^{1/2}, (ATCC no. CCL-226) or the mouse skeletal myoblast cell line, C2C12, (ATCC no. CRL-1772) was cultured in Dulbecco's Modified Eagle Medium (DMEM) (GibcoBRL) and supplemented with 10% fetal bovine serum (FBS) (GibcoBRL) and penicillin-streptomycin (GibcoBRL). The cells were refed and subcultured according to ATCC guidelines. Monc-1 cells were kindly provided by D. Anderson

(California Institute of Technology) and cultured on fibronectin-coated plates as described previously (Rao and Anderson, 1997).

C2C12 and C3H/10T^{1/2} cells were transfected in 100mm or 60mm plates by the calcium phosphate method as described (Sambrook et al., 1989). 5 μ g (100mm plate) or 3 μ g (60 mm plate) of experimental or control plasmid was cotransfected with equal amounts of hsp68-lacZ plasmid. β -galactosidase activity was used to normalize for transfection efficiency. Monc-1 cells were transfected by electroporation using 10 μ g of each plasmid. The cells were trypsinized and resuspended in chilled phosphate buffered saline (PBS) at a density of 10⁷ cells/ml. 10 μ g of reporter and hsp68lacZ plasmid was electroporated into 10⁷ cells (300V at a capacitance setting of 975 μ F). Cells were kept on ice for 10 min before replating and then grown for 36-48 hours.

Luciferase assays

Cells were harvested in passive lysis buffer (Promega) according to the manufacturer's instructions. Assays were performed using the Dual Luciferase Assay System (Promega) on a luminometer (Rosys Anthos Lucy 2) using a 10 second integration time for each reading. Assays for β -galactosidase activity were performed using an ONPG (o-nitrophenyl-galactopyranoside; Sigma) assay protocol as described (Sambrook et al., 1989).

References

- Baldini, A. 1999. Is the genetic basis of DiGeorge syndrome in HAND? *Nat Genet* **21**: 246-7.
- Bird, A.P. 1986. CpG-rich islands and the function of DNA methylation. *Nature* **321**: 209-13.
- Burbelo, P.D., G.R. Martin, and Y. Yamada. 1988. Alpha 1(IV) and alpha 2(IV) collagen genes are regulated by a bidirectional promoter and a shared enhancer. *Proc Natl Acad Sci U S A* **85**: 9679-82.
- Carlson, C., H. Sirotkin, R. Pandita, R. Goldberg, J. McKie, R. Wadey, S.R. Patanjali, S.M. Weissman, K. Anyane-Yeboah, D. Warburton, P. Scambler, R. Shprintzen, R. Kucherlapati, and B.E. Morrow. 1997. Molecular definition of 22q11 deletions in 151 velo-cardio-facial syndrome patients. *Am J Hum Genet* **61**: 620-9.
- Chapman, D.L., N. Garvey, S. Hancock, M. Alexiou, S.I. Agulnik, J.J. Gibson-Brown, J. Cebra-Thomas, R.J. Bollag, L.M. Silver, and V.E. Papaioannou. 1996. Expression of the T-box family genes, Tbx1-Tbx5, during early mouse development. *Dev Dyn* **206**: 379-90.
- Dallapiccola, B., A. Pizzuti, and G. Novelli. 1996. How many breaks do we need to CATCH on 22q11? *Am J Hum Genet* **59**: 7-11.
- Emanuel, B., Scambler, P. 1998 *Heart Development* (Harvey, R., Rosenthal, N., ed), pp. 463-478, Academic Press, San Diego.
- Gaston, K. and M. Fried. 1995. CpG methylation and the binding of YY1 and ETS proteins to the Surf-1/Surf-2 bidirectional promoter. *Gene* **157**: 257-9.
- Gavalas, A., J.E. Dixon, K.A. Brayton, and H. Zalkin. 1993. Coexpression of two closely linked avian genes for purine nucleotide synthesis from a bidirectional promoter. *Mol Cell Biol* **13**: 4784-92.
- Guarguaglini, G., A. Battistoni, C. Pittoggi, G. Di Matteo, B. Di Fiore, and P. Lavia. 1997. Expression of the murine RanBP1 and Htf9-c genes is regulated from a shared bidirectional promoter during cell cycle progression. *Biochem J* **325** (Pt 1): 277-86.
- Guris, D.L., J. Fantes, D. Tara, B.J. Druker, and A. Imamoto. 2001. Mice lacking the homologue of the human 22q11.2 gene CRKL phenocopy neurocristopathies of DiGeorge syndrome. *Nat Genet* **27**: 293-8.
- Hoppe, T., K. Matuschewski, M. Rape, S. Schlenker, H.D. Ulrich, and S. Jentsch. 2000.

- Activation of a membrane-bound transcription factor by regulated ubiquitin/proteasome-dependent processing. *Cell* **102**: 577-86.
- Ikeda, S., A. Mochizuki, A.H. Sarker, and S. Seki. 2000. Identification of functional elements in the bidirectional promoter of the mouse *Nthl1* and *Tsc2* genes. *Biochem Biophys Res Commun* **273**: 1063-8.
- Jerome, L.A. and V.E. Papaioannou. 2001. DiGeorge syndrome phenotype in mice mutant for the T-box gene, *Tbx1*. *Nat Genet* **27**: 286-91.
- Johnson, E.S., P.C. Ma, I.M. Ota, and A. Varshavsky. 1995. A proteolytic pathway that recognizes ubiquitin as a degradation signal. *J Biol Chem* **270**: 17442-56.
- Kirby, M.L. and K.L. Waldo. 1990. Role of neural crest in congenital heart disease. *Circulation* **82**: 332-40.
- Koepp, D.M., J.W. Harper, and S.J. Elledge. 1999. How the cyclin became a cyclin: regulated proteolysis in the cell cycle. *Cell* **97**: 431-4.
- Kothary, R., S. Clapoff, S. Darling, M.D. Perry, L.A. Moran, and J. Rossant. 1989. Inducible expression of an hsp68-lacZ hybrid gene in transgenic mice. *Development* **105**: 707-14.
- Lavia, P., D. Macleod, and A. Bird. 1987. Coincident start sites for divergent transcripts at a randomly selected CpG-rich island of mouse. *Embo J* **6**: 2773-9.
- Lindsay, E.A. and A. Baldini. 1998. Congenital heart defects and 22q11 deletions: which genes count? *Mol Med Today* **4**: 350-7.
- Lindsay, E.A., A. Botta, V. Jurecic, S. Carattini-Rivera, Y.C. Cheah, H.M. Rosenblatt, A. Bradley, and A. Baldini. 1999. Congenital heart disease in mice deficient for the DiGeorge syndrome region. *Nature* **401**: 379-83.
- Lindsay, E.A., F. Vitelli, H. Su, M. Morishima, T. Huynh, T. Pramparo, V. Jurecic, G. Ogunrinu, H.F. Sutherland, P.J. Scambler, A. Bradley, and A. Baldini. 2001. *Tbx1* haploinsufficiency in the DiGeorge syndrome region causes aortic arch defects in mice. *Nature* **410**: 97-101.
- Loebel, D., H. Huikeshoven, and S. Cotterill. 2000. Localisation of the DmCdc45 DNA replication factor in the mitotic cycle and during chorion gene amplification. *Nucleic Acids Res* **28**: 3897-903.
- Merscher, S., B. Funke, J.A. Epstein, J. Heyer, A. Puech, M.M. Lu, R.J. Xavier, M.B. Demay, R.G. Russell, S. Factor, K. Tokooya, B.S. Jore, M. Lopez, R.K. Pandita, M.

- Lia, D. Carrion, H. Xu, H. Schorle, J.B. Kobler, P. Scambler, A. Wynshaw-Boris, A.I. Skoultschi, B.E. Morrow, and R. Kucherlapati. 2001. TBX1 is responsible for cardiovascular defects in velo-cardio-facial/DiGeorge syndrome. *Cell* **104**: 619-29.
- Meyer, H.H., J.G. Shorter, J. Seemann, D. Pappin, and G. Warren. 2000. A complex of mammalian ufd1 and npl4 links the AAA-ATPase, p97, to ubiquitin and nuclear transport pathways. *Embo J* **19**: 2181-92.
- Novelli, G., A. Mari, F. Amati, A. Colosimo, F. Sangiuolo, M. Bengala, E. Conti, A. Ratti, R. Bordoni, A. Pizzuti, A. Baldini, R. Crinelli, F. Pandolfi, M. Magnani, and B. Dallapiccola. 1998. Structure and expression of the human ubiquitin fusion-degradation gene (UFD1L). *Biochim Biophys Acta* **1396**: 158-62.
- Novelli, G., F. Amati, and B. Dallapiccola. 2000. Individual haploinsufficient loci and the complex phenotype of DiGeorge syndrome. *Mol Med Today* **6**: 10-1.
- Orii, K.E., K.O. Orii, M. Souri, T. Orii, N. Kondo, T. Hashimoto, and T. Aoyama. 1999. Genes for the human mitochondrial trifunctional protein alpha- and beta-subunits are divergently transcribed from a common promoter region. *J Biol Chem* **274**: 8077-84.
- Osley, M.A., J. Gould, S. Kim, M.Y. Kane, and L. Hereford. 1986. Identification of sequences in a yeast histone promoter involved in periodic transcription. *Cell* **45**: 537-44.
- Rao, M.S. and D.J. Anderson. 1997. Immortalization and controlled in vitro differentiation of murine multipotent neural crest stem cells. *J Neurobiol* **32**: 722-46.
- Saha, P., K.C. Thome, R. Yamaguchi, Z. Hou, S. Weremowicz, and A. Dutta. 1998. The human homolog of *Saccharomyces cerevisiae* CDC45. *J Biol Chem* **273**: 18205-9.
- Sambrook, J., Fritsch, E.F., and Maniatis, T. 1989. *Molecular Cloning : A Laboratory Manual* (Nolan, C., ed) Vol. 3, pp. 16.30 – 16.39, 3 vols., Cold Spring Harbor Press.
- Schilling, L.J. and P.J. Farnham. 1995. The bidirectionally transcribed dihydrofolate reductase and rep-3a promoters are growth regulated by distinct mechanisms. *Cell Growth Differ* **6**: 541-8.
- Schug, J. and G.C. Overton. 1997. Modeling transcription factor binding sites with Gibbs Sampling and Minimum Description Length encoding. *Proc Int Conf Intell Syst Mol Biol* **5**: 268-71.
- Shaikh, T.H., S. Gottlieb, B. Sellinger, F. Chen, B.A. Roe, R.J. Oakey, B.S. Emanuel, and M.L. Budarf. 1999. Characterization of CDC45L: a gene in the 22q11.2 deletion region expressed during murine and human development. *Mamm Genome* **10**: 322-6.

- Smale, S.T. 1997. Transcription initiation from TATA-less promoters within eukaryotic protein-coding genes. *Biochim Biophys Acta* **1351**: 73-88.
- Srivastava, D. and H. Yamagishi. 1999. Reply: role of the dHAND-UFD1L pathway. *Trends Genet* **15**: 253-4.
- Tyers, M. and P. Jorgensen. 2000. Proteolysis and the cell cycle: with this RING I do thee destroy. *Curr Opin Genet Dev* **10**: 54-64.
- Yamagishi, H., V. Garg, R. Matsuoka, T. Thomas, and D. Srivastava. 1999. A molecular pathway revealing a genetic basis for human cardiac and craniofacial defects. *Science* **283**: 1158-61.
- Yamagishi, H., E.N. Olson, and D. Srivastava. 2000. The basic helix-loop-helix transcription factor, dHAND, is required for vascular development. *J Clin Invest* **105**: 261-70.
- Zhang, Y., S. Koushik, R. Dai, and N.F. Mivechi. 1998. Structural organization and promoter analysis of murine heat shock transcription factor-1 gene. *J Biol Chem* **273**: 32514-21.
- Zou, L. and B. Stillman. 1998. Formation of a preinitiation complex by S-phase cyclin CDK-dependent loading of Cdc45p onto chromatin. *Science* **280**: 593-6.

CHAPTER THREE

G α_Q AND G α_{11} PROTEINS MEDIATE ENDOTHELIN-1 SIGNALING IN NEURAL CREST-DERIVED PHARYNGEAL ARCH MESENCHYME

Background

Endothelin-A (ET_A) is a G-protein-coupled receptor expressed in the neural crest-derived mesenchyme of the pharyngeal arches during development. The ligand for ET_A, endothelin-1 (ET-1), is expressed in pharyngeal arch epithelium and binds the receptor after cleavage from its pro-form by the membrane-bound metalloprotease, endothelin converting enzyme-1 (ECE-1) (Xu et al., 1994). Activation of the ET_A receptor by ET-1 is required for proper development of neural crest-derived craniofacial structures, the cardiac outflow tract, and the great vessels. Proliferation and differentiation of cell populations contributing to these structures is determined by expression of transcription factors including gooseoid, Dlx-2, Dlx-3, dHAND, eHAND, and Barx1, all of which require ET-1 signaling for correct spatio-temporal expression in the pharyngeal arches.

Various components of the endothelin signaling pathway have been inactivated *in vivo* allowing study of their roles in development of neural crest cells. Mice with deficiencies in the genes encoding ET-1 (*Edn-1*) (Kurihara et al., 1994; 1995), ET_A (Clouthier et al., 1998), or ECE-1 (Yanagisawa et al., 1998) die shortly after birth with abnormal craniofacial bones, cleft palate, malformed thyroid and thymus, aortic arch

anomalies, and ventricular septal defects. These morphologic abnormalities correlate with the restricted expression patterns of ET-1 and ET_A. Signals from the ET_A receptor can potentially be transmitted by broadly expressed G proteins of the G_q, G_i, and/or G_s class, however little is known regarding the mechanisms of selectivity in ET_A–G protein coupling. Studies of ET-1 signaling in the context of myocardial hypertrophy have shown that ET-1 interaction with ET_A stimulates phospholipase C-β (PLC-β) isoforms through activation of the G_q class of G proteins. Indeed, adult cardiomyocyte hypertrophy is suppressed in mice with a cardiomyocyte-specific deletion of both Gα_q and Gα₁₁ (Wettschureck et al., 2001). By contrast, *Gα_q^(-/-)Gα₁₁^(-/-)* mice die around E11.0 apparently due to cardiomyocyte hypoplasia and heart failure. Interestingly, craniofacial development initiates prior to death, allowing us to assess the role of Gα_q/Gα₁₁ on the ET-1 signaling pathway in the pharyngeal arch mesenchyme.

Combined inactivation of *Gα_q* and *Gα₁₁* in mice results in alterations of neural crest-derived structures similar to, but less severe than, those observed upon disruption of ET-1 signaling (Offermanns et al., 1998). Mice with a single active allele of *Gα_q* or *Gα₁₁* survive up to 2 hours after birth but are born small, anoxic, and unresponsive to tactile stimuli. In addition, *Gα_q^(-/-)Gα₁₁^(+/-)* neonates exhibit malformation of neural crest-derived craniofacial structures, including the mandible, tympanic ring, and bones of the otic cup. These craniofacial malformations are not as severe as those caused by the absence of ET-1 or ET_A, presumably because one copy of *Gα₁₁* is able to transduce a fraction of the normal ET-1 signal. Both *Gα_q* and *Gα₁₁* are widely expressed and appear to be functionally redundant (Wilkie et al., 1991; Offermanns et al., 1998). Despite reduced fecundity, ataxia and platelet

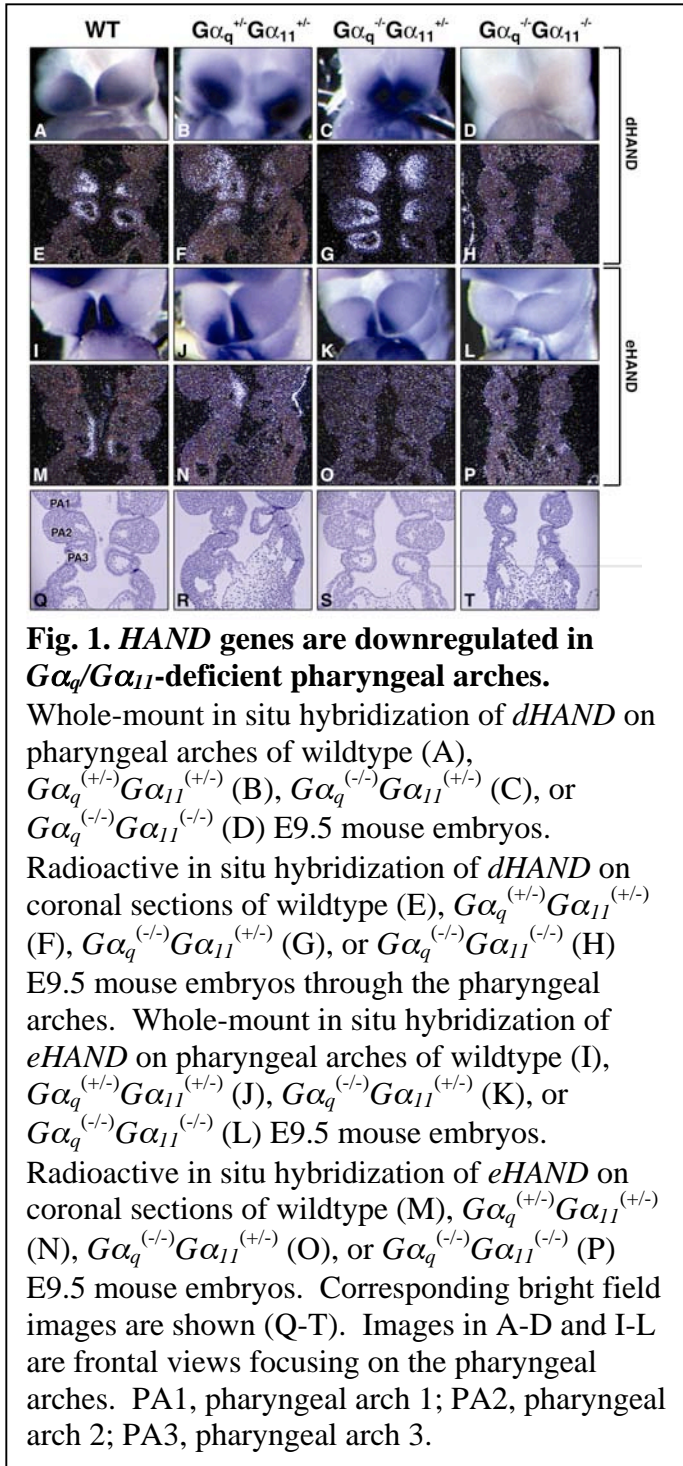
aggregation disorders in $G\alpha_q^{(-/-)}$ mice (Offermanns et al., 1997), any combination of two functional alleles of $G\alpha_q$ or $G\alpha_{11}$ is sufficient for survival, normal craniofacial development, and production of fertile adults.

The similarity of developmental defects seen in $G\alpha_q^{(-/-)}G\alpha_{11}^{(+/-)}$ mice compared to *Edn-1* or *ET_A*-null mice led us to hypothesize that the $G\alpha_q$ and $G\alpha_{11}$ proteins are the primary intracellular transducers of ET-1 signaling in the cranial neural crest. Here we show that expression of *ET_A*-dependent genes is altered in mice harboring inactive alleles of $G\alpha_q$ and $G\alpha_{11}$ while expression of other transcription factors in the pharyngeal arches remains unchanged, indicating that the $G\alpha_q$ and $G\alpha_{11}$ proteins mediate ET-1 signaling in the pharyngeal arches.

Results

HAND gene expression is downregulated in pharyngeal arches of $G\alpha_q/G\alpha_{11}$ -deficient embryos

Expression of the basic helix-loop-helix transcription factors dHAND and eHAND is downregulated in *Edn1*-null or *ET_A*-null (Thomas et al., 1998; Clothier et al., 2000) embryos, leading us to examine the effect of $G\alpha_q/G\alpha_{11}$ deficiency on expression of these two genes. Whole-mount *in situ* hybridization revealed high levels of expression of both *HAND* genes in wildtype and $G\alpha_q^{(+/-)}G\alpha_{11}^{(+/-)}$ embryos. $G\alpha_q^{(-/-)}G\alpha_{11}^{(+/-)}$ embryos expressed reduced amounts of both *HAND* genes while *HAND* gene expression was not detected in $G\alpha_q^{(-/-)}G\alpha_{11}^{(-/-)}$ embryos (Fig. 1).



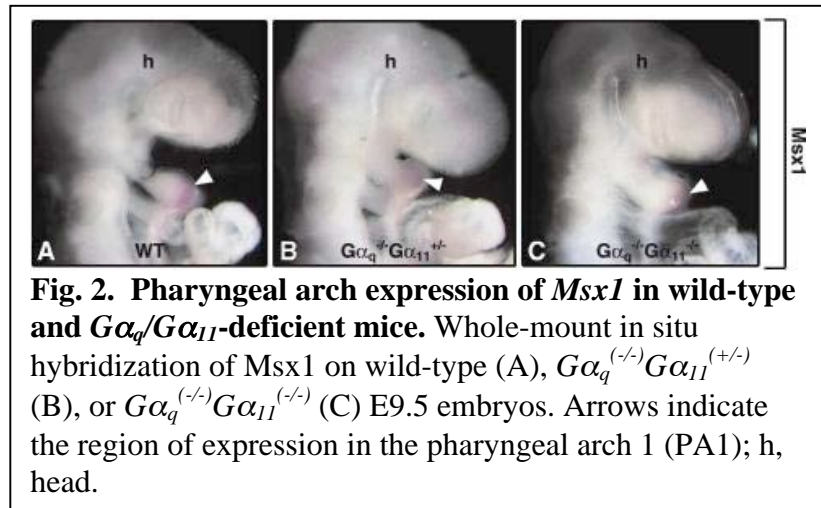
eHAND expression in this mutant.

In order to examine the regulation of *HAND* gene expression in the pharyngeal arch mesenchyme, we performed radioactive section *in situ* analysis on serial sections from various $G\alpha_q/G\alpha_{11}$ mutant embryos. High levels of *dHAND* expression were observed in the wildtype, $G\alpha_q^{(+/-)}G\alpha_{11}^{(+/-)}$ and $G\alpha_q^{(-/-)}G\alpha_{11}^{(+/-)}$ sections whereas *dHAND* expression was not detectable in the $G\alpha_q^{(-/-)}G\alpha_{11}^{(-/-)}$ sections. *eHAND* expression was similarly maintained in wildtype and $G\alpha_q^{(+/-)}G\alpha_{11}^{(+/-)}$ embryos, but was not detected in the $G\alpha_q^{(-/-)}G\alpha_{11}^{(+/-)}$ or $G\alpha_q^{(-/-)}G\alpha_{11}^{(-/-)}$ sections examined. The absence of *eHAND* expression in the $G\alpha_q^{(-/-)}G\alpha_{11}^{(+/-)}$ section most likely reflects the more narrow domain of

Msx1 and *Msx2* expression is maintained in the pharyngeal arches of $G\alpha_q/G\alpha_{11}$ -deficient embryos

Pharyngeal arch expression levels and patterns of other genes have been evaluated in *Edn1*-null mice. We examined expression of several of these genes on serial sections from the same embryos used for *HAND* gene expression analysis. As previously described for *Edn1*-null embryos,

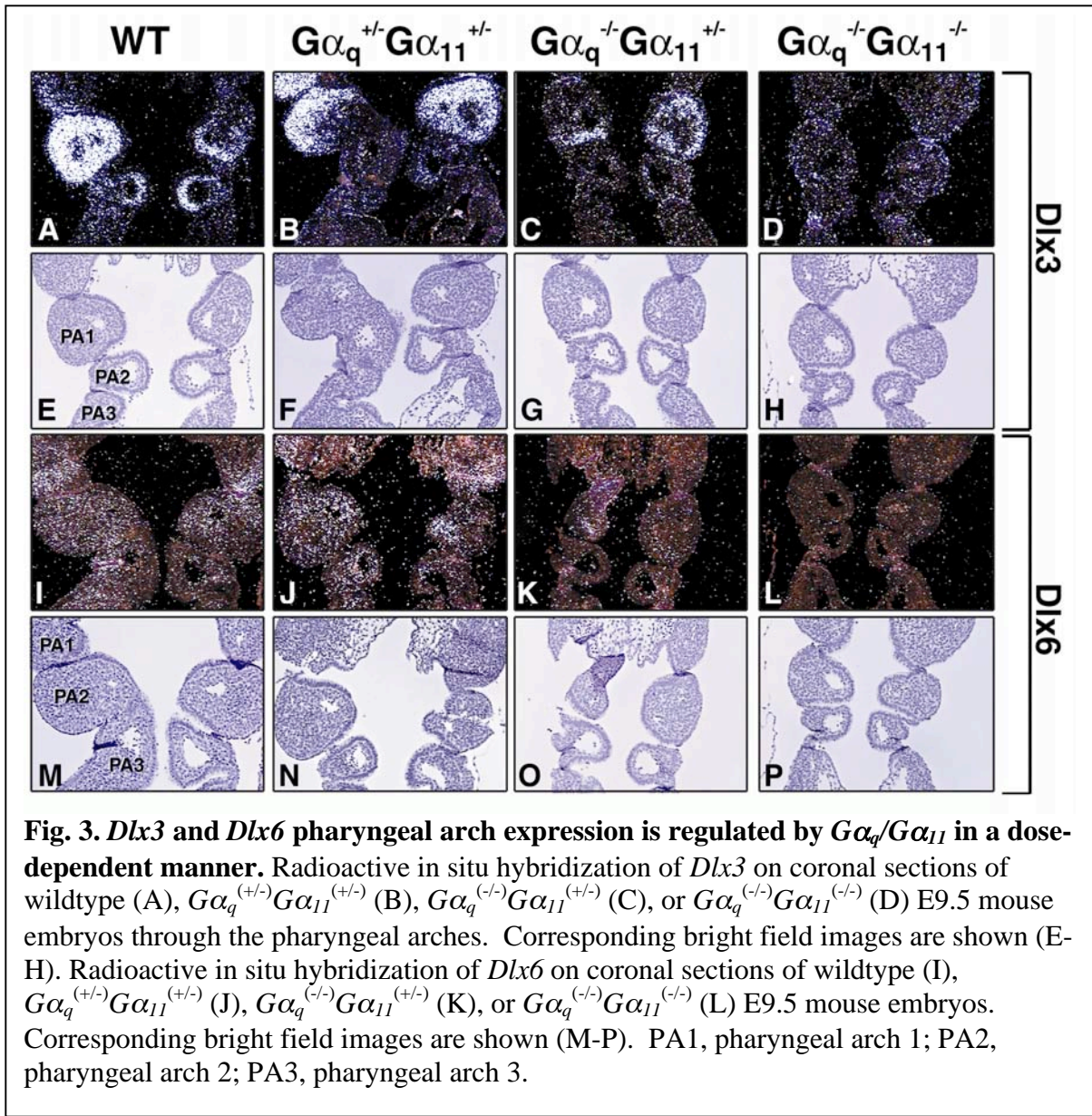
expression of the homeobox genes *Msx1* and *Msx2* is maintained in $G\alpha_q/G\alpha_{11}$ -deficient embryos (Fig. 2 and data not shown). Importantly, maintenance of *Msx1* and



Msx2 expression in $G\alpha_q/G\alpha_{11}$ -deficient embryos confirms that there is not an overall differentiation defect or a deficiency of cells in the pharyngeal arches of $G\alpha_q/G\alpha_{11}$ mutants and implies that the reduction of *HAND* gene expression observed in these embryos specifically reflects the absence of $G\alpha_q/G\alpha_{11}$ signaling.

Dlx3 and *Dlx6* expression is downregulated in $G\alpha_q/G\alpha_{11}$ -deficient embryos and maintained in *dHAND*-null embryos

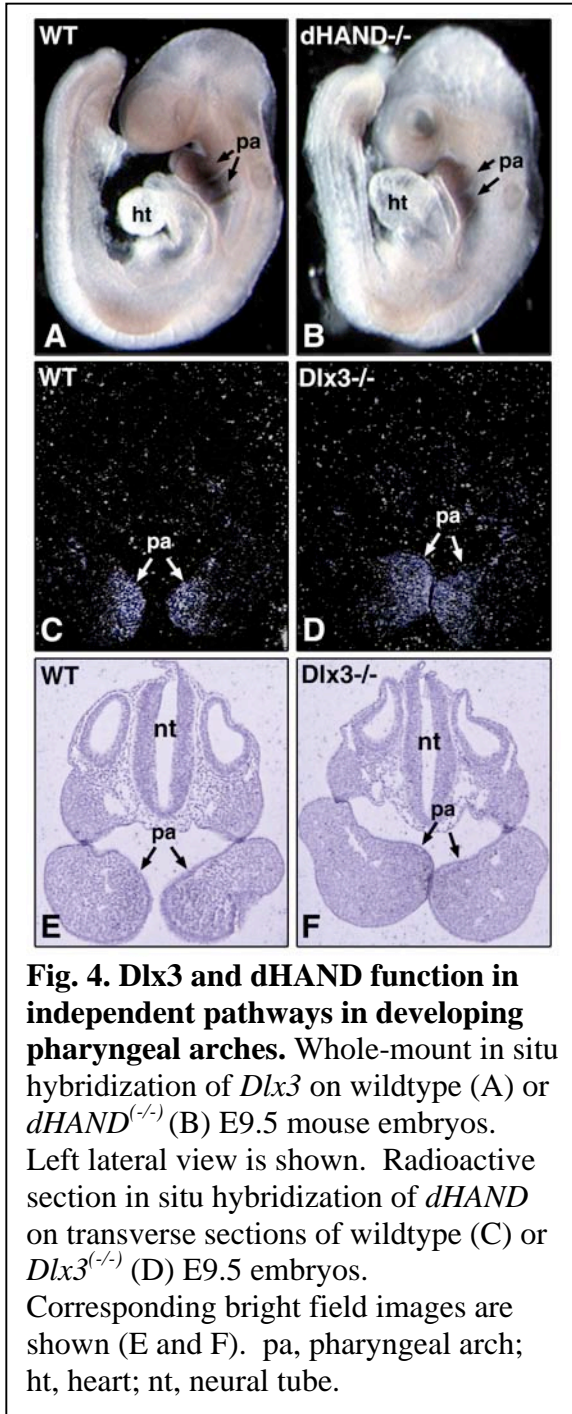
Expression of *Dlx3* and *Dlx6*, two homeobox-containing genes expressed in the distal mesenchyme and epithelium of the pharyngeal arches, is completely absent in the first and second arches of E9.5 *ET_A*-null embryos (Clouthier et al., 2000; Charite et al., 2001). *Dlx6* binds an *ET_A*-dependent neural crest enhancer required for expression of *dHAND* in the pharyngeal arches (Charite et al., 2001). To determine whether *Dlx3* and *Dlx6* are also



downregulated in $G\alpha_q/G\alpha_{11}$ mutant embryos, we examined their expression in E9.5 embryos with deletions of $G\alpha_q$ and/or $G\alpha_{11}$ genes. Whole mount *in situ* hybridization revealed expression of $Dlx3$ in wildtype E9.5 embryos, reduced expression levels in $G\alpha_q^{(-/-)}G\alpha_{11}^{(+/-)}$ embryos, and complete lack of expression in $G\alpha_q^{(-/-)}G\alpha_{11}^{(-/-)}$ embryos (data not shown).

We also examined $Dlx3$ and $Dlx6$ expression by radioactive section *in situ* hybridization on the various $G\alpha_q/G\alpha_{11}$ mutant embryos (Fig. 3). $Dlx3$ and $Dlx6$ expression was strong in wildtype sections and slightly diminished in sections from $G\alpha_q^{(+/-)}G\alpha_{11}^{(+/-)}$ embryos. Inactivation of three $G\alpha_q$ and $G\alpha_{11}$ alleles led to a dramatic decrease in both $Dlx3$ and $Dlx6$ expression consistent with the craniofacial defects of $G\alpha_q^{(-/-)}G\alpha_{11}^{(+/-)}$ mice. $Dlx3$ and $Dlx6$ expression was not detected in sections from $G\alpha_q^{(-/-)}G\alpha_{11}^{(-/-)}$ embryos. These findings are consistent with the increasing severity of phenotype observed as alleles of either $G\alpha_q$ or $G\alpha_{11}$ are deleted and, together with the data for the *HAND* genes and *Msx1* and *Msx2*, provides evidence that $G\alpha_q$ and $G\alpha_{11}$ transduce ET-1/ET_A signaling in neural crest cells to promote development of the pharyngeal arches.

Expression of *dHAND* in the pharyngeal arches has previously been shown to be dependent on ET-1 signaling. Additionally, *dHAND* is required for pharyngeal arch expression of *Msx1* (Thomas et al., 1998). To determine whether *dHAND* is also required for $Dlx3$ expression in the pharyngeal arches, we examined the expression of $Dlx3$ in E9.5 *dHAND*-null embryos. Pharyngeal arch expression of $Dlx3$ was not diminished in *dHAND*-null embryos (Fig. 4A) compared to wildtype littermates (Fig. 4B). Likewise, *dHAND* expression was not diminished in $Dlx3$ -null embryos (Fig. 4D). We conclude that $G\alpha_q/G\alpha_{11}$



mediates ET-1 activation of *dHAND* and *Dlx3* in parallel pathways in neural crest cells of the pharyngeal arch during craniofacial development.

Discussion

The similarity of craniofacial structures that were affected in *Gα_q*^{-/-}*Gα₁₁*^{+/-}, *ET_A* and *ET-1*-null mice led us to investigate whether these genes may function in a common signaling pathway. We examined whether the pharyngeal arch expression of several transcription factors, which is disrupted when ET-1 signaling is abolished, is similarly affected in *Gα_q/Gα₁₁*-deficient embryos. We found this to be the case for all such transcription factors examined—*Dlx3*, *Dlx6*, *dHAND*, and *eHAND*. Interestingly, while pharyngeal arch expression of these homeodomain and bHLH

genes is diminished in *Gα_q*^{-/-}*Gα₁₁*^{-/-}, *ET_A* and *ET-1*-null embryos, it is maintained in other developing structures including the limb buds and, in the case of *dHAND* and *eHAND*, the

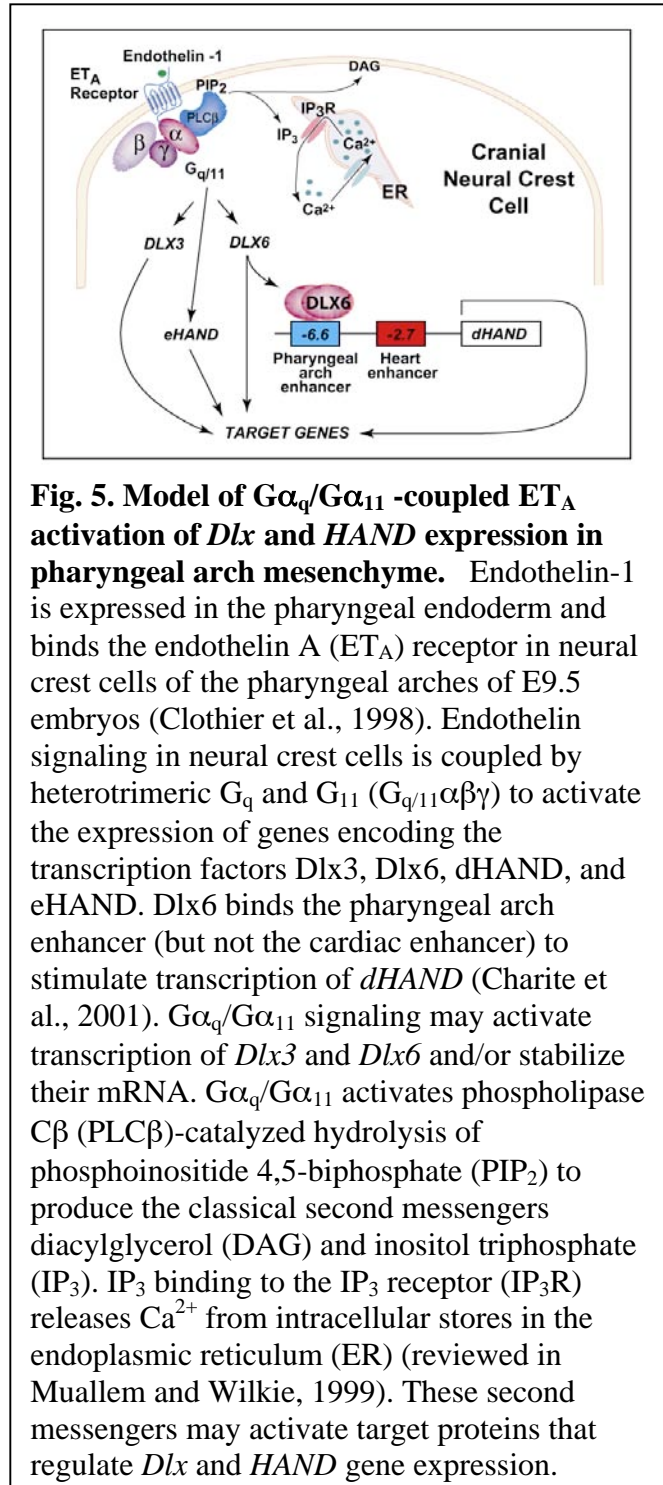
heart. Given that $G\alpha_q/G\alpha_{11}$ is required for *HAND* gene expression during craniofacial development, we tested whether $G\alpha_q/G\alpha_{11}$ signaling might also regulate the expression of bHLH genes required for neurogenesis (Guillemot, 1999) because we noted that mutant neonates expressing a single copy of either $G\alpha_q$ or $G\alpha_{11}$ exhibited phenotypes consistent with defective neural development (Offermanns et al., 1998). However, neural tube expression of the neurogenic bHLH transcription factors *Mash1*, *Math1*, *Ngn1*, and *Ngn2* appeared normal in $G\alpha_q^{(-/-)}G\alpha_{11}^{(-/-)}$ embryos at E9.5 (TMW and J. Johnson, unpublished). Thus, $G\alpha_q/G\alpha_{11}$ signaling was only found to be required for the expression of *Dlx* and *HAND* genes in the pharyngeal arches.

$G\alpha_q/G\alpha_{11}$ signaling regulates the activity of several transcription factors in various cell types, but little is known about the signaling hierarchy in cranial neural crest cells. $G\alpha_q$ and $G\alpha_{11}$ both activate PLC- β which, in turn, catalyzes the hydrolysis of phosphatidylinositol biphosphate into diacylglycerol and inositol triphosphate (Smrcka and Sternweis, 1993). This leads to intracellular calcium release and activation of protein kinase C (PKC), calmodulin activated kinase II (CaMKII), and the Ca^{2+} regulated phosphatase calcineurin. These kinases and phosphatases modulate the activity of several proteins that regulate transcription. For example, $G\alpha_q/G\alpha_{11}$ regulates activation of the transcription factor Pit-1 in a Raf-1-dependent pathway to control expression of the prolactin gene (Tian et al., 1995). In lymphocytes and cardiomyocytes, NF-AT nuclear translocation and activation of gene transcription is stimulated by calcineurin (Li et al., 1998; Molkenin et al., 1998; Boss et al., 1996). In B cells, NF κ B-dependent transcription is stimulated by $G\alpha_q/G\alpha_{11}$ -mediated activation of the Ca^{2+} -sensitive tyrosine kinase Pyk2 (Shi and Kehrl, 2001). Additionally, in

hypothalamic and retinal neurons, Gq-mediated depletion of phosphatidylinositol 4,5-biphosphate (PIP₂) at the plasma membrane apparently regulates nuclear translocation of the DNA-binding protein, tubby (Santagata et al., 2001). The MEF2 transcription factor is also regulated by G protein, calcineurin, CaM kinase and MAP kinase signaling (reviewed in McKinsey et al., 2002), making it an interesting potential target for G α_q /G α_{11} signaling cascades in the developing neural crest. Analysis of PIP₂ and calcium-dependent genes, MAP kinase targets, and CaMKII and PKC substrates in the context of the pharyngeal arch may uncover additional transcription factors that regulate *Dlx3*, *Dlx6*, *dHAND*, and *eHAND* and provide a mechanism for their activation.

G α_q /G α_{11} signaling in receptor complexes is dosage dependent. Inactivation of one or two out of the four alleles of *G α_q /G α_{11}* , in any combination, results in a craniofacial morphology indistinguishable from wild type. We found that transcription factors regulated by ET-1 maintain high expression levels in *G $\alpha_q^{(+/-)}$ G $\alpha_{11}^{(+/-)}$* embryos, reflecting the requirement of only two alleles of *G α_q /G α_{11}* for correct development and survival. By contrast, a single active copy of *G α_{11}* (*G $\alpha_q^{(-/-)}$ G $\alpha_{11}^{(+/-)}$*) resulted in reduced expression of *eHAND* and *G α_q /G α_{11}* -deficiency ablated expression of both *dHAND* and *eHAND*. This suggests a requirement of threshold levels of G α_q /G α_{11} protein for functional ET-1 signaling. It is possible that G α_{11} is expressed at lower levels than G α_q in the neural crest-derived mesenchyme of the pharyngeal arches, or couples ET_A receptor less efficiently, leading to the increased severity of defects observed in *G $\alpha_q^{(-/-)}$ G $\alpha_{11}^{(+/-)}$* mice compared to *G $\alpha_q^{(+/-)}$ G $\alpha_{11}^{(-/-)}$* mice.

We also found that although $G\alpha_q^{(-/-)}G\alpha_{11}^{(+/-)}$ embryos die shortly after birth with defects in neural crest-derived structures, these embryos do express high levels of *dHAND*. This probably reflects a requirement for other proteins, in addition to *dHAND*, whose expression is regulated by $G\alpha_q/G\alpha_{11}$ signaling to support development of the pharyngeal arch mesenchyme. *Dlx3* is a candidate for this role as its expression is markedly reduced in $G\alpha_q^{(-/-)}G\alpha_{11}^{(+/-)}$ embryos and is excluded from the pharyngeal arches of $G\alpha_q/G\alpha_{11}$ -null embryos. *Dlx3* and *dHAND* may act in parallel $G\alpha_q/G\alpha_{11}$ -dependent pathways because *Dlx3* expression is normal in *dHAND*-null embryos and *dHAND* expression remains unaltered in *Dlx3*-null embryos (Figs. 4 and 5). It is likely that



additional transcription factors regulated by ET-1 signaling are downregulated in

$G\alpha_q^{(-/-)}G\alpha_{11}^{(+/-)}$ embryos, and are required for development of neural crest-derived structures.

A genomic region upstream of *dHAND* containing four homeodomain binding sites is necessary and sufficient for pharyngeal arch expression of *dHAND* and is dependent on ET-1 signaling. *Dlx6* binds these sites in the *dHAND* pharyngeal arch enhancer and *Dlx6* expression is abolished in the pharyngeal arches of *ET_A*-null embryos (Charite et al., 2001). We have shown that *Dlx6* expression is $G\alpha_q/G\alpha_{11}$ -dose dependent indicating that *dHAND* pharyngeal arch expression is controlled by *Dlx6* in response to $G\alpha_q/G\alpha_{11}$ -mediated ET-1 signaling. We propose that $G\alpha_q/G\alpha_{11}$ signaling activates the expression of *Dlx3* and *Dlx6*. Consequently, *Dlx6* binds the *dHAND* pharyngeal arch enhancer to drive expression of *dHAND* in the pharyngeal arches during craniofacial development (Fig. 5). Analysis of the *Dlx6* regulatory region may lead to identification of intermediate factor(s) directly affected by $G\alpha_q/G\alpha_{11}$ -mediated signaling.

Pharyngeal arch expression of *Msx1* has previously been reported to be dependent on *dHAND* and is absent in *dHAND*-null embryos (Thomas et al., 1998). Although neither *Dlx6* nor *dHAND* expression was detected in sections from $G\alpha_q^{(-/-)}G\alpha_{11}^{(-/-)}$ embryos, *Msx1* expression was still maintained. This is consistent with data from *endothelin-1*-null embryos in which *dHAND* is expressed at very low levels, possibly allowing for normal expression of *Msx1* (Thomas et al., 1998). Perhaps there is some residual *dHAND* expression in $G\alpha_q^{(-/-)}G\alpha_{11}^{(-/-)}$ embryos below our level of detection that allows for expression of *Msx1*, possibly in combination with alternative mechanisms of *Msx1* activation.

We have shown that ET-1-dependent genes require $G\alpha_q/G\alpha_{11}$ for correct expression in the pharyngeal arches. Activation of these α -subunits is the first of many intracellular

events occurring downstream of the endothelin receptor that ultimately lead to transcription of target genes such as *Dlx3*, *Dlx6*, and the *HAND* genes during craniofacial development.

Materials and Methods

Harvesting and genotyping of embryos

$G\alpha_q^{(+/-)}G\alpha_{11}^{(+/-)}$ mice were intercrossed and embryos were collected at E9.5. Embryos were fixed in 4% paraformaldehyde overnight and stored at -20°C. Yolk sac DNA was genotyped for $G\alpha_q$ and $G\alpha_{11}$ by polymerase chain reaction (PCR). $G\alpha_q$ genotyping was performed using two forward primers, [TW140: 5'-AGGGCCCATGAGGACATGTATGC-3'], specific for the wildtype allele, and [TW36: 5'-AGGATCTCGTCGTGACCCATGGCGA-3'], specific for the knockout allele. The reverse primer, [TW71: 5'-TTCAAAGTATCACACTCACATCACAG-3'], is common to both alleles of $G\alpha_q$. $G\alpha_{11}$ genotyping was similarly achieved using two forward primers, [TW141: 5'-GACACTGCCATCTGTACAAGG-3'] and [α PGK5'-GCTAAAGCGCATGCTCCAGAC-3'] in combination with the reverse primer [CT26: 5'-GAGAATGACAGACGAGTTCTG-3']. Touchdown PCR was carried out under the following conditions: 94°C for 4 min; 94°C for 30 sec; 72°C for 30 sec; and 72°C for 30 sec (10 cycles, decreasing the annealing temperature by 2°C each cycle after the first cycle); 94°C for 30 sec; 55°C for 30 sec; and 72°C for 30 sec (20 cycles) and 72°C for 7 min. $G\alpha_q$ wild type and null alleles yielded products of 700 bp and 400 bp, respectively, while $G\alpha_{11}$ wild type and null alleles yielded products of 410 bp and 300 bp, respectively.

Whole-mount in situ hybridization

Whole-mount *in situ* hybridization was performed as previously described (Yamagishi et al., 1999) using digoxigenin-labeled antisense riboprobes synthesized from Dlx3, dHAND, and eHAND cDNAs linearized with NotI and transcribed with T3 polymerase.

Radioactive section in situ hybridization

³⁵S-labeled antisense riboprobes were synthesized from partial cDNAs of Msx1, Msx2, Dlx3, Dlx6, dHAND, and eHAND. cDNAs were linearized and transcribed using the following restriction enzymes and RNA polymerases: Msx1-BamHI, T7; Msx2-EcoRV, SP6; Dlx3-NotI, T3; Dlx6-SpeI, T7; dHAND-EcoRI, SP6; eHAND-BamHI, T7 (MAXIScript; Ambion Inc.). Radioactive section *in situ* hybridization was performed on paraffin-embedded sections of E9.5 mouse embryos using these riboprobes, as previously described (Nakagawa et al., 1999).

References

- Boss, V., Talpade, D.J., Murphy, T.J. (1996). Induction of NFAT-mediated transcription by Gq-coupled receptors in lymphoid and non-lymphoid cells. *J. Biol. Chem.* **271**, 10429-10432.
- Charite, J., McFadden, D. G., Merlo, G., Levi, G., Clouthier, D. E., Yanagisawa, M., Richardson, J. A., and Olson, E. N. (2001). Role of Dlx6 in regulation of an endothelin-1-dependent, dHAND branchial arch enhancer. *Genes Dev* **15**, 3039-49.
- Clouthier, D. E., Hosoda, K., Richardson, J. A., Williams, S. C., Yanagisawa, H., Kuwaki, T., Kumada, M., Hammer, R. E., and Yanagisawa, M. (1998). Cranial and cardiac neural crest defects in endothelin-A receptor- deficient mice. *Development* **125**, 813-24.
- Clouthier, D. E., Williams, S. C., Yanagisawa, H., Wieduwilt, M., Richardson, J. A., and Yanagisawa, M. (2000). Signaling pathways crucial for craniofacial development revealed by endothelin-A receptor-deficient mice. *Dev Biol* **217**, 10-24.
- Guillemot, F. (1999). Vertebrate bHLH genes and the determination of neuronal fates. *Exp Cell Res* **253**, 357-364.
- Ito, H., Hiroe, M., Hirata, Y., Fujisaki, H., Adachi, S., Akimoto, H., Ohta, Y., and Marumo, F. (1994). Endothelin ETA receptor antagonist blocks cardiac hypertrophy provoked by hemodynamic overload. *Circulation* **89**, 2198-203.
- Kurihara, Y., Kurihara, H., Suzuki, H., Kodama, T., Maemura, K., Nagai, R., Oda, H., Kuwaki, T., Cao, W. H., Kamada, N., and et al. (1994). Elevated blood pressure and craniofacial abnormalities in mice deficient in endothelin-1. *Nature* **368**, 703-10.
- Kurihara, Y., Kurihara, H., Oda, H., Maemura, K., Nagai, R., Ishikawa, T., and Yazaki, Y. (1995). Aortic arch malformations and ventricular septal defect in mice deficient in endothelin-1. *J Clin Invest* **96**, 293-300.
- Li, W., Llopis, J., Whitney, M., Zlokarnik, G., and Tsien, R.Y. (1998). Cell-permeant caged InsP₃ ester shows that Ca²⁺ spike frequency can optimize gene expression. *Nature* **392**, 936-941.
- McKinsey, T., Zhang, C.L., and Olson, E.N. (2002). MEF2: a calcium-dependent regulator of cell division, differentiation and death. *Trends Biochem Sci* **27**, 40-47.
- Molkentin, J.D., Lu, J.R., Antos, C.L., Markham, B., Richardson, J., Robbins, J., Grant, S.R., and Olson, E.N. (1998). A calcineurin-dependent transcriptional pathway for cardiac hypertrophy. *Cell* **93**, 215-228.

- Muallem, S., and Wilkie, T.M. (1999) G protein-dependent Ca^{2+} signaling complexes in secretory cells. *Cell Calcium* **26**, 173-180.
- Nakagawa, O., Nakagawa, M., Richardson, J. A., Olson, E. N., and Srivastava, D. (1999). HRT1, HRT2, and HRT3: a new subclass of bHLH transcription factors marking specific cardiac, somitic, and pharyngeal arch segments. *Dev Biol* **216**, 72-84.
- Offermanns, S., Heiler, E., Spicher, K., and Schultz, G. (1994). Gq and G11 are concurrently activated by bombesin and vasopressin in Swiss 3T3 cells. *FEBS Lett* **349**, 201-4.
- Offermanns, S., Toombs, C. F., Hu, Y. H., and Simon, M. I. (1997). Defective platelet activation in G alpha(q)-deficient mice. *Nature* **389**, 183-6.
- Offermanns, S., Zhao, L. P., Gohla, A., Sarosi, I., Simon, M. I., and Wilkie, T. M. (1998). Embryonic cardiomyocyte hypoplasia and craniofacial defects in G alpha q/G alpha 11-mutant mice. *Embo J* **17**, 4304-12.
- Santagata, S., Boggon, T.J., Baird, C.L., Gomez, C.A., Zhao, J., Shan, W.S., Myszka, D.G., and Shapiro, L. (2001). G-protein signaling through *tubby* proteins. *Science* **292**, 2041-2050.
- Shi, C.S., and Kehrl, J.H. (2001). PYK2 links Gq α and G13 α signaling to NF-kappa B activation. *J. Biol. Chem.* **276**, 31845-3150.
- Smrcka, A.V., and Sternweis, P.C. (1993). Regulation of purified subtypes of phosphatidylinositol-specific phospholipase C β by G protein α and $\beta\gamma$ subunits. *J. Biol. Chem.* **268**, 9667-9674.
- Thomas, T., Kurihara, H., Yamagishi, H., Kurihara, Y., Yazaki, Y., Olson, E. N., and Srivastava, D. (1998). A signaling cascade involving endothelin-1, dHAND and msx1 regulates development of neural-crest-derived branchial arch mesenchyme. *Development* **125**, 3005-14.
- Tian J., Ma, H.W., and Bancroft C. (1995). Constitutively active Gq α stimulates prolactin promoter activity via a pathway involving Raf activity. *Mol. Cell. Endocrinol.* **112**, 249-256.
- Wettschureck, N., Rutten, H., Zywiets, A., Gehring, D., Wilkie, T. M., Chen, J., Chien, K. R., and Offermanns, S. (2001). Absence of pressure overload induced myocardial hypertrophy after conditional inactivation of Galphaq/Galpha11 in cardiomyocytes. *Nat Med* **7**, 1236-40.

- Wilkie, T. M., Scherle, P. A., Strathmann, M. P., Slepak, V. Z., and Simon, M. I. (1991). Characterization of G-protein alpha subunits in the Gq class: expression in murine tissues and in stromal and hematopoietic cell lines. *Proc Natl Acad Sci U S A* **88**, 10049-53.
- Xu, D., Emoto, N., Giaid, A., Slaughter, C., Kaw, S., deWit, D., and Yanagisawa, M. (1994). ECE-1: a membrane-bound metalloprotease that catalyzes the proteolytic activation of big endothelin-1. *Cell* **78**, 473-85.
- Yamagishi, H., Garg, V., Matsuoka, R., Thomas, T., and Srivastava, D. (1999). A molecular pathway revealing a genetic basis for human cardiac and craniofacial defects. *Science* **283**, 1158-61.
- Yanagisawa, H., Yanagisawa, M., Kapur, R. P., Richardson, J. A., Williams, S. C., Clouthier, D. E., de Wit, D., Emoto, N., and Hammer, R. E. (1998). Dual genetic pathways of endothelin-mediated intercellular signaling revealed by targeted disruption of endothelin converting enzyme-1 gene. *Development* **125**, 825-36.

CHAPTER FOUR

HIF2 α , AP2 β , AND ET-1 COOPERATIVELY REGULATE DEVELOPMENT OF DUCTUS ARTERIOSUS SMOOTH MUSCLE

Background

Differentiation of smooth muscle cells in the developing embryo occurs in response to reciprocal signaling from surrounding cells and is marked by transcriptional initiation of smooth muscle-specific genes. The earliest of these markers to be expressed include smooth muscle alpha-actin and smooth muscle myosin while caldesmon and calponin mark more highly differentiated smooth muscle cells (reviewed in Owens, 2000). The repertoire of cytoskeletal and contractile proteins expressed determines the differentiation state of a given smooth muscle cell, giving rise to a spectrum of smooth muscle phenotypes from synthetic to contractile and maintenance of the differentiation state requires continuous input of positive and negative signals (Blau and Baltimore, 1991).

Smooth muscle cells arise from various embryonic progenitors including lateral plate mesoderm, cranial mesenchyme, and neural crest cells. During development, visceral smooth muscle differentiates from the lateral splanchnic mesoderm and contributes to the internal organs. Consistent with the embryo's early reliance on the circulatory system, vascular smooth muscle, arising in part from migratory neural crest cells, tends to differentiate earlier than smooth muscle of the lung, gut or bladder. In fact, markers of

smooth muscle differentiation first appear in the outflow tract where powerful arterial blood flow requires strong vascular integrity and modulation of arterial pressure relies on contractile tone (Miano et al., 1994). Neural crest cells contribute largely to the outflow tract and aortic arch and neural crest ablation causes loss or improper development of those vessels (reviewed in Hutson and Kirby, 2003).

Among the developing aortic arch structures, the ductus arteriosus, a specialized fetal vessel, contains the most highly differentiated smooth muscle and expresses high levels of calponin (Slomp et al., 1997). Mammalian fetal circulation relies on this shunt to deliver blood from the placenta, where it has the highest oxygen content, to the heart, brain, head, and upper torso while the lower body and placenta receive less oxygenated blood. At birth, ductal closure separates the pulmonary and systemic circulations so that fully oxygenated blood is delivered to all of the organs following gas exchange in the lungs. Closure of the ductus arteriosus occurs through a program involving oxygen sensing by the specialized smooth muscle cells of the ductus arteriosus as well as response to a decrease in the circulating levels of the vasodilating hormone prostaglandin E_2 . Failure of this process results in patent ductus arteriosus (PDA), the third most common congenital heart defect (Hoffman and Kaplan, 2002).

Although the physiology of the ductus arteriosus has been well described, little is known about the transcriptional pathways that specify this unique vessel. In humans, DNA-binding mutations in the gene encoding the transcription factor AP2 β are associated with patent ductus arteriosus (Satoda et al., 2000; Zhao et al., 2001). Targeted deletion of *Tfap2 β* in mice causes apoptosis of renal epithelial cells resulting in polycystic kidney disease and

postnatal lethality (Moser et al., 1997), but the patency of the *Tfap2 β ^{-/-}* ductus arteriosus has not been assessed.

Endothelin-1 (Et-1) is also thought to play a role in appropriate development and closure of the ductus arteriosus. Et-1, as previously mentioned, is a small signaling peptide generally expressed in and secreted from vascular endothelial cells. Cleavage of the pro-form of Et-1 by the endothelin converting enzyme allows it to bind to its receptor, Et_A, expressed in adjacent vascular smooth muscle cells (Xu et al., 1994). Et_A signaling is required for development of neural crest-derived structures as targeted deletion of any of the components of the Et_A signaling pathway results in craniofacial and outflow tract abnormalities (Kurihara et al., 1994; Clouthier et al., 1998; Yanagisawa et al., 1998). Results of many in vivo and in vitro studies strongly support a role for endothelin signaling in oxygen-induced constriction of the ductus arteriosus (Coceani et al., 1991; Coceani et al., 1999; Momma et al., 2003; Taniguchi et al., 2003).

Although endothelin-1 has been described as the effector of oxygen signaling in the ductus arteriosus due to its requirement for oxygen-induced constriction, it lacks inherent oxygen sensing capabilities. Among the better-characterized oxygen-sensing factors are members of the family of hypoxia-inducible factors (Hifs), which are bHLH/PAS domain-containing transcription factors. Under normoxic conditions, Hifs are hydroxylated by particular oxygen-sensitive prolyl hydroxylases leading to their ubiquitination and proteasomal degradation. But during hypoxia, Hifs are stabilized and imported to the nucleus where they become activated, heterodimerize with Arnt, another bHLH/PAS

domain-containing protein, and bind DNA to regulate transcription of target genes (reviewed in Bruick, 2003).

Here, we show that an individual with patent ductus arteriosus carried a heterozygous nonsense mutation in the gene encoding the endothelin receptor, Et_A , and that *Et-1*, which encodes an Et_A ligand, was uniquely expressed in the smooth muscle of the ductus arteriosus together with *Hif2 α* and *Tfap2 β* . *Ap2 β* was required for expression of *Hif2 α* and *Et-1* specifically in the smooth muscle cells of the ductus arteriosus. *Tfap2 β ^{-/-}* mice had abnormal ductal smooth muscle differentiation and subsequently, delayed ductal closure. Finally, we found that *Hif2 α* functioned in a negative autoregulatory loop by disrupting sequence-specific DNA binding by *Ap2 β* . These results suggest that *Hif2 α* , *Ap2 β* and *Et-1* are important for the appropriate development and maturation of the smooth muscle of the ductus arteriosus.

Results

Et-1 is specifically expressed in the smooth muscle of the ductus arteriosus during development

To determine potential genetic contributions to the etiology of congenital heart disease, our laboratory has begun to analyze the DNA sequence of candidate genes necessary for cardiogenesis from patients with sporadic cases of congenital heart disease. One of these patients, who had PDA, carried a heterozygous nonsense mutation within the gene encoding the endothelin receptor, ET_A (Fig. 1a). The mutation in this individual introduced a premature stop codon, truncating the receptor and eliminating its cytoplasmic tail. This

mutation was not found in 300 control chromosomes and a similar truncation rendered the receptor non-functional (Hashido et al., 1992). Since constriction of mouse ductal smooth muscle is impaired in the absence of endothelin signaling (Coceani et al., 1999) and Et_A is critical for development of neural crest-derived structures such as the ductus arteriosus (Clothier et al., 1998), we suspected that this individual's PDA could be attributed to decreased Et_A signaling. To determine whether the expression pattern of Et_A is consistent with a role for endothelin signaling in specifying the uniquely contractile smooth muscle of the ductus arteriosus, we examined Et_A mRNA expression in the great vessels of embryonic day (E) 13.5 mouse embryos, when remodeling of the outflow tract has occurred, separating the pulmonary artery from the aorta, and fetal circulation has become dependent on the arterial duct (Fig. 1b). We found that Et_A was expressed in smooth muscle cells throughout the great vessels but did not uniquely mark the smooth muscle cells of the ductus arteriosus.

Since Et-1 is the major ligand that signals through the Et_A receptor, we examined expression of $Et-1$ mRNA in the great vessels of E13.5 mouse embryos (Fig. 1d). In addition to the known expression of $Et-1$ in endothelial cells throughout the developing vasculature, we detected $Et-1$ mRNA specifically in the smooth muscle of the ductus arteriosus with distinct borders at the aortic and pulmonary artery junctions. Although the presence of a nonsense mutation in an individual with PDA does not prove that the condition is caused by the mutated ET_A allele, that observation in conjunction with the specific expression of $Et-1$ in the smooth muscle of the ductus arteriosus is consistent with a role for endothelin signaling in development of this specialized smooth muscle.

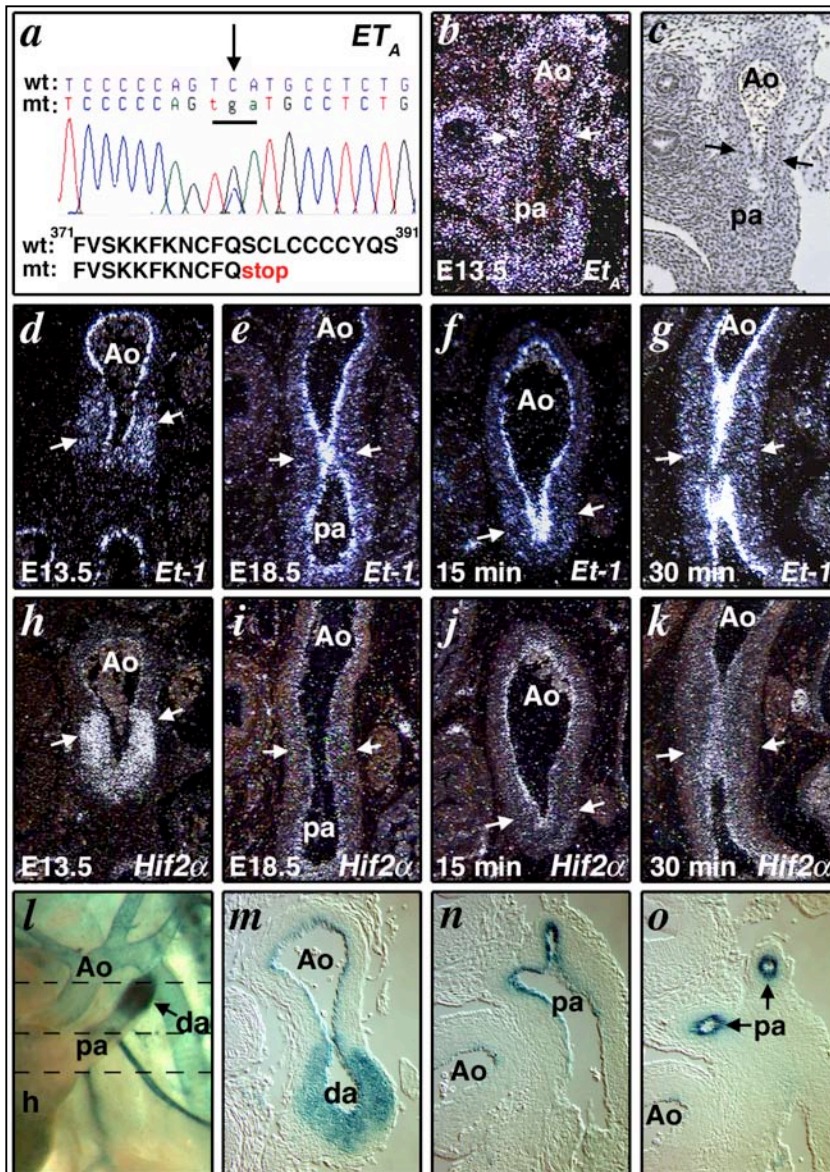


Figure 1. Endothelin and Hif2 α in the smooth muscle of the ductus arteriosus during development.

Chromatograph showing a partial sequence from the *ET_A* locus of an individual with PDA (a). Wildtype (wt) and mutant (mt) allele are shown and mutated nucleotide is indicated (arrow). Partial amino acid sequences of the wild-type and mutant allele are shown below. Radioactive section in situ hybridization using an *Et_A* mRNA probe showed uniform expression of *Et_A* in the smooth muscle throughout aorta (Ao), pulmonary artery (pa) and ductus arteriosus (arrows) (b). Corresponding bright field image is shown (c). Radioactive section in situ using an *Et-1*

mRNA probe revealed ductal smooth muscle expression at E13.5 (d) which was absent in animals harvested at E18.5 (e) and 15 (f) or 30 minutes (g) after birth while endothelial expression persisted. Radioactive section in situ using a *Hif2 α* mRNA probe showed overlapping temporo-spatial expression with *Et-1* (h-k). LacZ- stained E14.5 *Hif2 α ^{+/-lacZ}* embryo showed strong β -galactosidase expression in the ductus arteriosus (da) (l). Histological analysis of LacZ-stained *Hif2 α ^{+/-lacZ}* embryo confirmed strong ductal smooth muscle expression (m) while expression in the aorta (m), pulmonary trunk (n), and distal branches of the pulmonary artery (o) was confined to the vascular endothelium.

In lambs, Et-1 release from ductal smooth muscle cells during the perinatal period is associated with constriction of the vessel at birth (Coceani et al., 1991). We examined *Et-1* expression in the ductus arteriosus of E18.5 mouse embryos and in neonatal mice harvested at 15 or 30 minutes after birth to determine whether mouse ductal smooth muscle expresses *Et-1* perinatally (Fig 1e-g). We found that by E18.5, the smooth muscle expression of *Et-1* in the ductus arteriosus was extinguished and that it was not re-initiated after birth, although endothelial expression remained. The ductal smooth muscle expression of *Et-1* during development, in addition to its expression in the endothelium, likely results in especially high levels of endothelin signaling in the arterial duct that may contribute to the unique development and oxygen-sensitivity of the ductal smooth muscle later at the time of parturition.

Hif2 α , a potential transcriptional regulator of Et-1, is specifically expressed in the smooth muscle of the ductus arteriosus during development

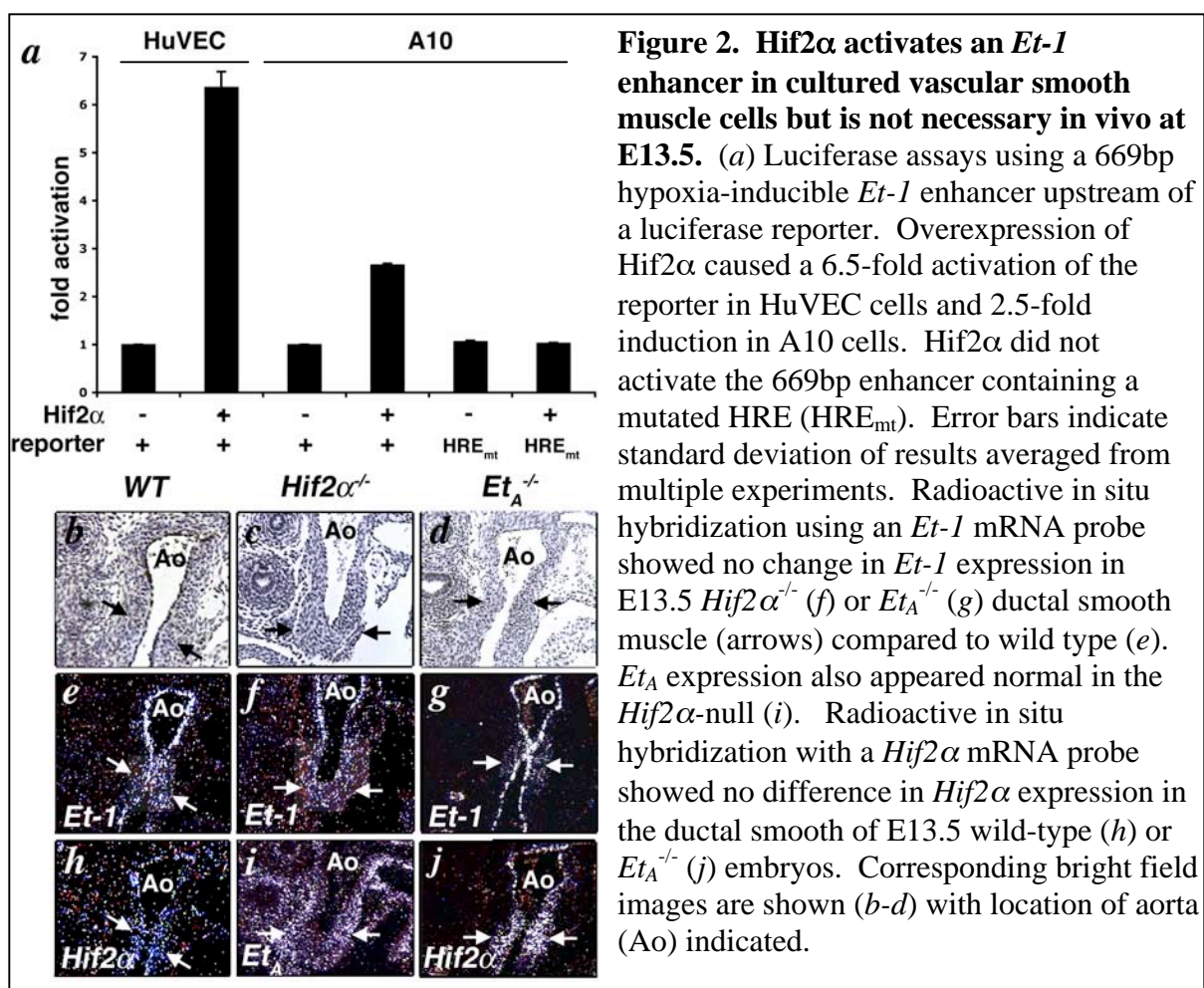
Hypoxic induction of *Et-1* expression occurs through a Hif response element upstream of *Et-1* (Yamashita et al., 2001). Therefore, we asked whether the unique ductal smooth muscle expression of *Et-1* might be under control of a member of the Hif protein family. We examined expression of the genes encoding Hif1 α , -2 α , and -3 α to determine whether any of these three genes were expressed in the smooth muscle of the ductus arteriosus. At E13.5, both *Hif1 α* and *Hif3 α* were ubiquitously expressed throughout the developing embryo (data not shown), while *Hif2 α* was expressed primarily in vascular endothelial cells, as previously described (Tian et al., 1997) (Fig. 1h). However, we found

that *Hif2α* was also expressed specifically in the smooth muscle of the ductus arteriosus, similarly to *Et-1*. We examined the expression of *Hif2α* at E18.5, and 15 or 30 minutes after birth and found that, like *Et-1*, *Hif2α* expression declined by E18.5 in the ductal smooth muscle but was maintained in the vascular endothelium (Fig. 1i-k). To visualize expression of *Hif2α* at higher resolution, we obtained E13.5 *Hif2α*^{+/-} embryos whose targeted allele contains a *LacZ* cassette in place of the second exon (Tian et al., 1998) and observed strong β-galactosidase activity in the ductus arteriosus (Fig. 1l). Histological analysis through the outflow tract of these β-gal-stained embryos revealed that while *LacZ* expression was restricted to vascular endothelial cells of the aorta, pulmonary trunk, and distal pulmonary arteries, staining extended from the endothelial cells into the smooth muscle layer only within the ductus arteriosus, consistent with the results of radioactive section in situ hybridization for *Hif2α* mRNA (Fig. 1m-o). *Hif2α* expression was not observed in any other smooth muscle of the embryo at this stage.

Hif2α and Et-1 are not required for one another's expression in the smooth muscle of the ductus arteriosus

Because *Et-1* and *Hif2α* were specifically coexpressed in the smooth muscle of the ductus arteriosus at E13.5, we investigated the possibility of an epistatic relationship between the two genes. A Hif response element (HRE) at position -118 upstream of the *Et-1* transcription start site is required for hypoxic induction of *Et-1* mRNA expression in cultured vascular endothelial cells (Hu et al., 1998). Using a 669 base pair enhancer corresponding to the upstream region of the *Et-1* locus to drive expression of luciferase, we performed reporter

assays to test whether Hif2 α was able to activate transcription through this HRE in smooth muscle cells (Fig. 2a). All transfections were carried out with a mutant form of Hif2 α containing alanine residues in place of both prolines that would otherwise be hydroxylated during normoxia, resulting in a stable form of the protein. Overexpression of Hif2 α caused a



6.5-fold induction of the reporter in HuVEC cells, confirming the activity of Hif2 α on this enhancer. We also found that Hif2 α was able to activate the reporter to a lesser extent in an A10 aortic smooth muscle cell line. Mutation of the HRE abolished the transcriptional

activation by Hif2 α indicating that Hif2 α can act through that site to initiate transcription in cultured vascular smooth muscle cells.

To determine whether Hif2 α was required for expression of *Et-1* in the smooth muscle of the ductus arteriosus in vivo, we compared expression of *Et-1* mRNA in E13.5 *Hif2 α ^{-/-}* embryos and their wild-type littermates. We found that *Et-1* mRNA expression was maintained in the absence of Hif2 α in both the vascular endothelium and ductal smooth muscle cells (Fig. 2e,f). We also examined *Et_A* expression in the *Hif2 α -null* and found it to be comparable to the wild type (Fig. 2i). Given the co-expression of *Hif2 α* and *Et-1*, we also examined expression of *Hif2 α* and *Et-1* mRNA in *Et_A^{-/-}* animals to determine whether *Hif2 α* expression in the smooth muscle of the ductus arteriosus was dependent on endothelin signaling and whether *Et-1* expression was altered in the absence of its receptor. We found that E13.5 *Et_A^{-/-}* embryos and their wild-type littermates had equivalent levels of both *Hif2 α* and *Et-1* mRNA expression in both the vascular endothelium and ductal smooth muscle cells (Fig. 2g,j). This result, along with the maintenance of *Et-1* expression in the *Hif2 α ^{-/-}*, indicated that there was not an epistatic relationship between *Hif2 α* and *Et-1* at E13.5 and that while Hif2 α could activate *Et-1* in tissue culture, it was not required in vivo.

Tfap2 β is expressed in the smooth muscle of the ductus arteriosus and Tfap2 β ^{-/-} mice have delayed ductal closure

Targeted deletion of *Hif2 α* in mice results in embryonic lethality beginning around E11.5, preceding formation of the ductus arteriosus (Tian et al., 1998). Because the early demise of *Hif2 α ^{-/-}* embryos precluded analysis of ductal development, we examined an

alternative genetic model of impaired ductal development to determine *Hif2α*'s potential role in vivo. Since *TFAP2β* is important for development and closure of the human ductus arteriosus, we hypothesized that *Tfap2β*^{-/-} mouse embryos may display defects of ductal development, thus serving as an appropriate model for our studies. To determine whether *Tfap2β* was normally expressed in the developing mouse ductus arteriosus, we assayed *Tfap2β* mRNA expression in embryonic mouse arterial ducts. At E13.5, *Tfap2β* mRNA was strongly expressed in the smooth muscle of the ductus arteriosus with sharp borders at the aortic and pulmonary artery ends, similar to *Hif2α* (Fig. 3). However, *Tfap2β* was not expressed in vascular endothelial cells.

Tfap2β^{-/-} animals survive several days postnatally (Moser et al., 1997) allowing assessment of their ductal patency. We observed that in wild-type pups, the ductus arteriosus begins to constrict by about thirty minutes after birth and that functional closure occurs as early as one hour after birth and is universally completed by two hours postnatally. We found that ductal closure in wild-type and *Tfap2β*^{+/-} pups always occurred within two hours of birth, but that *Tfap2β*^{-/-} animals had delayed ductal closure. These results reveal that *Tfap2β*^{-/-} mice display delayed ductal closure but that alternative pathways can compensate for the absence of *Tfap2β* in mice, unlike in humans, ultimately resulting in closure of the ductus arteriosus. Also, the early expression of *Tfap2β* suggests that it is important for ductal smooth muscle development in preparation for

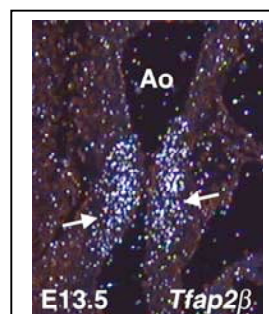
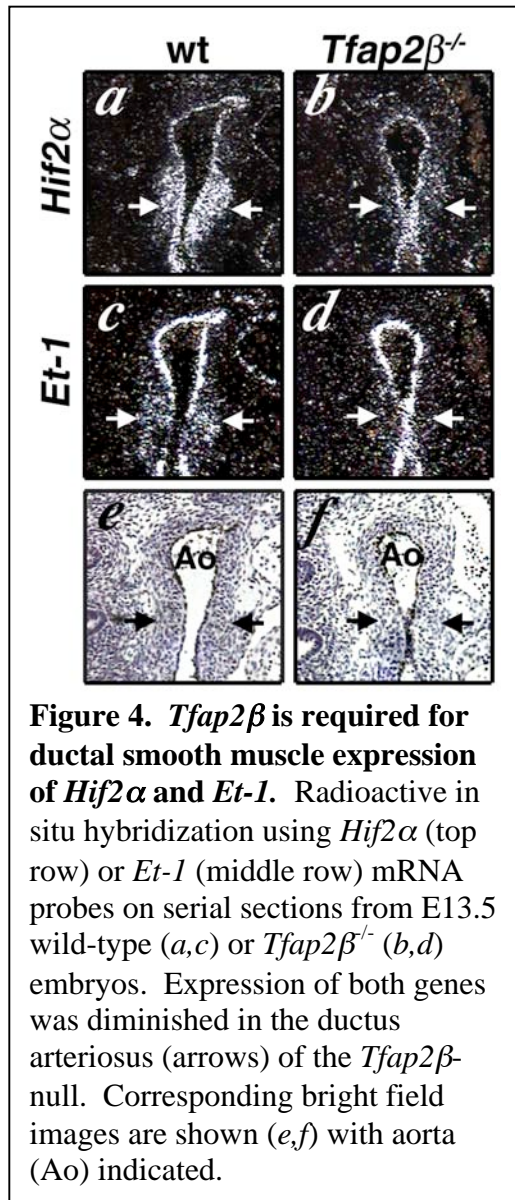


Fig. 3. *Tfap2β* is expressed in the smooth muscle of the ductus arteriosus.

Radioactive in situ hybridization using a *Tfap2β* mRNA probe on a section through the great vessels of an E13.5 mouse embryo. Arrows indicate the location of the ductus arteriosus adjacent to the aorta (Ao).

the closure events that occur at birth. Finally, the survival of *Tfap2* $\beta^{-/-}$ pups into the postnatal period provided a model of impaired ductal development suitable for further analysis of *Hif2* α .



Tfap2 β is required for ductal smooth muscle expression of *Hif2* α and *Et-1*

Given *Tfap2* β 's essential role in ductal smooth muscle cells, we compared both *Hif2* α and *Et-1* expression in wild-type and *Tfap2* $\beta^{-/-}$ mouse embryos to determine whether lack of *Ap2* β would affect expression of either of these genes. We found that at E13.5, *Tfap2* $\beta^{-/-}$ mouse embryos had decreased *Hif2* α and *Et-1* mRNA expression specifically in the smooth muscle of the ductus arteriosus, compared to endothelial expression within the same embryo (Fig. 4). This result demonstrated a dependence on *Tfap2* β specifically for ductal smooth muscle expression enhancement of *Hif2* α and *Et-1* and suggests that *Hif2* α or *Et-1* may function in a transcriptional pathway downstream of *Tfap2* β to control development of

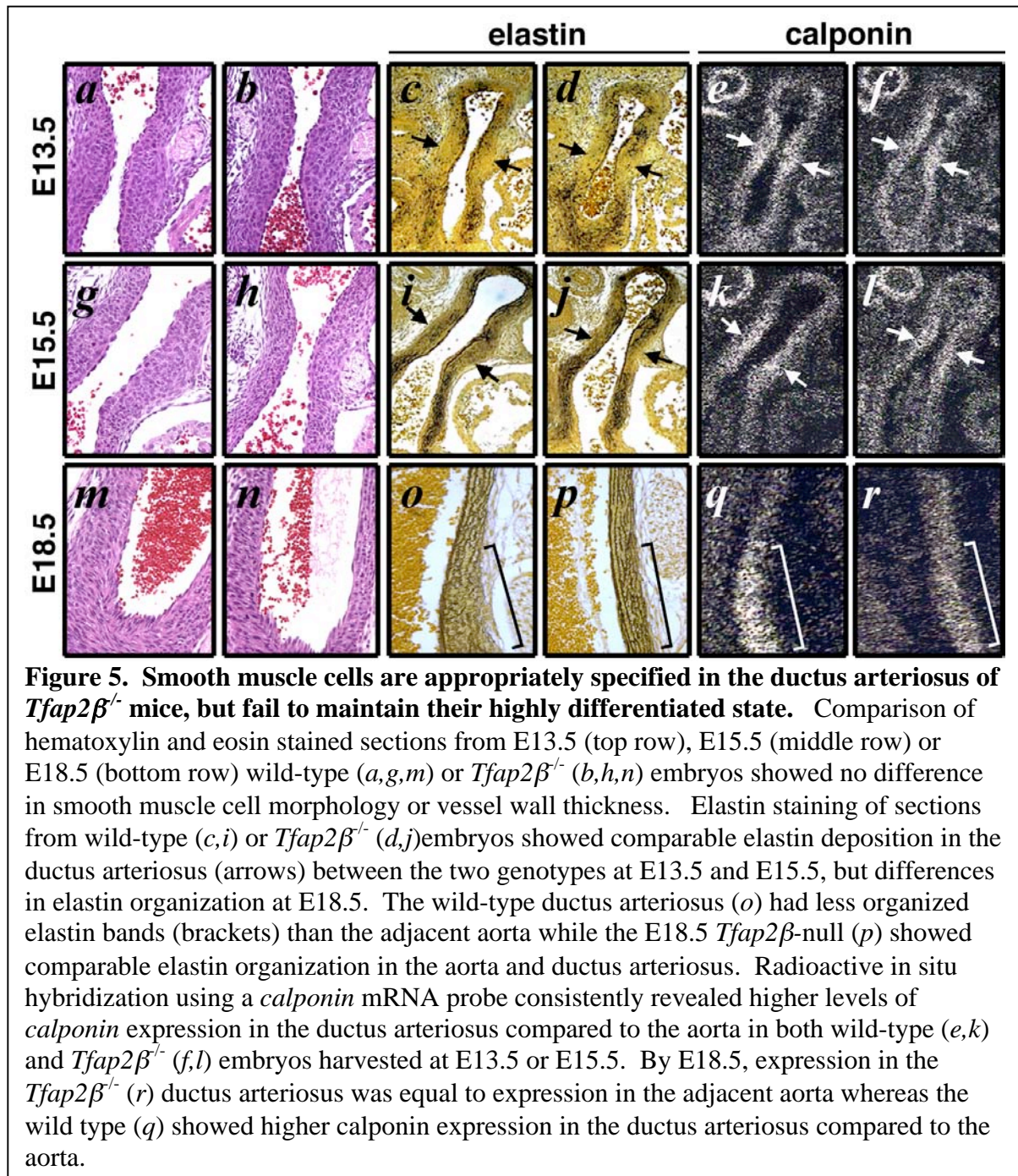
the unique smooth muscle cells of the ductus arteriosus.

Smooth muscle cells are appropriately specified in the ductus arteriosus of $Tfap2\beta^{-/-}$ mice, but fail to maintain their highly differentiated state

Delayed ductal closure and diminished expression of *Hif2 α* and *Et-1* in $Tfap2\beta^{-/-}$ pups could result from absence of smooth muscle cells or a lack of appropriately differentiated smooth muscle cells in the ductus arteriosus of these animals. To determine whether ductal smooth muscle was present and correctly specified as contractile, we performed histological analysis of wild-type or $Tfap2\beta^{-/-}$ embryos harvested at E13.5, E15.5 or E18.5 (Fig. 5). Analysis of hematoxylin and eosin (H&E) stained sections from wild-type and mutant embryos revealed no difference in ductal smooth muscle cell morphology between the two genotypes. We also noted that the diameter of the vascular wall appeared comparable in the wild-type and $Tfap2\beta^{-/-}$ embryos at all stages examined. To assess whether the differentiation of ductal smooth muscle was affected by the absence of *Tfap2 β* , we examined elastin deposition by performing Verhoeff-van Gieson staining on serial sections from the same embryos used for H&E analysis. We found that both the wild-type and $Tfap2\beta^{-/-}$ ductus arteriosus contained less elastin than the aorta or pulmonary artery from E13.5 through E15.5 but this difference was lost by E18.5. However, while elastin levels appeared comparable in the ductus arteriosus of wild-type and $Tfap2\beta^{-/-}$ embryos at E18.5, we observed a difference in fiber organization between the two genotypes. In the wild type, elastin fibers of the ductus arteriosus appeared less organized than in the aorta, consistent with the highly differentiated and contractile state of ductal smooth muscle compared to aortic smooth muscle. But in the $Tfap2\beta^{-/-}$, elastin fibers were well organized in both the aorta and ductus arteriosus,

suggesting that loss of *Tfap2* β resulted in a defect of ductal smooth muscle differentiation.

We also examined expression of *calponin*, a marker of highly differentiated, contractile smooth muscle cells, on serial sections from the same embryos used for previous histological



analysis. Radioactive in situ hybridization using an ^{35}S -labelled *calponin* mRNA probe revealed higher levels of *calponin* mRNA expression in ductal smooth muscle of both wild-type and *Tfap2 β ^{-/-}* embryos from E13.5 through E15.5 relative to the adjacent smooth muscle of the aorta and pulmonary artery. Preferential expression of *calponin* in the ductal smooth muscle persisted at E18.5 in the wild type. However, in the absence of *Tfap2 β* , enhancement of *calponin* expression in the ductal smooth muscle was lost by E18.5. These results indicated that the smooth muscle of the mouse ductus arteriosus matures earlier than the aortic or pulmonary artery smooth muscle and is less elastic, consistent with previous reports on the developing human ductus arteriosus (Slomp et al., 1997). However, *Tfap2 β* was necessary to maintain the highly differentiated state of ductal smooth muscle, and this may contribute to the delayed ductal closure we observed in *Tfap2 β ^{-/-}* neonates. Further, our results show that smooth muscle cells were present and appropriately specified in the absence of *Tfap2 β* , and therefore, down-regulation of *Hif2 α* and *Et-1* in the *Tfap2 β* mutants is unlikely to be due to a lack of ductal smooth muscle cells in these embryos.

Hif2 α blocks transcriptional activation by Ap2 β by preventing DNA-binding by Ap2 β

Since the transcription factors Ap2 β and Hif2 α are uniquely coexpressed in the smooth muscle of the ductus arteriosus and the ability of Ap2 β to act as a transcriptional activator is well established, we asked whether Hif2 α could affect the transactivation potential of Ap2 β . To study this, we utilized a chloramphenicol acetyltransferase (CAT) reporter assay system whereby an expression vector containing three tandem copies of an Ap2 binding element upstream of a CAT cDNA was cotransfected into NIH-3T3 cells with or

without a *Tfap2 β* expression vector. We found that while Ap2 β could activate this reporter as previously described (Satoda et al., 2000), Hif2 α not only failed to activate the reporter, but when co-transfected with Ap2 β , also blocked Ap2 β -induced activation (Fig. 6a). Since Ap2 β and Hif2 α both rely of the transcriptional coactivator P300 for their transactivation activity, we considered the possibility that negative regulation of Ap2 β by Hif2 α could be explained by sequestration of P300 by the overexpressed Hif2 α . To test this idea, we cotransfected excess P300 with Ap2 β , Hif2 α , or both and found that, although overexpression of P300 was able to enhance the transactivation potential of Ap2 β , it could not rescue the negative regulation by Hif2 α , indicating that sequestration of P300 by Hif2 α was not the mechanism by which Hif2 α negatively regulated Ap2 β activity. Because the decrease in Ap2 β activity upon cotransfection with Hif2 α could also be caused by a decrease in Ap2 β expression, we assayed Ap2 β expression by performing western analysis on the cell lysates used for ELISA. We found that Ap2 β protein expression was actually increased upon coexpression with Hif2 α and P300, and yet, Ap2 β transactivation activity declined (Fig 6). Thus, Hif2 α negatively regulated transactivation by Ap2 β independently of P300 sequestration or changes in Ap2 β expression.

We speculated that negative regulation of Ap2 β by Hif2 α could occur through one of two mechanisms—either Hif2 α could form a complex on DNA with Ap2 β , thereby prohibiting transactivation by Ap2 β or, alternatively, Hif2 α could disrupt DNA binding by Ap2 β altogether, thus preventing transactivation. To distinguish between these two possibilities, we performed electrophoretic mobility shift assays (EMSAs) using *in vitro* transcribed and translated Ap2 β or Hif2 α protein and a ³²P-labelled oligonucleotide

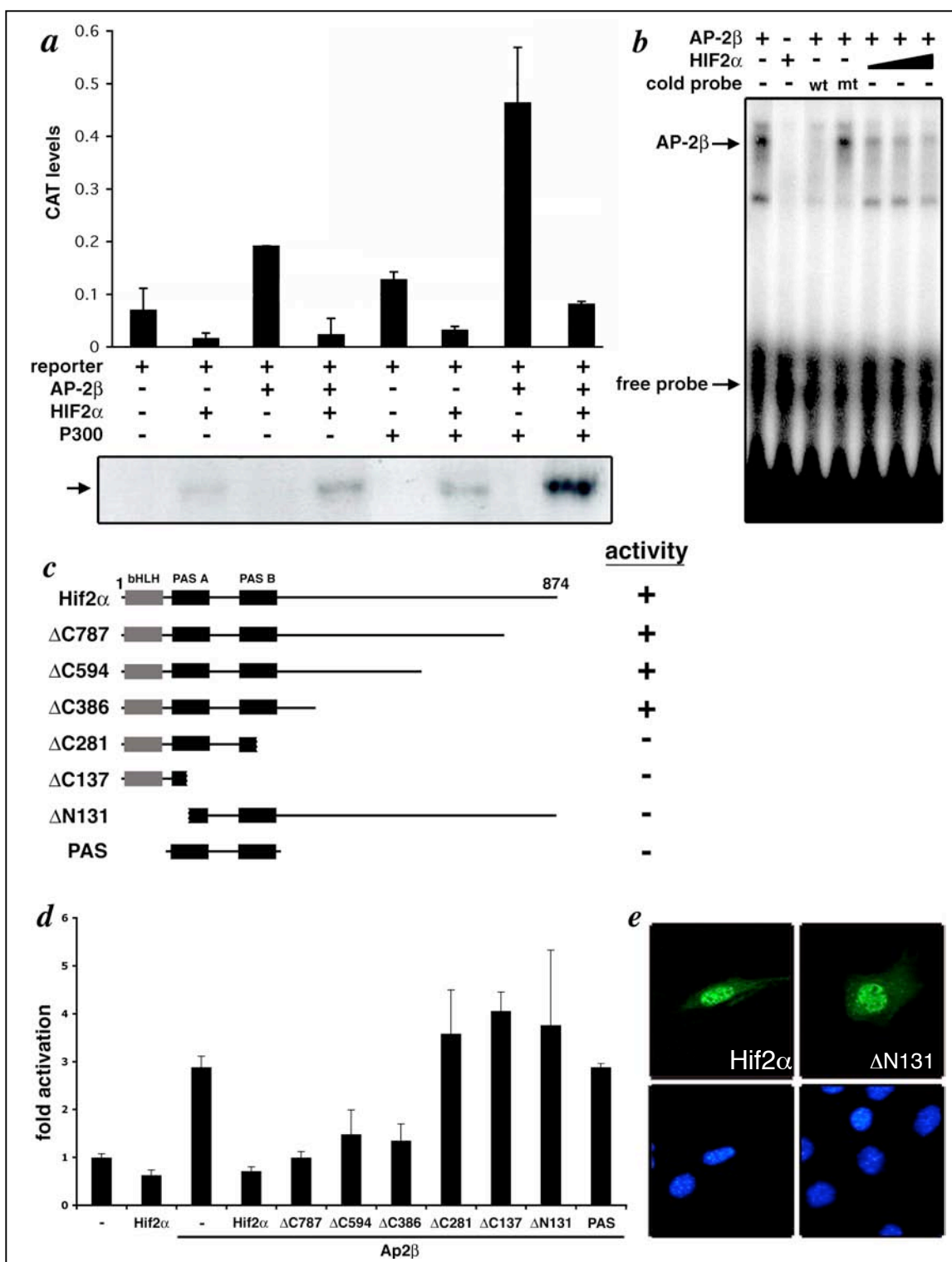


Figure 6. Hif2 α negatively regulates activity through inhibition of DNA-binding. (a) ELISAs measuring chloramphenicol acetyltransferase (CAT) protein levels in cell lysates. NIH-3T3 cells were transfected with a CAT reporter containing three copies of an Ap2 binding element. Ap2 β , Hif2 α , or P300 were cotransfected as indicated. Ap2 β activated the reporter and this activation was decreased in the presence of Hif2 α . Cotransfection of P300 did not rescue the loss of activation. Error bars indicate standard deviation of results averaged from several experiments. Western analysis of Ap2 β protein in each sample is shown. (b) Electromobility shift assays performed using *in vitro* transcribed and translated Ap2 β or Hif2 α protein and a 32 P-labeled oligo containing an Ap2 binding site. 100x cold wild-type oligo (wt) competed for Ap2 β binding, while 100x cold mutant oligo (mt) failed to compete, demonstrating sequence-specific binding to the probe by Ap2 β . Hif2 α failed to shift the probe, but reduced the amount of oligo shifted in the presence of Ap2 β in a dose-dependent manner signifying its ability to disrupt DNA binding by Ap2 β . (c) Schematic showing amino-terminal and carboxy-terminal truncations of Hif2 α used in reporter assays and EMSAs and summary of activation data. (d) ELISAs measuring chloramphenicol acetyltransferase (CAT) protein levels in cell lysates. NIH-3T3 cells were transfected with a CAT reporter containing three copies of an Ap2 binding element. Ap2 β , Hif2 α , or truncations of Hif2 α were cotransfected as indicated. Error bars indicate standard deviation of results averaged from several experiments. (e) Immunocytochemistry detecting overexpressed Hif2 α or Δ N131 in NIH-3T3 cells. Both forms of the protein are localized to the nucleus. Corresponding DAPI-staining shown below.

containing an Ap2 consensus binding site. We found that, while Ap2 β was able to specifically shift the radioactive oligonucleotide, addition of Hif2 α with Ap2 β resulted in a dose-dependent decrease in the amount of DNA bound to Ap2 β (Fig. 6b). This result indicated that negative regulation of Ap2 β by Hif2 α was due to a decrease of site-specific DNA binding by Ap2 β in the presence of Hif2 α .

The N-terminus of Hif2 α containing the PAS domains is required to block DNA binding and transcriptional activation by Ap2 β

The amino-terminus of Hif2 α contains a bHLH domain, important for DNA binding and dimerization, and two PAS domain repeats, whose function remain unknown (Tian et al., 1997) while the carboxy-terminus consists of regions that have been characterized as transcriptional activation domains (O'Rourke et al., 1999). To determine which domains of Hif2 α were responsible for its ability to block transcriptional activation by Ap2 β , we generated truncations of Hif2 α (Fig. 6d) and tested them in our CAT reporter assay. We found that, while 386 amino acids of the amino-terminus containing the bHLH and PAS domains was sufficient to negatively affect the activity of Ap2 β , deletion of half of the second PAS domain resulted in failure to block Ap2 β 's activity suggesting that the PAS domains are required for this function. Further, deleting as little as 131 amino acids from the amino-terminus of Hif2 α resulted in the loss of its ability to block transcriptional activation by Ap2 β (Fig. 6e). However, the PAS domains alone were not sufficient to elicit this effect indicating that combinatorial action by the bHLH and PAS domains is required to block transcription by Ap2 β . Western analysis on the cell lysates used to measure CAT protein levels revealed no significant difference in Ap2 β protein levels (data not shown). Additionally, immunohistochemical analysis showed that Hif2 α mutants were appropriately localized to the nucleus (Fig. 6f). Thus, changes in Ap2 β expression or Hif2 α localization were not responsible for the observed differences in activation. These results indicated that the amino-terminus of Hif2 α was both necessary and sufficient to block DNA binding by Ap2 β , resulting in disruption of reporter transactivation. Since Ap2 β is required for ductal smooth muscle expression of Hif2 α , the negative feedback regulation of Ap2 β by Hif2 α may allow finer control of Ap2 β -dependent gene expression during development.

Discussion

Although the development and closure of the ductus arteriosus has been studied by anatomists and physiologists for decades, the transcriptional program regulating development of the specialized smooth muscle cells contained within this structure remains poorly understood. Clues from human genetics as well as pharmacological studies in lambs and rats (Coceani et al., 1991; Shen et al., 2002; Momma et al., 2003; Taniguchi et al., 2003) led us to study the interplay between hypoxic and endothelin signaling cascades and the transcription factor *Tfap2 β* during development of this ductal smooth muscle. We found that *Hif2 α* , *Et-1*, and *Tfap2 β* were coexpressed in the smooth muscle of the ductus arteriosus and that *Tfap2 β* was necessary for timely ductal closure and expression of both *Hif2 α* and *Et-1*. Although present in *Tfap2 β* mutants, ductal smooth muscle cells failed to maintain their uniquely differentiated state, which may have contributed to the delayed ductal closure. Finally, we found that *Ap2 β* activity was regulated by *Hif2 α* in a P300-independent manner through inhibition of sequence-specific DNA binding by *Ap2 β* , suggesting a negative feedback loop through which *Hif2 α* may titrate expression of *Ap2 β* target genes during ductal development.

Hif2 α protein vs. mRNA expression

We initially hypothesized that *Hif2 α* may play a role in ductal closure at the time of birth by acting as an oxygen-sensing transcription factor to maintain ductal patency during development, when vascular oxygen tension is low. According to that model, *Hif2 α* protein

would be degraded immediately following birth as a result of rising vascular oxygen levels, thus changing gene transcription programs in the ductal smooth muscle cells, allowing the arterial duct to constrict. However, we found that *Hif2 α* mRNA expression was absent by E18.5, preceding birth by at least 2 days. This does not rule out the possibility that Hif2 α protein remains for some time after mRNA expression is abolished, but the lack of a Hif2 α antibody that can be used for immunohistochemistry on mouse sections has prevented us from examining Hif2 α protein levels in the ductus arteriosus. However, it is unlikely that the Hif2 α protein is stable for more than two days in order to be present at high levels in the neonatal ductus arteriosus. Therefore, we believe that our expression data indicate that Hif2 α must be acting in ductal smooth muscle cells during late mid-gestation and may be contributing to ductal patency, development or maturation during that time period. In addition to directing transcription of specific target genes during ductal development, our data suggest that the role of Hif2 α includes balancing the transactivation potential of Ap2 β by negatively regulating Ap2 β -DNA binding.

Et-1 expression in the smooth muscle of the mouse ductus arteriosus declines prenatally

Previous studies indicate that endothelin-1 is expressed in the smooth muscle of the ductus arteriosus of near-term fetal lambs and its release is dependent on oxygen availability (Coceani et al., 1991). Our data show that in mice, endothelin-1 is not expressed perinatally within the ductal smooth muscle, although it is highly expressed in endothelial cells throughout the great vessels. This may indicate a species-specific difference with respect to the dependence on endothelin signaling for ductal closure. Indeed, comparison of mouse and

rat studies regarding endothelin signaling and ductal closure seem to indicate a difference between these two closely related rodent species with regard to their dependence on endothelin. In vivo, *Et_A*-null mice die postnatally of asphyxiation due to jaw deformation (Clouthier et al., 1998) and pharmacological inhibition of *Et_A* signaling in rats has recently been reported to result in similar defects in neural crest-derived structures (Taniguchi et al., 2003). However, administration of *Et_A* antagonists to rats during late gestation results in postnatal lethality without a jaw phenotype, and these mice were found to die from a patent ductus arteriosus (Taniguchi et al., 2003) unlike *Et_A^{-/-}* mice whose ducts close normally when intubated (Coceani et al., 1999). While this apparent disparity in endothelin signaling requirement for ductal closure could be due to the difference between pharmacological interference and targeted gene deletion, it likely reflects species variation in ductal closure mechanisms between mouse and rat. Conversely, both species may depend on Et-1 expression in the ductal smooth muscle during development, not to induce constriction, but to pattern the ductal smooth muscle in preparation for its physiological changes at birth.

It has been previously proposed that larger species, such as the rat and particularly the lamb, because of their larger vessel lumen diameter, rely more heavily on oxygen-induced constriction of the arterial duct at birth, which may be mediated by a factor such as endothelin, in order to bring the opposing vessel walls into close enough proximity to permit further closure events (Bergwerff et al., 1999). Smaller animals, such as the mouse, may not depend on dramatic endothelin-mediated constriction at birth, since less constriction would be required to restrict blood flow through their smaller duct. Alternatively, since the ductal smooth muscle layer is thicker in larger animals, secretion of endothelin from endothelial

cells alone may be insufficient to reach endothelin receptors on the smooth muscle cells within the interior of the smooth muscle layer, resulting in a need for endothelin expression and secretion from the smooth muscle cells themselves and this may have been implemented during the course of evolution. Further analysis of the time course of Et-1 expression in the ductus arteriosus of various species may reveal a correlation between vessel wall thickness and smooth muscle Et-1 expression at birth.

Human vs. mouse phenotypes with respect to Tfap2 β

In humans, heterozygous mutations resulting in single amino acid substitutions within the DNA binding or transactivation domains of TFAP2 β are associated with Char syndrome and result in facial dysmorphism, PDA and various degrees of hand anomalies (Satoda et al., 2000; Zhao et al., 2001). These mutant forms of TFAP2 β have been shown to dimerize normally with other Ap2 proteins and therefore have dominant-negative effects on transactivation. Therefore, DNA-binding mutations will affect not only the level of active Ap2 β homodimers and heterodimers containing Ap2 β , but also homo- and heterodimers of other AP2 family members which may be sequestered by inactive Ap2 β . In contrast, targeted deletion of Ap2 β in mice simply eliminates Ap2 β homodimers and heterodimers containing Ap2 β , but is not expected to affect homo- and heterodimers of other Ap2 family members. Although the expression of other Ap2 proteins in the ductus arteriosus of wild-type and Tfap2 β ^{-/-} embryos has not been examined, compensation by the remaining Ap2 family members may account for the delayed closure, rather than PDA, we observed in Tfap2 β ^{-/-} pups. Alternatively, the human ductus arteriosus may simply be more sensitive to

Ap2 β protein levels, whereas the mouse ductus arteriosus is able to overcome a lack of Ap2 β protein and the consequential effects on ductal smooth muscle differentiation. In fact, targeted deletion of smooth muscle myosin in mice, which would be expected to result in PDA due to the inability of the smooth muscle to contract without this structural protein, also results in postponement, but not failure of ductal closure (Morano et al., 2000) indicating that the mouse ductus arteriosus is able to close independently of smooth muscle constriction, albeit in a delayed manner. To date, the only genetic mouse models of patent ductus arteriosus arise from targeted deletion of genes encoding elements of the prostaglandin pathway. These include knockouts of the prostaglandin receptor, EP₄ (Nguyen et al., 1997), the prostaglandin dehydrogenase, Pgdh (Coggins et al., 2002), and compound knockouts of the cyclooxygenases, Cox-1 and Cox-2 (Loftin et al., 2001).

Clinical implications

Closure of the ductus arteriosus is vital for healthy extrauterine life. However, in the case of particular congenital heart defects including interrupted aortic arch or left ventricular hypoplasia, systemic blood flow is absolutely dependent on maintenance of ductal patency. Understanding the transcriptional regulation of normal ductal development, maturation and closure by factors such as Hif2 α , Ap2 β and Endothelin-1 will provide targets for rational drug design to either close or open the ductus arteriosus as needed and may help to elucidate pathways that result in changes that occur in other vascular structures in response to oxygen.

Materials and methods

Luciferase reporter assays

Luciferase assays were carried out in HuVEC or A10 cell lines (ATCC) transiently transfected with the indicated plasmids as well as a *LacZ* expression vector using Fugene6 (Roche) with the total amount of transfected DNA held constant using an empty expression vector. The reporter construct (kindly provided by N. Bishopric) consisted of 669bp from the promoter region of the *Et-1* locus cloned upstream of a luciferase reporter. Assays were performed using the Luciferase Assay System (Promega) on a luminometer (Rosys Anthos Lucy 2). Results were normalized to β -galactosidase activity as detected using an ONPG (*o*-nitrophenyl-galactopyranoside; Sigma) assay protocol as previously described (Sambrook et al., 1989).

LacZ staining

Timed matings were set up between *Hif2* $\alpha^{+/-}$ males and wild-type C57B6 females and pregnant mothers were sacrificed 14 days later. Embryos were harvested, fixed and stained for β -galactosidase (β -gal) activity as described previously (Yamagishi et al., 2000).

Embryo harvesting and histology

Mice of the appropriate genotype were intercrossed and embryos were collected at E13.5, E14.5, E15.5 or E18.5. In the case of neonate collection, pregnant females were kept under observation and pups were collected at the indicated time after birth, decapitated, and their chest cavity was opened. Embryos and pups were fixed in 4% paraformaldehyde overnight

at 4°C and then stored at -20°C in 70% ethanol. Genotype of *Hif2α*, *Tfap2β*, or *Et_A* was determined by polymerase chain reaction (PCR) performed on genomic DNA isolated from tails as described previously. Animals were then rehydrated in PBS, paraffin embedded and sectioned transversely.

Radioactive in situ hybridization

³⁵S-labeled antisense probes were synthesized from partial cDNAs of *Hif2α*, *Tfap2β*, *Et-1*, or *calponin*. cDNAs were linearized and transcribed using the following restriction enzymes and RNA polymerases: *Hif2α*-BamHI, SP6; *Tfap2β*-XbaI, T7; *Et-1*-EcoRV; SP6 (Ambion Inc.). Radioactive section in situ hybridization was performed on paraffin-embedded sections of mouse embryos using these riboprobes as previously described.

Transfections, CAT assays and western analysis

Transfections and CAT assays were performed as described previously (Satoda et al., 2000). Briefly, NIH-3T3 cells (ATCC) were transiently transfected with the indicated expression vectors using Fugene6 (Roche) and total amount of transfected DNA was held constant using an empty expression vector. Cells were harvested after 48 hours and CAT protein levels were measured in duplicate using a CAT ELISA kit (Roche). Each transfection was performed a minimum of three times. Western analysis to measure Ap2β protein levels was performed on cell lysates using a polyclonal Ap2β antibody (Santa Cruz Biotechnology), HRP-conjugated donkey anti-rabbit IgG (Santa Cruz Biotechnology) and Western Blotting Luminol Reagent (Santa Cruz Biotechnology).

Electrophoretic mobility shift assays

Oligonucleotides containing a consensus Ap2 binding site were synthesized (Integrated DNA Technologies) as follows: Control- 5'-GGGATCGAACTGACCGCCCGCGGCCCGT-3', 5'-GGGACGGGCCGCGGGCGGTCAGTTCGATC-3'; Mutant- 5'-GGGATTGTCAGACGTCTGTCGTCTGC-3', 5'-GGGCAGACGACAGACGTCTGACAAT-3'. Oligonucleotides were resuspended, combined in oligo annealing buffer, boiled for 5 minutes and slowly cooled to room temperature. Annealed oligonucleotides were radiolabeled with [α - 32 P]dCTP using a Klenow DNA polymerase and purified on Sephadex G-25 spin columns (Roche). Hif2 α and Ap2 β proteins were in vitro transcribed and translated using the TNT T7-coupled reticulocyte lysate system (Promega), using full-length cDNA templates cloned into pcDNA vectors (Invitrogen). DNA binding assays were performed in Gel Shift Binding 5X Buffer (Promega) in a 20 μ l total volume with the indicated volumes of each protein and 2 μ l of labeled oligonucleotide at 50,000 cpm. Amount of reticulocyte lysate used in each condition was held constant. 100X unlabeled wild-type or mutant competitor oligonucleotide was added to reactions as indicated. DNA-protein complexes were resolved on a 6% non-denaturing polyacrylamide gel in 0.5X TBE. Gels were exposed to a Phosphor screen and read in a PhosphorImager (Molecular Dynamics).

Hif2 α truncations

All truncations of *Hif2 α* were generated by PCR using a cDNA encoding a stable form of murine *Hif2 α* (Hif2 α P405A,P530V) (kindly provided by C. Simon) contained in pCDNA3 (Invitrogen) as template. Primer sequences available on request. PCR products were then subcloned back into pCDNA3 and resulting constructs were verified by sequencing.

References

- Bergwerff, M., M.C. DeRuiter, and A.C. Gittenberger-de Groot. 1999. Comparative anatomy and ontogeny of the ductus arteriosus, a vascular outsider. *Anat Embryol (Berl)* **200**: 559-71.
- Blau, H.M. and D. Baltimore. 1991. Differentiation requires continuous regulation. *J Cell Biol* **112**: 781-3.
- Bruick, R.K. 2003. Oxygen sensing in the hypoxic response pathway: regulation of the hypoxia-inducible transcription factor. *Genes Dev* **17**: 2614-23.
- Clouthier, D.E., K. Hosoda, J.A. Richardson, S.C. Williams, H. Yanagisawa, T. Kuwaki, M. Kumada, R.E. Hammer, and M. Yanagisawa. 1998. Cranial and cardiac neural crest defects in endothelin-A receptor-deficient mice. *Development* **125**: 813-24.
- Coceani, F. and L. Kelsey. 1991. Endothelin-1 release from lamb ductus arteriosus: relevance to postnatal closure of the vessel. *Can J Physiol Pharmacol* **69**: 218-21.
- Coceani, F., Y. Liu, E. Seidlitz, L. Kelsey, T. Kuwaki, C. Ackerley, and M. Yanagisawa. 1999. Endothelin A receptor is necessary for O₂ constriction but not closure of ductus arteriosus. *Am J Physiol* **277**: H1521-31.
- Coggins, K.G., A. Latour, M.S. Nguyen, L. Audoly, T.M. Coffman, and B.H. Koller. 2002. Metabolism of PGE₂ by prostaglandin dehydrogenase is essential for remodeling the ductus arteriosus. *Nat Med* **8**: 91-2.
- Hashido, K., T. Gamou, M. Adachi, H. Tabuchi, T. Watanabe, Y. Furuichi, and C. Miyamoto. 1992. Truncation of N-terminal extracellular or C-terminal intracellular domains of human ETA receptor abrogated the binding activity to ET-1. *Biochem Biophys Res Commun* **187**: 1241-8.
- Hoffman, J.I. and S. Kaplan. 2002. The incidence of congenital heart disease. *J Am Coll Cardiol* **39**: 1890-900.
- Hu, J., D.J. Discher, N.H. Bishopric, and K.A. Webster. 1998. Hypoxia regulates expression of the endothelin-1 gene through a proximal hypoxia-inducible factor-1 binding site on the antisense strand. *Biochem Biophys Res Commun* **245**: 894-9.
- Hutson, M.R. and M.L. Kirby. 2003. Neural crest and cardiovascular development: a 20-year perspective. *Birth Defects Res Part C Embryo Today* **69**: 2-13.
- Kurihara, Y., H. Kurihara, H. Suzuki, T. Kodama, K. Maemura, R. Nagai, H. Oda, T. Kuwaki, W.H. Cao, N. Kamada, and et al. 1994. Elevated blood pressure and

- craniofacial abnormalities in mice deficient in endothelin-1. *Nature* **368**: 703-10.
- Loftin, C.D., D.B. Trivedi, H.F. Tiano, J.A. Clark, C.A. Lee, J.A. Epstein, S.G. Morham, M.D. Breyer, M. Nguyen, B.M. Hawkins, J.L. Goulet, O. Smithies, B.H. Koller, and R. Langenbach. 2001. Failure of ductus arteriosus closure and remodeling in neonatal mice deficient in cyclooxygenase-1 and cyclooxygenase-2. *Proc Natl Acad Sci U S A* **98**: 1059-64.
- Miano, J.M., P. Cserjesi, K.L. Ligon, M. Periasamy, and E.N. Olson. 1994. Smooth muscle myosin heavy chain exclusively marks the smooth muscle lineage during mouse embryogenesis. *Circ Res* **75**: 803-12.
- Momma, K., T. Nakanishi, and S. Imamura. 2003. Inhibition of in vivo constriction of fetal ductus arteriosus by endothelin receptor blockade in rats. *Pediatr Res* **53**: 479-85.
- Morano, I., G.X. Chai, L.G. Baltas, V. Lamounier-Zepter, G. Lutsch, M. Kott, H. Haase, and M. Bader. 2000. Smooth-muscle contraction without smooth-muscle myosin. *Nat Cell Biol* **2**: 371-5.
- Moser, M., A. Pscherer, C. Roth, J. Becker, G. Mucher, K. Zerres, C. Dixkens, J. Weis, L. Guay-Woodford, R. Buettner, and R. Fassler. 1997. Enhanced apoptotic cell death of renal epithelial cells in mice lacking transcription factor AP-2beta. *Genes Dev* **11**: 1938-48.
- Nakagawa, O., M. Nakagawa, J.A. Richardson, E.N. Olson, and D. Srivastava. 1999. HRT1, HRT2, and HRT3: a new subclass of bHLH transcription factors marking specific cardiac, somitic, and pharyngeal arch segments. *Dev Biol* **216**: 72-84.
- Nguyen, M., T. Camenisch, J.N. Snouwaert, E. Hicks, T.M. Coffman, P.A. Anderson, N.N. Malouf, and B.H. Koller. 1997. The prostaglandin receptor EP4 triggers remodelling of the cardiovascular system at birth. *Nature* **390**: 78-81.
- Owens, G.K. 1991. Role of contractile agonists in growth regulation of vascular smooth muscle cells. *Adv Exp Med Biol* **308**: 71-9.
- Satoda, M., F. Zhao, G.A. Diaz, J. Burn, J. Goodship, H.R. Davidson, M.E. Pierpont, and B.D. Gelb. 2000. Mutations in TFAP2B cause Char syndrome, a familial form of patent ductus arteriosus. *Nat Genet* **25**: 42-6.
- Shen, J., T. Nakanishi, H. Gu, S. Miyagawa-Tomita, G.R. Wu, K. Momma, and M. Nakazawa. 2002. The role of endothelin in oxygen-induced contraction of the ductus arteriosus in rabbit and rat fetuses. *Heart Vessels* **16**: 181-8.
- Slomp, J., A.C. Gittenberger-de Groot, M.A. Glukhova, J. Conny van Munsteren, M.M.

- Kockx, S.M. Schwartz, and V.E. Koteliansky. 1997. Differentiation, dedifferentiation, and apoptosis of smooth muscle cells during the development of the human ductus arteriosus. *Arterioscler Thromb Vasc Biol* **17**: 1003-9.
- Taniguchi, T. and I. Muramatsu. 2003. Pharmacological knockout of endothelin ET(A) receptors. *Life Sci* **74**: 405-9.
- Tian, H., R.E. Hammer, A.M. Matsumoto, D.W. Russell, and S.L. McKnight. 1998. The hypoxia-responsive transcription factor EPAS1 is essential for catecholamine homeostasis and protection against heart failure during embryonic development. *Genes Dev* **12**: 3320-4.
- Tian, H., S.L. McKnight, and D.W. Russell. 1997. Endothelial PAS domain protein 1 (EPAS1), a transcription factor selectively expressed in endothelial cells. *Genes Dev* **11**: 72-82.
- Xu, D., N. Emoto, A. Giaid, C. Slaughter, S. Kaw, D. deWit, and M. Yanagisawa. 1994. ECE-1: a membrane-bound metalloprotease that catalyzes the proteolytic activation of big endothelin-1. *Cell* **78**: 473-85.
- Yamagishi, H., J. Maeda, M. Tokumura, S. Yoshiba, E. Takahashi, H. Fukushima, C. Yamagishi, N. Matsuo, and Y. Kojima. 2000. Ventricular septal defect associated with microdeletions of chromosome 22q11.2. *Clin Genet* **58**: 493-6.
- Yamashita, K., D.J. Discher, J. Hu, N.H. Bishopric, and K.A. Webster. 2001. Molecular regulation of the endothelin-1 gene by hypoxia. Contributions of hypoxia-inducible factor-1, activator protein-1, GATA-2, AND p300/CBP. *J Biol Chem* **276**: 12645-53.
- Yanagisawa, H., R.E. Hammer, J.A. Richardson, S.C. Williams, D.E. Clouthier, and M. Yanagisawa. 1998. Role of Endothelin-1/Endothelin-A receptor-mediated signaling pathway in the aortic arch patterning in mice. *J Clin Invest* **102**: 22-33.
- Zhao, F., C.G. Weismann, M. Satoda, M.E. Pierpont, E. Sweeney, E.M. Thompson, and B.D. Gelb. 2001. Novel TFAP2B mutations that cause Char syndrome provide a genotype-phenotype correlation. *Am J Hum Genet* **69**: 695-703.

CHAPTER FIVE

CONSIDERATIONS AND FUTURE DIRECTIONS

Dissecting Independent Roles of Endothelin-1

In addition to its many effects on postnatal physiology, Et-1 also plays several different roles during development. This is evidenced by mice with targeted deletion of genes encoding proteins important in the endothelin signaling cascade such as Et-1 (Kurihara et al., 1994), Et_A (Clouthier et al., 1998), or Ece-1 (Yanagisawa et al., 1998), which fail to form neural crest-derived structures of the head and face. My analysis of G α_q and G α_{11} -deficient mice has added to our understanding of how downstream effectors of endothelin signaling differ between various tissues such as the pharyngeal arch mesenchyme and neuronal cell populations. Also, my novel observation of Et-1 expression in the developing smooth muscle of the ductus arteriosus, as well as its dependence on Ap2 β expression in that tissue, further supports a role for endothelin in development, maturation, and/or physiological response of this vessel as it constricts in response to rising oxygen tension at birth. However, the exact role that endothelin is playing in smooth muscle of the arterial duct during mid-late gestation remains to be discovered.

Pharmacological studies in mice, rats, or lambs treated with agonists or antagonists of the Et_A receptor at various times during gestation or after birth have permitted further dissection of the time-periods during which Et_A affects growth and development of particular structures. In fact, Et_A receptor blockade in rats during late gestation specifically causes

patent ductus arteriosus, while exposure to the drug earlier during development will also lead to craniofacial abnormalities through its adverse effect on neural crest development (Taniguchi et al., 2003). This finding supports the idea that endothelin can directly promote constriction of the ductus arteriosus in addition to patterning the neural crest cells that ultimately contribute to the smooth muscle of the arterial duct which behave uniquely at birth.

Endothelin-1 has also been shown to promote proliferation of pulmonary smooth muscle cells, where it is endogenously produced in hypertensive adults (Wort et al., 2001). Additionally, endothelin is upregulated in ischemic or hypoxic tissues where it activates genes and signaling pathways required for the hypoxic response (reviewed in Goraca, 2002). Clearly, endothelin signaling is critical for neural crest development, smooth muscle cell proliferation, and response of multiple cell types to hypoxia and future studies will be necessary to discern when and how endothelin is specifically affecting these processes in the smooth muscle of the ductus arteriosus and what, if any, interdependence there is between the three events.

Retinoic Acid and Neural Crest

Perturbations of retinoic acid (RA) signaling cause defects in development of the neural crest. Compound knockout of the retinoic acid receptor (*RAR*) genes leads to embryonic or perinatal lethality with a number of developmental abnormalities (Mendelsohn et al., 1994). In addition to genetic models, pharmacological studies of both maternal vitamin A deficiency or over-ingestion of vitamin A by the mother during gestation have

revealed a syndrome of malformations affecting, among other structures, the neural crest-derived aortic arch arteries (Warkany et al., 1948; Wilson et al., 1953).

RA has unique effects on the smooth muscle of the ductus arteriosus during late gestation. Although the contractile machinery is normally functional in the pre-term ductus arteriosus, the smooth muscle lacks the ability to respond to experimentally increased O_2 levels. However, maternal administration of RA has been shown to enhance the contractility of fetal rat ductal smooth muscle in response to oxygen (Wu et al., 2001). This effect is believed to be due to the ability of RA to accelerate maturation of the O_2 -sensing mechanism of arterial duct smooth muscle although that mechanism is not fully understood. RA has also been shown to upregulate particular markers of smooth muscle cell differentiation in the developing pulmonary system. Since I found that ductal smooth muscle cells in the $Ap2\beta^{-/-}$ were unable to maintain their highly differentiated state during late gestation, it is possible that there is some relationship between this phenotype and RA signaling in the $Ap2\beta^{-/-}$. In the absence of $Ap2\beta$, it is possible that ductal smooth muscle cells are impaired in their ability to metabolize vitamin A or receive signals from available retinoic acid. In this case, there may be decreased retinoic acid receptor expression or activity in the smooth muscle of the $Ap2\beta$ -null compared to wild-type littermates. Differences in RAR expression between wild-type and $Ap2\beta^{-/-}$ embryos could be determined using in situ hybridization to detect the various *RAR* mRNAs. However, this approach would not address whether activity of those receptors was altered in the absence of $Ap2\beta$.

A unique mouse model has been generated that could also help to answer the question of whether endogenous RA signaling is perturbed in the smooth muscle of the $Ap2\beta^{-/-}$ ductus

arteriosus. Colbert et al. created a transgenic mouse carrying a retinoic acid response element-*lacZ* (RARE-*lacZ*) transgene that expresses β -galactosidase in response to endogenous RA signaling during development (Colbert et al., 1996). Analysis of embryonic mice carrying this transgene revealed strong β -galactosidase expression in the ductus arteriosus and this staining colocalized with expression of SM2, a splice variant of smooth muscle myosin heavy chain and a marker of embryonic ductal smooth muscle cells. By breeding the RARE-*lacZ* transgene into *Ap2 β* -deficient mice, we could generate *Ap2 β ^{-/-};RARE-*lacZ** embryos to test whether *Ap2 β* is required for RA signaling in ductal smooth muscle. While altered expression of this transgene in the smooth muscle of the *Ap2 β ^{-/-}* ductus arteriosus would indicate inappropriate RA signaling in that tissue, correct expression would still leave open the reverse possibility that RA signaling is important for *Ap2 β* expression. This could easily be tested by administering RA to rodent dams and analyzing expression of *Ap2 β* at various time points in the unborn mice.

Implications for the Ductus Venosus

The ductus venosus is another fetal vessel that closes at the time of parturition. The venous duct traverses the liver, allowing blood to bypass the developing organ and travel to the placenta for detoxification. Unlike the ductus arteriosus, the ductus venosus is not derived from neural crest cells and, as a vein, lacks the highly differentiated and contractile smooth muscle layer characteristic of the arterial duct. For decades, closure of the ductus venosus was thought to occur passively as part of the major hemodynamic changes brought about at birth, contrasting the active constriction of the ductus arteriosus in response to

prostaglandin withdrawal and endothelin upregulation. However, patency of the ductus venosus does persist in some humans after birth, causing hepatic dysfunction and liver steatosis. More recently, familial cases of patent ductus venosus have even been reported, suggesting that closure of the vessel is a heritable trait controlled by products of specific genes (Uchino et al., 1996; Jacob et al., 1999).

Genetic control of ductus venosus closure has been further demonstrated by targeted deletion of the gene encoding the aryl hydrocarbon receptor (Ahr) in mice. Ahr is a bHLH/PAS domain-containing transcription factor similar to Hif2 α and *Ah*^{-/-} mice die during the neonatal period (Lahvis et al., 2000). Hemodynamic analysis of *Ah*^{-/-} newborns revealed persistently patent venous ducts that likely contributed to their early death. Interestingly, the ductus arteriosus of these animals closed normally further supporting the idea that different transcriptional cascades control closure of these two fetal vessels.

The arterial and venous ducts serve to divert blood away from the lungs and liver, respectively, during fetal development and closure of both vessels is critical for extrauterine survival. Evolution of both structures allowed animals to develop within the mother where the fetus depends on the placenta for exchange of gas and waste—functions that would normally be carried out by the lungs and liver. Given the parallels between the two ducts, it is interesting to entertain the idea that they evolved similar mechanisms of closure, both relying on a bHLH/PAS domain-containing transcription factor with sensing capabilities suitable to their individual needs. In this respect, the venous duct may be utilizing the aryl hydrocarbon receptor, a regulator of

biological responses to environmental toxins and elements that would normally be neutralized by the liver. Perhaps, in a similar manner, the arterial duct has evolved to use Hif2 α , an oxygen-sensing transcription factor, to promote its closure at birth or to maintain its patency during gestation. Due to the embryonic lethality of *Hif2 α ^{-/-}* mice (Tian et al., 1998), analysis of ductal patency in late gestation or neonatal mice lacking Hif2 α has not been possible. However, given my finding that vascular smooth muscle expression of *Hif2 α* is restricted to the ductus arteriosus, it would be possible to generate a tissue-specific knockout of *Hif2 α* using an existing *Sm22-Cre* mouse (Holtwick et al., 2002). Although Sm22 is expressed throughout developing arterial smooth muscle and expression of Cre recombinase under its control would excise Hif2 α in all of those cells, the consequence would be targeted deletion of *Hif2 α* in ductal smooth muscle cells—the only vascular smooth muscle known to express *Hif2 α* during development. Further expression analysis of *Hif2 α* and *Ah* in both the ductus arteriosus and ductus venosus may also help to substantiate or invalidate this idea of parallel closure mechanisms.

Technological Advances in Gene Regulation Discovery

A critical next step for the projects outlined in this thesis and one of the most important goals of labs studying transcriptional regulation of development is to identify transcriptional targets of a particular genetic regulatory cascade. It is also one of the most difficult questions to answer given our current technologies, particularly as we seek to identify *direct* targets of transcription factors. Candidate approaches can only go so far toward identifying transcriptional targets and, due to obvious limitations, may not reveal

new genetic pathways that will open novel lines of study. Subtractive hybridization and microarray analysis have been widely used to compare gene expression profiles in specific tissues of wild-type animals with those lacking or overexpressing the transcription factor of interest in an effort to identify transcriptional targets. However, both applications come with inherent challenges that make identification of verifiable, biologically relevant, direct transcriptional targets difficult. First, since targeted deletion of many of the genes important for heart development results in early embryonic lethality, the amount of tissue available for RNA extraction is often limited and associated developmental delay or the dying condition of the embryo can complicate the analysis since transcripts related to those processes will be over-represented in the mutant. Secondly, such screens require a secondary approach to eliminate false positives and this is perhaps the most tedious part of the analysis. Finally, neither technique enriches for direct targets, so any gene whose expression is found to be affected must be analyzed by additional methods to determine whether it is a direct target or occurs further downstream in the transcriptional cascade.

Chromatin immunoprecipitation (ChIP) is a promising technique for identifying direct transcriptional targets of a particular protein since, in theory, recovered DNA fragments should represent enhancer elements directly bound by the transcription factor under investigation. Of course, even under optimal conditions, a large portion of the recovered fragments are actually false positives, so a secondary screen is again required to enrich for true targets. New technologies and novel uses of preexisting techniques have recently been applied to this quest with some success. One such application

involves serial immunoprecipitation (IP) such that, after the first round of IP, the output is eluted and precipitated again using the same antibody or a second antibody with varying affinity. The advantage of this approach is that it greatly reduces false positives due to the extreme unlikelihood of repeated, non-specific IP of unwanted fragments (Weinmann et al., 2001). The downside of this methodology, both as reported in the literature and from my own experience, is that the number of false negatives is dramatically increased. That is to say, many known direct targets of a particular transcription factor will not be cloned using this method, limiting its utility for identification of unknown targets.

An alternative and, I believe, more promising secondary screen is to couple ChIP to CpG island microarray analysis—a technique known as ChIP on chip (Weinmann et al., 2002). Since transcription factors regulate gene expression through interactions with enhancer elements, it would be useful to select for clones recovered from ChIP that can be identified as enhancers, as they are more likely to represent biologically relevant targets. We know empirically that enhancers often contain an inordinately high percentage of CpG dinucleotides and we refer to these regions as CpG islands. By identifying and amplifying CpG islands from the human genome, a CpG island microarray has been generated to which ChIP output can be hybridized. Direct, uncloned ChIP output is linearly amplified, fluorescently labeled and hybridized to the chip along with output from a negative control ChIP, usually performed without addition of antibody or on cells not expressing the transcription factor of interest. CpG island microarray features which are preferentially bound by experimental ChIP clones, compared to negative control ChIP clones, are considered for verification as enhancer elements

controlled by the transcription factor under investigation. This verification process is simplified with ChIP on chip because the investigator can easily retrieve the sequence of the positive CpG island features, allowing for in silico identification of conserved, aligned transcription factor binding sites. Further, sequence knowledge allows generation of PCR primers flanking these sites for use in subsequent ChIP experiments followed by amplification of potential target sequences to look for enrichment of those targets in experimental versus negative control samples.

Although dHAND, which is required for development of the right ventricle as well as the neural crest-derived pharyngeal arches (Srivastava et al., 1997), was cloned a decade ago (Srivastava et al., 1995) and its function during development has been extensively studied since, no direct targets of dHAND have been identified in the developing heart or pharyngeal arch arteries. In addition to its normal expression in the heart, limbs, and neural crest-derived structures during development, dHAND is known to be highly expressed in neuroblastomas—fetal tumors of the adrenal gland that arise as a result of inappropriate neural crest cell growth and differentiation (Gestblom et al., 1999). Using resected neuroblastomas, I have performed ChIP with a polyclonal dHAND antibody to identify direct, developmental targets of dHAND. As a negative control, I made use of biopsies from normal kidneys, which do not express dHAND at any measurable level. After hybridization of the experimental and negative control ChIP output to a human CpG island microarray, I have identified many interesting candidate targets, which I plan to test for direct regulation by dHAND.

Another useful new tool that has become available during the course of this work is the ECR browser—an online navigation tool from the Comparative Genomics Center at Lawrence Livermore National Laboratory (<http://ecrbrowser.dcode.org/>). This is a tool for visualizing and studying evolutionary relationships between the sequenced vertebrate and non-vertebrate genomes including human, dog, mouse, rat, chicken, frog, pufferfish, zebrafish, and fruit fly (Ovcharenko et al., 2004). The ECR browser is an extremely powerful and user-friendly database with dynamic outputs for varying types of queries. After simply entering the name of a gene for which one is interested in identifying enhancer elements, an easy to read alignment of the genomic locus from multiple organisms is generated, highlighting the evolutionary conserved regions (ECRs). Given their maintenance through evolutionary time and selective pressure, these ECRs, which often appear in non-coding regions of the genome, are likely to contain regulatory elements bound by specific transcription factors to promote temporo-spatial expression of nearby genes. The ECR browser also allows for extraction of the exact sequences corresponding to the ECR and is coupled to a second tool, rVISTA 2.0, for identifying conserved, aligned transcription factor binding sites within those ECRs (Loots and Ovcharenko, 2004).

As CpG island microarrays become available for additional model organisms, it will be possible to perform ChIP on chip on a variety of tissue and cell types. In this way, investigators studying transcriptional regulation can potentially identify exponentially more enhancers and actively utilized, biologically relevant transcription factor binding sites, uncovering entire transcriptional cascades important for

development, normal biological activities, and progression of disease. Just as tools have been developed to allow access to the masses of information generated by genome sequencing projects, gifted bioinformatics specialists will need to create solutions that permit investigators to visualize the web of genomic elements important for transcriptional regulation. Since a single gene can have numerous enhancers regulating its expression at various times and in different tissues, and a single enhancer can be shared by multiple genes, it would be useful to have this information integrated into a single accessible location, rather than scattered through assorted publications. Expansion of the ECR browser could address this need through additional annotation of existing alignments. Through visual indication of known enhancer elements and verified transcription factor binding sites both inside and outside of the ECRs, a wealth of information would be available for further identification of important enhancers. Perhaps by integrating all of this information in a visual way, evolutionary, sequence, or positional patterns will emerge that can accelerate discovery of how expression of our genes is regulated.

References

- Clouthier, D.E., K. Hosoda, J.A. Richardson, S.C. Williams, H. Yanagisawa, T. Kuwaki, M. Kumada, R.E. Hammer, and M. Yanagisawa. 1998. Cranial and cardiac neural crest defects in endothelin-A receptor-deficient mice. *Development* **125**: 813-24.
- Colbert, M.C., M.L. Kirby, and J. Robbins. 1996. Endogenous retinoic acid signaling colocalizes with advanced expression of the adult smooth muscle myosin heavy chain isoform during development of the ductus arteriosus. *Circ Res* **78**: 790-8.
- Gestblom, C., A. Grynfeld, I. Ora, E. Ortoft, C. Larsson, H. Axelson, B. Sandstedt, P. Cserjesi, E.N. Olson, and S. Pahlman. 1999. The basic helix-loop-helix transcription factor dHAND, a marker gene for the developing human sympathetic nervous system, is expressed in both high- and low-stage neuroblastomas. *Lab Invest* **79**: 67-79.
- Goraca, A. 2002. New views on the role of endothelin (minireview). *Endocr Regul* **36**: 161-7.
- Holtwick, R., M. Gotthardt, B. Skryabin, M. Steinmetz, R. Potthast, B. Zetsche, R.E. Hammer, J. Herz, and M. Kuhn. 2002. Smooth muscle-selective deletion of guanylyl cyclase-A prevents the acute but not chronic effects of ANP on blood pressure. *Proc Natl Acad Sci U S A* **99**: 7142-7.
- Jacob, S., G. Farr, D. De Vun, H. Takiff, and A. Mason. 1999. Hepatic manifestations of familial patent ductus venosus in adults. *Gut* **45**: 442-5.
- Kurihara, Y., H. Kurihara, H. Suzuki, T. Kodama, K. Maemura, R. Nagai, H. Oda, T. Kuwaki, W.H. Cao, and N. Kamada. 1994. Elevated blood pressure and craniofacial abnormalities in mice deficient in endothelin-1. *Nature* **368**: 703-10.
- Lahvis, G.P., S.L. Lindell, R.S. Thomas, R.S. McCuskey, C. Murphy, E. Glover, M. Bentz, J. Southard, and C.A. Bradfield. 2000. Portosystemic shunting and persistent fetal vascular structures in aryl hydrocarbon receptor-deficient mice. *Proc Natl Acad Sci U S A* **97**: 10442-7.
- Loots, G. and Ovcharenko, I. 2004. rVista 2.0: evolutionary analysis of transcription factor binding sites. *Nucleic Acids Research*, **32**: W217-W221.
- Mendelsohn, C., D. Lohnes, D. Decimo, T. Lufkin, M. LeMeur, P. Chambon, and M. Mark. 1994. Function of the retinoic acid receptors (RARs) during development (II). Multiple abnormalities at various stages of organogenesis in RAR double mutants. *Development* **120**: 2749-71.

- Ovcharenko, I., Nobrega, M.A., Loots, G.G., and Stubbs, L. 2004. ECR Browser: a tool for visualizing and accessing data from comparisons of multiple vertebrate genomes. *Nucleic Acids Research*, **32**: W280-W286.
- Srivastava, D., P. Cserjesi, and E.N. Olson. 1995. A subclass of bHLH proteins required for cardiac morphogenesis. *Science* **270**: 1995-9.
- Srivastava, D., T. Thomas, Q. Lin, M.L. Kirby, D. Brown, and E.N. Olson. 1997. Regulation of cardiac mesodermal and neural crest development by the bHLH transcription factor, dHAND. *Nat Genet* **16**: 154-60.
- Taniguchi, T. and I. Muramatsu. 2003. Pharmacological knockout of endothelin ET(A) receptors. *Life Sci* **74**: 405-9.
- Tian, H., R.E. Hammer, A.M. Matsumoto, D.W. Russell, and S.L. McKnight. 1998. The hypoxia-responsive transcription factor EPAS1 is essential for catecholamine homeostasis and protection against heart failure during embryonic development. *Genes Dev* **12**: 3320-4.
- Uchino, T., F. Endo, S. Ikeda, K. Shiraki, Y. Sera, and I. Matsuda. 1996. Three brothers with progressive hepatic dysfunction and severe hepatic steatosis due to a patent ductus venosus. *Gastroenterology* **110**: 1964-8.
- Warkany, J., Roth, C.B., and Wilson, J.G. 1948. Multiple congenital malformations : a consideration of etiologic factors. *Pediatrics* **1**: 462-471
- Weinmann, A.S., S.M. Bartley, T. Zhang, M.Q. Zhang, and P.J. Farnham. 2001. Use of chromatin immunoprecipitation to clone novel E2F target promoters. *Mol Cell Biol* **21**: 6820-32.
- Weinmann, A.S., P.S. Yan, M.J. Oberley, T.H. Huang, and P.J. Farnham. 2002. Isolating human transcription factor targets by coupling chromatin immunoprecipitation and CpG island microarray analysis. *Genes Dev* **16**: 235-44.
- Wilson, J.G., C.B. Roth, and J. Warkany. 1953. An analysis of the syndrome of malformations induced by maternal vitamin A deficiency. Effects of restoration of vitamin A at various times during gestation. *Am J Anat* **92**: 189-217.
- Wort, S.J., M. Woods, T.D. Warner, T.W. Evans, and J.A. Mitchell. 2001. Endogenously released endothelin-1 from human pulmonary artery smooth muscle promotes cellular proliferation: relevance to pathogenesis of pulmonary hypertension and vascular remodeling. *Am J Respir Cell Mol Biol* **25**: 104-10.
- Wu, G.R., S. Jing, K. Momma, and T. Nakanishi. 2001. The effect of vitamin A on

contraction of the ductus arteriosus in fetal rat. *Pediatr Res* **49**: 747-54.

Yanagisawa, H., M. Yanagisawa, R.P. Kapur, J.A. Richardson, S.C. Williams, D.E. Clouthier, D. de Wit, N. Emoto, and R.E. Hammer. 1998. Dual genetic pathways of endothelin-mediated intercellular signaling revealed by targeted disruption of endothelin converting enzyme-1 gene. *Development* **125**: 825-36.

VITAE

Kathryn Nicole Ivey was born in Waynesboro, Pennsylvania on January 13, 1976 to Roger Lee Ivey and Margaret Mary O'Toole Ivey. In 1980, one year after the birth of her brother Kevin Lee Ivey, her family moved to San Antonio, Texas where she ultimately graduated Magna cum Laude from James Madison High School in 1994. She graduated from Texas A&M University in College Station, Texas with a Bachelor of Science degree in Molecular and Cell Biology in 1998. She then moved to Dallas, Texas where she worked for one year in the laboratory of Leon Eidels, Ph.D. as a research technician before entering the Ph.D. program in the Division of Cell and Molecular Biology at The University of Texas Southwestern Medical Center. In 1999, she joined the Integrative Biology program and began her doctoral research in the laboratory of Deepak Srivastava, M.D. She married her long-time love, Christopher David Kline in September of 2002.

Permanent Address: 4332 Mesa Dr.
Carrollton, TX 75010